

# UC Berkeley

## UC Berkeley Electronic Theses and Dissertations

### Title

The roles of HipBA Toxin-Antitoxin Systems in *Caulobacter crescentus* Persistence and Stress Tolerance

### Permalink

<https://escholarship.org/uc/item/2dc9z32q>

### Author

Huang, Charlie

### Publication Date

2019

Peer reviewed|Thesis/dissertation

The roles of HipBA Toxin-Antitoxin Systems in *Caulobacter crescentus* Persistence and Stress Tolerance

By

Charlie Huang

A dissertation submitted in partial satisfaction of the

requirements for the degree of

Doctor of Philosophy

in

Microbiology

in the

Graduate Division

of the

University of California, Berkeley

Committee in charge:

Professor Kathleen R. Ryan, Chair  
Professor Matthew Traxler  
Professor Roberto Zoncu

Summer 2019



## Abstract

The roles of HipBA Toxin-Antitoxin Systems in *Caulobacter crescentus* Persistence and Stress Tolerance

by

Charlie Huang

Doctor of Philosophy in Microbiology

University of California, Berkeley

Professor Kathleen R. Ryan, Chair

Toxin-Antitoxin Systems are evolutionarily successful genetic modules that have proliferated across almost all free-living bacteria. The ubiquitous Type II modules encode a toxic protein and a corresponding antitoxin protein that forms a tight complex with the toxin to inhibit its activity. Originally thought to be merely selfish genetic elements, TA systems are now implicated in a wide variety of processes from biofilm formation to bacterial persistence. Persistence is low frequency phenomenon that permits a small subpopulation within a larger growing population to survive various stresses, including antibiotic treatment. These tolerant persister cells enter a transient dormant state and are genetically identical to the larger population. Once the antibiotic is removed, persister cells resume normal growth and become sensitive to the antibiotic once again. A popular mainstream model describing how TA systems interface with bacterial persistence has come under considerable scrutiny and major tenets of the model have been invalidated. Thus, there is a critical need to carefully reassess the biological roles of TA systems.

This dissertation focuses on the *hipBA* TA system; the link between the *hipBA* module and persister cell formation was first reported over thirty years ago and endures these recent challenges. The *hipBA* operon encodes a HipA toxin and a HipB antitoxin. The HipA toxin is a serine/threonine kinase that functions as a protein synthesis inhibitor. In *Escherichia coli*, HipA phosphorylates the glutamyl tRNA synthetase, GltX, to inhibit tRNA charging. The buildup of uncharged tRNAs activates the Stringent Response, a highly conserved stress response that is implicated in persister cell formation. The precise mechanism by which HipA mediates persister cell formation is under debate and the *hipBA* system has only been rigorously studied in *E. coli*; thus, there is a need to validate the role of *hipBA* in bacterial persistence in other organisms and dissect the mechanism of persister cell formation. *Caulobacter crescentus* is an aquatic alphaproteobacteria that is adapted to survive in environments with very low nutrient availability. Curiously, the *C. crescentus* NA1000 chromosome contains three *hipBA* modules. This dissertation characterizes each of these modules and assesses their contribution to bacterial persistence in *C. crescentus*. Furthermore, this work

dissects the biological role of each module in helping *C. crescentus* survive its stressful environment.

The first chapter, to be submitted as a primary research article, focuses on bacterial persistence in *C. crescentus*. Each *hipBA* module is experimentally validated as a functional TA system with a kinase HipA toxin capable of inhibiting growth and a corresponding HipB antitoxin. All three HipAs inhibit protein synthesis and several tRNA synthetases are identified as HipA kinase targets. This work is the first published report of persistence in *C. crescentus*. The persister fraction is quantified in rich PYE media; The persister frequency was consistently  $\sim 10^{-5}$  -  $10^{-6}$  during exponential growth and  $\sim 10^{-4}$  -  $10^{-5}$  in stationary phase against various antibiotics: carbenicillin, streptomycin and vancomycin. Two of the modules, *hipBA*<sub>1</sub> and *hipBA*<sub>2</sub>, are responsible for the increase in persister frequency between exponential growth and stationary phase. Without these modules, *C. crescentus* does not accumulate persister cells in stationary phase cultures grown in PYE media. Curiously, all three HipAs are capable of increasing persister frequencies  $\sim 10$ - $100$  fold when ectopically expressed. HipA mediated persister cell formation is dependent on the Stringent Response. While we validate the biological role of *hipBA* modules in bacterial persistence through a similar pathway as that in *E. coli*, persistence is never abolished even in a strain that entirely lacks the Stringent Response. Therefore, there are multiple pathways through which persister cells form in *C. crescentus*.

The second chapter contains unpublished material examining the *hipBA*<sub>3</sub> module. While the role of *hipBA*<sub>1</sub> and *hipBA*<sub>2</sub> in increasing persister cell frequencies in stationary phase cultures grown in PYE media was identified, no biological role was assigned to *hipBA*<sub>3</sub>. Here, we report a novel integration of a *hipBA* module into stress tolerance. Instead of being stochastically active in a small subpopulation, *hipBA*<sub>3</sub> responds to environmental cues. The HipB<sub>3</sub> antitoxin is degraded by the HslUV protease in response to phosphate limitation. Strains lacking the *hipBA*<sub>3</sub> module are ultrasensitive to peroxide stress during the exponential-to-stationary phase transition in cultures grown in PYE media. Supplementing phosphate or functional HipA<sub>3</sub> kinase complements this ultrasensitivity. Dps is a ferritin-like protein implicated in *C. crescentus* survival against peroxide stress. Ectopic Dps expression complements the peroxide ultrasensitivity in the  $\Delta hipBA_3$  strain. *dps* transcript abundance is reduced in a  $\Delta hipBA_3$  strain and ectopic HipA<sub>3</sub> expression upregulates *dps*. Thus, HipA<sub>3</sub> phosphorylates a downstream target that results in the transcriptional upregulation of *dps*. A model detailing how phosphate potentiates Dps function and the importance of translating Dps as phosphate becomes limiting is proposed.

## Chapter 1

### ***hipBA* toxin-antitoxin systems and persistence in *Caulobacter crescentus***

Charlie Y. Huang, Carlos Gonzales-Lopez, Kathleen R. Ryan

Department of Plant & Microbial Biology, University of California, Berkeley, USA

## Abstract

Antibiotic persistence is a transient phenotypic state during which a bacterium can withstand otherwise lethal antibiotic exposure or environmental stresses. In *Escherichia coli*, persistence is promoted by the HipBA toxin-antitoxin system. The HipA toxin functions as a serine/threonine kinase that inhibits cell growth; the HipB antitoxin neutralizes the toxin. *E. coli* HipA inactivates the glutamyl-tRNA synthetase GltX, which inhibits translation and triggers the highly conserved stringent response. Although *hipBA* operons are widespread in bacterial genomes, it is unknown if this mechanism is conserved. Here we describe the functions of three *hipBA* modules in the alpha-proteobacterium *Caulobacter crescentus*. The HipA toxins have different effects on growth and macromolecular syntheses, and they phosphorylate distinct substrates. HipA<sub>1</sub> and HipA<sub>2</sub> contribute to antibiotic persistence during stationary phase by phosphorylating the aminoacyl-tRNA synthetases GltX and TrpS. The stringent response regulator SpoT is required for HipA-mediated antibiotic persistence, but persister cells can form in the absence of all *hipBA* operons or *spoT*, indicating that multiple pathways converge on persistence in *C. crescentus*.

## Introduction

Toxin-antitoxin (TA) modules are small operons that encode a toxic protein and a corresponding antitoxin<sup>1</sup>. In Type II TA systems, the antitoxin is a protein that binds and neutralizes the toxin (**Fig. 1-1**)<sup>2</sup>. When free of inhibition, the toxin acts on various targets to inhibit cell growth or cause death<sup>3</sup>. While the toxin is long-lived, the antitoxin is labile and degraded by proteases. Therefore, the antitoxin must be continually produced to keep the toxin in check<sup>4</sup>. Both the antitoxin alone and the toxin-antitoxin complex can repress their own transcription; thus, as the antitoxin is degraded, the repression is relieved and the operon is transcribed to replenish the antitoxin supply<sup>5,6</sup>.

TA modules were initially found to promote plasmid maintenance via post-segregational killing of cells that did not inherit a plasmid<sup>7</sup>. Subsequently, however, TA modules were found to be highly abundant in the chromosomes of almost all free-living bacteria, raising questions about additional biological functions<sup>2,8</sup>. TA systems can provide stability to mobile genetic elements in bacterial chromosomes, but a growing body of work indicates that TA modules are involved in additional processes including biofilm formation, phage resistance, stress responses, and antibiotic persistence<sup>9-13</sup>.

Antibiotic persistence is thought to play an important role in chronic infections and facilitates the evolution of antibiotic resistance<sup>14</sup>. In contrast to resistance, in which a heritable genetic change renders an entire bacterial population able to grow in the presence of an antibiotic, persister cells are genetically identical their susceptible relatives and they tolerate antibiotics and other stresses by entering a transient, non-replicating state<sup>15,16</sup>. Persister cells can resume normal growth once the stressor is removed, but they are once again sensitive to the stress<sup>16</sup>. Persistence is viewed as a bet-hedging strategy against unexpected environmental threats; the dormant cells temporarily sacrifice replication in exchange for stress tolerance<sup>17,18</sup>.

TA systems were first implicated in antibiotic persistence when a screen for *Escherichia coli* mutants with increased levels of persister cell formation retrieved the gain-of-function *hipA7* allele<sup>19</sup>. Named for *high incidence of persistence*, the *hipBA* module encodes two proteins, the HipB antitoxin and the HipA toxin, which functions as a serine/threonine kinase (**Fig. 1-2**)<sup>20-22</sup>. The G22S amino acid substitution in HipA7 is thought to increase the likelihood of HipA activity by interfering with HipA dimerization within HipA/HipB/operator complexes at the *hipBA* promoter<sup>23</sup>. Mutations in *hipA* are reported to arise in half of *E. coli* clinical isolates associated with chronic urinary tract infections, indicating a need for further studies to understand how HipA toxins promote antibiotic persistence<sup>24</sup>.

To date, the HipBA system has only been mechanistically studied in *E. coli*, where free HipA phosphorylates and inactivates the glutamyl-tRNA synthetase GltX<sup>25</sup>. The accumulation of uncharged tRNAs is detected by the ribosome-associated protein RelA, which synthesizes the alarmone (p)ppGpp to signal a state of amino acid starvation, known as the stringent response<sup>26,27</sup>. (p)ppGpp binding to additional target proteins, such as RNA polymerase and primase, reprograms transcription, downregulates macromolecular syntheses, and promotes dormancy<sup>28</sup>. However, other substrates of *E. coli* HipA have recently been identified, and additional phosphorylation events may stimulate persister formation<sup>26</sup>.

*hipBA* operons are present in numerous, phylogenetically distinct bacterial genomes, yet it is unknown if all HipBA modules influence persistence, or if all HipA toxins phosphorylate the same substrates. To address these questions, we are studying HipBA systems in *Caulobacter crescentus* NA1000, a Gram-negative alpha-proteobacterium that lives in nutrient-limited freshwater environments and maintains three *hipBA* operons in its chromosome<sup>29,30</sup>. Here we report that all three *hipBA* operons encode active TA systems, and that two of them are responsible, via the stringent response, for the majority of antibiotic persistence during stationary phase. The three HipA toxins phosphorylate distinct sets of substrates, of which specific aminoacyl-tRNA synthetases are critical targets for the development of antibiotic persistence. Importantly, persister cells are still observed after elimination of all three *hipBA* operons or the stringent response regulator *spoT*, indicating that there are multiple pathways leading to antibiotic persistence in *C. crescentus*.



## Results

A blastp search of the NA1000 genome for proteins similar to *E. coli* HipA revealed three predicted *hipBA* operons: *hipBA*<sub>1</sub>, *CCNA\_00481-2*, *hipBA*<sub>2</sub>, *CCNA\_02822-1*, and *hipBA*<sub>3</sub>, *CCNA\_02859-8* (**Fig 1-3**). When ectopically expressed under control of an inducible *riboA* promoter on a low-copy plasmid, each HipA toxin inhibited growth in exponential-phase NA1000 cultures, albeit to different degrees (**Fig. 1-4A**). HipA<sub>1</sub> and HipA<sub>2</sub> significantly impacted cell viability, while HipA<sub>3</sub> had a bacteriostatic effect. While no organism with multiple HipA toxins has been studied, coactivation of different TA systems has been reported, and we could not discount the possibility of crosstalk between *hipBA* modules<sup>31,32</sup>. To assess the effect of each HipA toxin without the possibility of crosstalk, we expressed each HipA from a low-copy plasmid in a strain with all three *hipBA* operons deleted from the chromosome ( $\Delta hipBA_{1,2,3}$ ). Each HipA toxin can independently inhibited growth in this strain (**Fig. 1-4B**). HipA<sub>2</sub> or HipA<sub>3</sub> expression resulted in slightly more potent growth inhibition in  $\Delta hipBA_{1,2,3}$  than in NA1000, likely due to the absence of chromosomally encoded HipB antitoxins that would mitigate the effects of ectopic HipA expression. In contrast, HipA<sub>1</sub> was less toxic when expressed in the  $\Delta hipBA_{1,2,3}$  strain than in NA1000, suggesting that its deleterious effects are enhanced in wild-type cells by coactivation of another HipA.

All three HipA toxins in NA1000 maintain the conserved active site residues of serine/threonine kinases (**Fig. 1-5**)<sup>33</sup>. We generated an aspartate-to-glutamine (D-Q) substitution in the active site of each HipA, modeled on a corresponding substitution used to create a kinase-dead *E. coli* HipA protein<sup>34</sup>. Each HipA D-Q variant was ectopically expressed in the  $\Delta hipBA_{1,2,3}$  strain to determine if kinase activity is necessary for growth inhibition (**Fig. 1-4A**). Although each kinase-dead HipA protein was expressed (**Fig. 1-4B**), we observed no growth inhibition, indicating that the toxic effects of the wild-type HipA proteins are mediated by phosphorylation of downstream targets.

Once released from antitoxin inhibition, *E. coli* HipA eventually autophosphorylates on a serine residue, which structurally blocks its kinase activity<sup>34</sup>. In persister cells generated due to HipA activity, autophosphorylation is likely important for the resumption of normal growth, also known as persister resuscitation<sup>34</sup>. To confirm the kinase activity of each HipA protein, we examined autophosphorylation using Phos-tag mobility shift assays in combination with Western blotting. When expressed in the  $\Delta hipBA_{1,2,3}$  strain, we observed retardation of a portion of each wild type HipA protein indicative of autophosphorylation, but no mobility shift occurred when the kinase-dead HipA variants were expressed (**Fig. 1-4B**).

We expected each HipA toxin to be counteracted by binding to the HipB antitoxin encoded in its operon. Promiscuity between toxin and antitoxin partners is rare, even in bacteria harboring multiple paralogous toxins, but crosstalk in HipA-HipB interactions has never been investigated<sup>35,36</sup>. To determine the cognate HipB antitoxin(s) for each HipA toxin, we coexpressed all combinations of HipA and HipB in a  $\Delta hipBA_{1,2,3}$  background (**Fig. 1-4C**). As expected, the growth arrest caused by ectopically expressing each HipA is mitigated by coexpressing the HipB in its own operon. Unexpectedly, the toxicity of HipA<sub>1</sub> or HipA<sub>2</sub> was counteracted by coexpression of either

HipB<sub>1</sub> or HipB<sub>2</sub>, indicating that the *hipBA*<sub>1</sub> and *hipBA*<sub>2</sub> modules can influence each other's phenotypic effects.

### **HipA toxins in NA1000 do not require the stringent response to arrest growth**

*E. coli* HipA is significantly less toxic in a strain that does not have RelA, and HipA has been proposed to rely on the stringent response to inhibit DNA replication and transcription<sup>27</sup>. However, it is not known if interaction with the stringent response is a universal feature of HipA activity. The stringent response in *C. crescentus* relies on a single (p)ppGpp synthetase/hydrolase SpoT<sup>37</sup>. SpoT associates with the translating ribosome and responds to amino acid limitation, but only in combination with a separate cue indicating either carbon or nitrogen starvation<sup>38</sup>. Thus, the accumulation of uncharged tRNAs, such as those produced by HipA-mediated phosphorylation of GltX, would be insufficient on its own to activate the *C. crescentus* stringent response.

To investigate the relationship between *Caulobacter* HipAs and the SpoT-mediated stringent response, we first asked if the stringent response was required for growth inhibition by HipA toxins in NA1000. We found that each HipA toxin is equally capable of inhibiting growth in the wild-type and  $\Delta spoT$  backgrounds (**Fig. 1-6A**). To determine if the stringent response is activated by ectopic HipA expression, we measured the transcription of three genes that are highly upregulated and two genes that are significantly downregulated during the stringent response using<sup>38</sup>. In contrast to incubation in minimal medium lacking a carbon source, expression of individual HipA toxins does not produce the characteristic transcriptional changes (**Fig. 1-6B**). We therefore conclude that the HipA toxins do not require the stringent response for growth inhibition, and their expression is not sufficient to activate the stringent response in *C. crescentus* during exponential growth.

### **HipAs affect protein synthesis**

The best-understood effects of *E. coli* HipA are upon protein synthesis, via GltX phosphorylation, but it has also been reported to inhibit DNA and RNA synthesis<sup>25,39</sup>. To determine if macromolecular syntheses are affected by *C. crescentus* HipA toxins, we measured <sup>35</sup>S-methionine, <sup>3</sup>H-thymidine, and <sup>3</sup>H-uridine incorporation following induction of each HipA. <sup>35</sup>S-methionine incorporation is sharply reduced in wild-type and  $\Delta hipBA_{1,2,3}$  cultures expressing HipA<sub>1</sub> or HipA<sub>2</sub>, but only mildly reduced over time in cultures expressing HipA<sub>3</sub> (**Figs. 1-7A-B**). While HipA<sub>2</sub> is equally capable of inhibiting translation when expressed in either genetic background, HipA<sub>1</sub> inhibits protein synthesis more weakly in the  $\Delta hipBA_{1,2,3}$  strain. This observation is consistent with the weaker overall growth inhibition by HipA<sub>1</sub> in  $\Delta hipBA_{1,2,3}$  cells (**Fig. 1-4B**) and suggests that HipA<sub>1</sub> coactivates HipA<sub>2</sub>. <sup>3</sup>H-thymidine incorporation is mildly reduced after several hours when any HipA is expressed (**Fig. 1-7C**); however, this may be due to indirect effects of growth arrest. <sup>3</sup>H-uridine incorporation was unchanged when any HipA was expressed, indicating that RNA synthesis is not targeted (**Fig. 1-7D**). Thus, HipA<sub>1</sub> and HipA<sub>2</sub> sharply and quickly inhibit translation, while no *C. crescentus* HipA toxin strongly inhibits DNA or RNA synthesis.

## HipA<sub>1</sub> and HipA<sub>2</sub> phosphorylate tRNA synthetases

From an initial phosphoproteomics analysis of unstressed NA1000 during exponential growth, we noted that the aminoacyl-tRNA synthetases GltX, LysS, and TrpS were phosphorylated on serine residues. No kinase was previously known to phosphorylate these proteins, and the HipA and Doc toxins are the only predicted serine/threonine kinases encoded in the NA1000 genome. By analogy with *E. coli* HipA, and based on their inhibition of protein synthesis, we hypothesized that HipA<sub>1</sub> and/or HipA<sub>2</sub> phosphorylate GltX, TrpS, and LysS. We used Phos-tag mobility shift assays to examine the phosphorylation of aminoacyl-tRNA synthetases in  $\Delta hipBA_{1,2,3}$  cells expressing individual HipA toxins. HipA<sub>2</sub> expression caused retardation of LysS, TrpS and GltX, while HipA<sub>1</sub> expression slowed the migration of LysS and GltX (**Fig. 1-8A**). Consistent with its much weaker effect on protein synthesis, HipA<sub>3</sub> did not affect the migration of LysS or TrpS and only caused the retardation of a small fraction of GltX after an extended period of toxin expression (**Fig. 1-8B**). Although it is formally possible that HipA<sub>1</sub> and/or HipA<sub>2</sub> activate an unknown kinase that phosphorylates these targets, the simplest interpretation is that HipA<sub>1</sub> and HipA<sub>2</sub> directly phosphorylate overlapping sets of aminoacyl-tRNA synthetases, which inhibits translation.

## *hipBA*<sub>1</sub> and *hipBA*<sub>2</sub> contribute to persistence in *C. crescentus* via phosphorylation of TrpS and GltX

Antibiotic persistence has not previously been reported in *C. crescentus*. We used Minimum Duration for Killing (MDK) assays to measure bacterial survival over time after exposure to saturating antibiotic concentrations (10-500 times the minimal inhibitory concentration)<sup>40</sup>. When plotted, cultures that contain a sensitive population and a persister fraction generate a biphasic killing curve that reflects the different survival rates of the two populations (**Fig. 1-9**). An increase in persister fraction shifts the second phase of the curve upwards, while a decrease moves the second phase downwards<sup>41</sup>. With enough MDK measurements, the biphasic curve can be used to estimate the frequency of persister cells and describe the survival rate over time of each population. While much of the work on persistence and HipA employs beta-lactam antibiotics to kill the susceptible population, *C. crescentus* NA1000 expresses an active beta-lactamase enzyme Bla<sup>42</sup>. We report persistence toward carbenicillin in a  $\Delta bla$  strain (**Fig. 1-10**), but we focus on other antibiotics to dissect the contributions of the *hipBA* modules to persistence in *C. crescentus*.

We selected an aminoglycoside, streptomycin, and a cell wall synthesis inhibitor, vancomycin, for their rapid bactericidal activity against *C. crescentus*. We observed a biphasic killing curve in exponential phase cultures (**Fig. 1-11A**); however, the lower frequency of persistence and the lower cell density during exponential growth make measurements challenging, as the second phase of the killing curve quickly moves below the detection limit of our assay. These results are consistent with reports of other bacteria, where persisters are rarer during exponential growth than during stationary phase. Consequently, we focused on persistence during stationary phase. We observed

biphasic killing in NA1000 cultures that had reached full cell density ( $OD_{660} \sim 1.0$ , after 24 hours of growth from  $OD_{660} = 0.02$ ) when saturating antibiotic concentrations were applied. The wild-type persister fraction was estimated to be  $\sim 10^{-4}$ - $10^{-5}$  in stationary phase cultures grown in PYE medium and was consistent across carbenicillin, streptomycin and vancomycin treatments (**Fig. 1-10, Figs. 1-11A-B**).

To determine if one or more *C. crescentus hipBA* modules contribute to persistence, we first measured the persister fraction in a strain lacking all *hipBA* operons (**Fig. 1-11A**). The  $\Delta hipBA_{1,2,3}$  strain showed a significant  $\sim 5$ - $10$ -fold reduction in persister frequency in stationary phase cultures grown in PYE medium when treated with streptomycin and vancomycin. Interestingly, persisters were not entirely abolished in the  $\Delta hipBA_{1,2,3}$  strain, and the remaining persister fraction had a survival rate similar to that of wild-type persisters. We conclude from these results that at least one *hipBA* module is required for the formation of  $>80\%$  of *C. crescentus* persister cells, but that persisters which do form in the absence of *hipBA* modules are just as able to withstand antibiotic killing as those possessing a full complement of *hipBA* systems.

To dissect the contributions of individual *hipBA* modules, we measured persistence in individual and double *hipBA* knockout strains. Single *hipBA* deletions had no significant effects, (**Fig. 1-11C**), but we observed the same  $\sim 5$ - $10$ -fold reduction in persister frequency in a  $\Delta hipBA_{1,2}$  strain as in  $\Delta hipBA_{1,2,3}$  (**Figs. 1-11 A-B**). The reduction in persister frequency in  $\Delta hipBA_{1,2,3}$  cells was complemented by low-copy plasmids bearing *hipBA*<sub>1</sub> and/or *hipBA*<sub>2</sub> (**Fig. 1-11B**). All strains lacking one or more *hipBA* operons have growth rates very similar to the wild-type strain (**Fig. 1-12**), so the reduction in persister frequency is not likely to be caused by a pleiotropic fitness defect. We infer that *hipBA*<sub>1</sub> and *hipBA*<sub>2</sub> are the primary determinants of persister cell formation in stationary phase, and that there is some level of functional redundancy between these modules. In contrast, the *hipBA*<sub>3</sub> module appears to play no significant role in antibiotic persistence under during stationary phase.

As HipA<sub>1</sub> and HipA<sub>2</sub> phosphorylate tRNA synthetases, we asked if these targets are important for persister cell formation. Overexpression of GltX or TrpS reduced the persister fraction in stationary phase to the same level as seen in  $\Delta hipBA_{1,2}$  cultures (**Fig. 1-13A**). In contrast, strains expressing LysS or the control, methionyl-tRNA synthetase MetG, had persister frequencies indistinguishable from NA1000. Overexpression of GltX or TrpS could reduce the persister fraction either by bolstering tRNA synthetase activity and maintaining active translation, or by titrating HipA<sub>1</sub> or HipA<sub>2</sub> away from substrates that are truly critical for persister cell formation. The fact that overexpression of LysS, also a target of HipA<sub>1</sub> and HipA<sub>2</sub>, was not able to reduce the persister fraction argues against a nonspecific titration effect. These results strongly suggest that GltX and TrpS are critical targets through which HipA<sub>1</sub> and HipA<sub>2</sub> mediate persister cell formation, and they demonstrate further that not all phosphorylated substrates are important for HipA-mediated persistence.

### **The stringent response is responsible for the accumulation of persister cells in stationary phase**

Although ectopic HipA expression in exponential phase cells did not activate the stringent response and was not required for HipA-induced growth arrest (**Fig. 1-6**), the stringent response is important for persister cell formation in some bacteria<sup>43</sup>. We therefore asked if the (p)ppGpp synthase/hydrolase SpoT affects persistence in *C. crescentus*.  $\Delta spoT$  cells divide slightly faster than a wild-type cells, but they lose viability more quickly than wild-type cells during long-term nutrient-limited conditions like stationary phase (**Fig. 1-13D**) or carbon starvation<sup>37,44</sup>. Biphasic killing was observed in exponential and stationary phase cultures of a  $\Delta spoT$  strain grown in PYE medium when challenged with streptomycin or vancomycin, indicating that *C. crescentus* can form persisters without the stringent response. During exponential growth, the  $\Delta spoT$  strain had a persister frequency similar to NA1000 (**Fig. 1-11A**). However, the fraction of persisters in stationary phase PYE cultures was reduced in the  $\Delta spoT$  mutant by ~5-10 fold, and both the sensitive and persister populations were killed faster than the corresponding wild-type populations. Significantly, the  $\Delta spoT$  strain had similar persister frequencies in exponential and stationary phases, indicating that SpoT is important for the accumulation of persister cells during stationary phase.

The  $\Delta spoT$  and  $\Delta hipBA_{1,2}$  mutants displayed similar reductions in persister frequency specifically during stationary phase. Thus, HipA toxins may mediate persister formation in stationary phase through the stringent response or vice versa. Since deletion of *hipBA* modules or overexpression of specific aminoacyl-tRNA synthetase substrates reduced persister frequencies (**Figs. 1-11A, 1-12A**), we wondered if expressing HipA toxins themselves could increase the persister fraction. To answer this question, we briefly induced expression of each HipA in NA1000,  $\Delta hipBA_{1,2,3}$  or  $\Delta spoT$  cells prior to antibiotic exposure in the persistence assay. Toxins were expressed during exponential phase because protein induction during stationary phase was inconsistent and yielded noisy, unreproducible MDK measurements. To avoid excessive loss of viability from the more toxic HipA proteins, expression was induced for three hours before washing the cells and adding lethal concentrations of antibiotics. Ectopic expression of each HipA increased the persister frequency in NA1000; however, no HipA could increase the persister frequency in a  $\Delta spoT$  background (**Figs. 1-12 B-C**). We conclude that while no HipA in NA1000 requires or activates the stringent response to arrest growth, HipA-induced persister formation does require the stringent response.

## Discussion

The *C. crescentus* NA1000 chromosome contains three functional *hipBA* modules, each with a distinct effect on growth, viability, and macromolecular syntheses when ectopically expressed in exponential-phase cultures. HipA<sub>2</sub> is the most toxic, reducing translation to  $\leq 25\%$  of the wild-type level within 1 hour and reducing the viable cell count by 10-100-fold within 2 hours. HipA<sub>1</sub> also immediately inhibits protein synthesis, but to a lesser degree than HipA<sub>2</sub>, and begins to reduce viability after 12 hours of expression. HipA<sub>3</sub>, which is bacteriostatic, causes a gradual and less severe reduction in translation over 4 hours. Since our ectopic expression system produces comparable amounts of the three HipA toxins (**Fig. 1-4D**), these phenotypes suggest each toxin has different levels of kinase activity and/or phosphorylate distinct groups of

substrates. In agreement with this prediction, we observed that the HipAs have different activity toward selected aminoacyl-tRNA synthetases: HipA<sub>2</sub> phosphorylates TrpS, GltX and LysS; HipA<sub>1</sub> phosphorylates LysS and GltX; and HipA<sub>3</sub> only weakly phosphorylates GltX (**Fig. 1-8B**). These results pave the way for examining kinase-substrate specificity in HipA toxins and suggest that HipA<sub>3</sub> arrests growth by a mechanism distinct from HipA<sub>1</sub> and HipA<sub>2</sub>.

Since *C. crescentus* contains three *hipBA* modules, we assessed the possibility of crosstalk between them by co-expressing non-cognate HipA and HipB proteins. The toxicity of HipA<sub>1</sub> or HipA<sub>2</sub> was counteracted by co-expression of either HipB<sub>1</sub> or HipB<sub>2</sub>, while HipA<sub>3</sub> could only be inhibited by HipB<sub>3</sub>. Since non-native promoters were used for co-expression, these results indicate crosstalk at the level of protein-protein interaction, where HipB from one module blocks the activity of HipA from another module. In support of this finding, ectopic HipA<sub>1</sub> expression is somewhat less toxic (**Fig5. 1-3 A-B**) and less capable of inhibiting protein synthesis (**Figs. 1-7 A-B**) in the  $\Delta hipBA_{1,2,3}$  strain than in a wild-type strain, suggesting that HipA<sub>1</sub> achieves some of its toxicity by coactivating HipA<sub>2</sub>. Based on examination of the *hipBA*<sub>1</sub> and *hipBA*<sub>2</sub> operons, we speculate that they also engage in transcriptional crosstalk. In *E. coli*, HipB alone or HipA/HipB complexes bind inverted repeat sequences with distinct spacing to autoregulate *hipBA* transcription<sup>24,45</sup>. In the promoter regions of *hipBA*<sub>1</sub> and *hipBA*<sub>2</sub>, we noted a series of identical inverted repeats that occur in intervals consistent with the higher-order structure of *E. coli* HipA/HipB/promoter complexes (**Fig. 1-14**). Based on these observations, we speculate that cross-regulation may exist in other bacteria harboring multiple HipBA systems.

In contrast to *E. coli*, ectopic expression of the *C. crescentus* HipA toxins during exponential phase neither activates the stringent response nor requires SpoT to inhibit growth. This discrepancy is likely due to the different criteria for stringent response activation in the two bacteria. In *E. coli*, RelA synthesizes (p)ppGpp when uncharged tRNAs enter the ribosome, indicative of amino acid starvation<sup>46,47</sup>. In contrast, *C. crescentus* SpoT synthesizes (p)ppGpp only when it senses amino acid starvation in combination with a separate signal of carbon or nitrogen starvation<sup>38</sup>. Thus, to stimulate the (p)ppGpp synthase activity of SpoT in *C. crescentus*, a HipA toxin expressed during exponential growth would need to phosphorylate targets that generate two independent starvation signals, despite the presence of adequate nutrients in the medium. Our phosphorylation and persistence results imply that HipA<sub>1</sub> and HipA<sub>2</sub> inhibit the charging of specific tRNAs, supplying the amino acid starvation signal, but they do not by themselves provide a separate signal indicating nitrogen or carbon starvation.

As an organism adapted to aquatic environments with low nutrient levels, *C. crescentus* may not be expected to encounter frequent antibiotic stress. However, persister cells are tolerant of a variety of stresses, such as starvation, that *C. crescentus* may face in a rapidly shifting environment<sup>18</sup>. We report the first measurements of antibiotic persistence in *C. crescentus*, in exponential growth and in stationary phase. The persister frequency was consistently  $\sim 10^{-5}$ - $10^{-6}$  during exponential growth and  $\sim 10^{-}$

$4 \cdot 10^{-5}$  in stationary phase across all antibiotics tested (carbenicillin, streptomycin and vancomycin) and was similar to the persister frequencies reported in pathogens<sup>15</sup>. Deletion mutants reveal that *hipBA*<sub>1</sub>, *hipBA*<sub>2</sub>, and *spoT* play significant roles in *C. crescentus* persister cell formation during stationary phase, while *hipBA*<sub>3</sub> is dispensable. The  $\Delta$ *spoT* strain does not have a significantly reduced persister frequency compared to wild-type during exponential growth in PYE medium, but it fails to accumulate persister cells in stationary phase, indicating that the stringent response mediates a large (~5-10 fold) increase in persister cells that normally occurs during stationary phase. Both the sensitive and persister sub-populations of the  $\Delta$ *spoT* strain were killed more rapidly by antibiotics during stationary phase persistence assays, but not during exponential-phase persistence assays. This difference survival may reflect the reduced ability of  $\Delta$ *spoT* cells to survive the nutrient-depleted conditions of the stationary phase persistence assay (**Fig. 1-13D**)<sup>37</sup>, rather than a specific reduction in antibiotic tolerance. In contrast, persister cells formed by *C. crescentus* lacking all three *hipBA* operons were killed by antibiotics at the same rate as wild-type persisters (**Figs. 1-11A, 1-11C**), suggesting that HipBA TA systems primarily affect persister formation. Importantly, persistence in stationary phase is not abolished even when all *hipBA* operons or *spoT* is deleted, indicating that additional mechanisms can support persister formation.

Ectopic expression of each HipA during exponential growth in a wild-type background increased the persister fraction ~10-100 fold, but only in the presence of an intact *spoT* gene, indicating that all three *C. crescentus* HipA proteins mediate persister formation through the stringent response. Further, our results provide genetic evidence that HipA-mediated phosphorylation of specific aminoacyl-tRNA synthetases contributes to persister formation. Overexpression of GltX or TrpS reduces the persister fraction to a level that phenocopies the  $\Delta$ *hipBA*<sub>1,2</sub> strain, but overexpression of another HipA<sub>2</sub> substrate, LysS, has no effect on persistence. We interpret these results to mean that phosphorylation of GltX and TrpS are critical events in HipA-induced persister formation, whereas LysS phosphorylation is not.

*E. coli* HipA phosphorylates GltX on Ser<sup>239</sup> within a conserved motif that binds and positions the catalytic ATP molecule<sup>25,26</sup>. Phosphorylation by *E. coli* HipA or substitution of an aspartate residue for Ser<sup>239</sup> blocked the tRNA charging activity of GltX *in vitro*<sup>25</sup>. In addition, a related toxin, HipT, found specifically in *E. coli* O127, was recently reported to activate the stringent response by phosphorylating TrpS on the analogous residue, Ser<sup>197</sup><sup>48</sup>. Our preliminary data suggest that *C. crescentus* TrpS is phosphorylated on the analogous conserved residue, Ser<sup>210</sup>, consistent with HipA<sub>2</sub> inactivating TrpS. In LysS (encoded by *CCNA\_00082*), the analogous serine residue, Ser<sup>322</sup>, was also phosphorylated in our phosphoproteome data, yet LysS overexpression did not reduce the fraction of persister cells in stationary phase. These results suggest either that LysS is not inactivated by phosphorylation, or that a second lysyl-tRNA synthetase encoded by *CCNA\_00757* provides activity in our conditions. Finally, our preliminary data suggest that *C. crescentus* GltX is phosphorylated on Ser<sup>2</sup>, rather than Ser<sup>242</sup>, the residue analogous to Ser<sup>239</sup> in *E. coli* GltX. Ser<sup>2</sup> is present in a six-amino acid N-terminal peptide not shared by *E. coli* GltX, but, based on the structure of the *Thermus thermophilus* homolog GluRS bound to its substrates, phosphorylation

of an amino acid near the N-terminus of the enzyme could interfere with the binding of tRNA<sup>Glu 49,50</sup>.

Although ectopic expression of either HipA<sub>1</sub> or HipA<sub>2</sub> can arrest growth population-wide, by a mechanism that includes inhibiting translation, the same ectopic expression does not uniformly activate the stringent response and produces at most 10<sup>-3</sup> persister cells. These results suggest that one or more stochastic processes downstream of HipA govern persister formation. We propose that HipA<sub>1</sub> or HipA<sub>2</sub> provides the amino acid starvation signal necessary to activate SpoT by phosphorylating and inactivating TrpS and/or GltX, while a signal for nitrogen or carbon starvation occurs stochastically, increasing in likelihood as cells enter stationary phase. In *E. coli*, the stringent response is necessary for persister formation, but above some threshold, the level of (p)ppGpp is not predictive of the persistent phenotype<sup>43</sup>. Instead, a stochastic process related to (p)ppGpp-dependent transcriptional reprogramming is thought to drive a sub-population of cells toward the persister fate. By analogy with *E. coli*, *C. crescentus* persister formation in stationary phase may also rely on a second stochastic process downstream of SpoT activation. Intriguingly, deletion of *hipBA*<sub>3</sub> does not reduce the persister fraction in stationary phase, but overexpression of HipA<sub>3</sub> in exponential phase increases persister formation, dependent upon *spoT*. Based on these results, we propose that HipA<sub>3</sub> promotes persister formation under environmental conditions that remain to be identified, either by phosphorylating tRNA synthetases that we have not investigated, or by phosphorylating cellular targets that provide a nitrogen or carbon starvation signal to SpoT.



## Methods

**Strains and growth conditions.** Strains used in this study are listed in Table 1-1. All *Caulobacter crescentus* strains derive from the laboratory strain NA1000. *Caulobacter* strains were grown at 30°C in rich PYE or in minimal medium supplemented with 0.2% glucose (M2G)<sup>29,51</sup>. PYE medium was supplemented with antibiotics when appropriate at the following concentrations (µg/mL): kanamycin (5); chloramphenicol (1); nalidixic acid (20); oxytetracycline (1); streptomycin (5). *E. coli* was grown in Luria broth at 37°C, supplemented with antibiotics when appropriate at the following concentrations (µg/mL) for liquid (L) or solid (S) medium: kanamycin, 30 (L), 50 (S); chloramphenicol, 20 (L), 30 (S); tetracycline, 12 (L/S); spectinomycin, 50 (L/S)<sup>52</sup>.

**Plasmid construction.** *Caulobacter crescentus* NA1000 genomic DNA or purified plasmids were used as template with Q5 High Fidelity DNA Polymerase (New England Biolabs (NEB)) to amplify fragments for cloning. Fragments were isolated after gel electrophoresis using the Zymoclean Gel DNA Recovery kit (Zymo Research). NEB restriction enzymes were used to digest purified plasmids. Gibson assembly was performed using NEB Hi-Fi DNA Assembly Master Mix. Plasmid constructs were confirmed by DNA sequencing. Plasmid descriptions are listed in Table 1-2, and primers used in plasmid construction are listed in Table 1-3.

**Strain construction.** TA module knockout plasmids (e.g.  $\Delta hipBA_1$ ) were generated using derivatives of the pNPTS138 suicide vector that carries the kanamycin resistance determinant (*nptI*) and a counterselectable marker that restricts growth in the presence of sucrose (*sacB*). Genome modifications were made with these pNPTS138 derivatives using two-step recombination. Knockout plasmids were transferred into *C. crescentus* NA1000 by conjugation using *E. coli* S17-1, with selection on PYE plates containing kanamycin and nalidixic acid. Colonies containing the integrated plasmid at the target locus were grown to saturation in PYE under nonselective conditions and plated on PYE agar containing 3% (wt/vol) sucrose to select for loss of the *sacB* marker. Sucrose-resistant colonies were screened for kanamycin sensitivity, and the resulting kanamycin-sensitive colonies were screened for the desired deletion at the genomic locus by diagnostic PCR using primers indicated in Table 1-3.

pCYH1, pCYH2, and pCYH3. For *hipBA* knockout constructs, flanking homology regions were amplified using the following primer pairs: pCYH1 5'-region (*hipBA*<sub>1</sub> Up F and *hipBA*<sub>1</sub> Up R), pCYH2 5'-region (*hipBA*<sub>2</sub> Up F and *hipBA*<sub>2</sub> Up R), pCYH3 5'-region (*hipBA*<sub>3</sub> Up F and *hipBA*<sub>3</sub> Up R), pCYH1 3'-region (*hipBA*<sub>1</sub> Down F and *hipBA*<sub>1</sub> Down R), pCYH2 3'-region (*hipBA*<sub>2</sub> Down F and *hipBA*<sub>2</sub> Down R), pCYH3 3'-region (*hipBA*<sub>3</sub> Down F and *hipBA*<sub>3</sub> Down R) The final plasmid was assembled via Gibson cloning into a HindIII/EcoRI-digested pNPTS138 backbone.

*hipA*<sub>1</sub>, *hipA*<sub>2</sub>, and *hipA*<sub>3</sub>. For these over expression vectors, *hipA*<sub>1</sub>, *hipA*<sub>2</sub>, and *hipA*<sub>3</sub> were placed under control of the *riboA* promoter on the low-copy plasmid pMR20. PCR fragments representing the *riboA* promoter and each coding region were inserted into HindIII/EcoRI digested pMR20 using Gibson Assembly. PCR fragments for Gibson assembly were amplified using the following primer pairs: *hipA*<sub>1</sub>: P<sub>riboA</sub> (*riboA* to

pMR10/pMR20 F and *riboA* to *hipA*<sub>1</sub> R), *hipA*<sub>1</sub> (*hipA*<sub>1</sub> to *riboA* F and *hipA*<sub>1</sub> R). *hipA*<sub>2</sub>: P<sub>riboA</sub> (*riboA* to pMR10/pMR20 F and *riboA* to *hipA*<sub>2</sub> R), *hipA*<sub>2</sub> (*hipA*<sub>2</sub> to *riboA* F and *hipA*<sub>2</sub> R). *hipA*<sub>3</sub>: P<sub>riboA</sub> (*riboA* to pMR10/pMR20 F and *riboA* to *hipA*<sub>3</sub> R), *hipA*<sub>3</sub> (*hipA*<sub>3</sub> to *riboA* F and *hipA*<sub>1</sub> R).

pFLAG-*hipA*<sub>1</sub>, pFLAG-*hipA*<sub>2</sub>, pFLAG-*hipA*<sub>3</sub>. For these over expression vectors, the coding region of *hipA*<sub>1</sub>, *hipA*<sub>2</sub>, and *hipA*<sub>3</sub> were N-terminally fused to a 1xFLAG tag (amino acid sequence: DYKDDDDK) and placed under control of the *riboA* promoter on the low-copy plasmid pMR20. PCR fragments representing the *riboA* promoter and each coding region with N-terminal 1xFLAG tag fusion were inserted into HindIII/EcoRI digested pMR20 using Gibson Assembly. PCR fragments for Gibson assembly were amplified using the following primer pairs: pFLAG-*hipA*<sub>1</sub>: P<sub>riboA</sub> (*riboA* to pMR10/pMR20 F and *riboA* to FLAG R), *hipA*<sub>1</sub> (*hipA*<sub>1</sub> F and *hipA*<sub>1</sub> R). pFLAG-*hipA*<sub>2</sub>: P<sub>riboA</sub> (*riboA* to pMR10/pMR20 F and *riboA* to FLAG R), *hipA*<sub>2</sub> (*hipA*<sub>2</sub> F and *hipA*<sub>2</sub> R). pFLAG-*hipA*<sub>3</sub>: P<sub>riboA</sub> (*riboA* to pMR10/pMR20 F and *riboA* to FLAG R), *hipA*<sub>3</sub> (*hipA*<sub>3</sub> F and *hipA*<sub>3</sub> R).

pFLAG-*hipA*<sub>1</sub><sup>D301Q</sup>, pFLAG-*hipA*<sub>2</sub><sup>D308Q</sup>, pFLAG-*hipA*<sub>3</sub><sup>D326Q</sup>. For these overexpression vectors, pFLAG-*hipA*<sub>1</sub>, pFLAG-*hipA*<sub>2</sub>, pFLAG-*hipA*<sub>3</sub> were amplified using mutagenic primers to introduce a substitution in the kinase active site. The amplified plasmid fragment was treated with KLD enzyme mix (NEB) before transformation into *E. coli* competent cells. PCR fragments were amplified using the following primer pairs: pFLAG-*hipA*<sub>1</sub><sup>D301Q</sup>: (*hipA*<sub>1</sub><sup>D301Q</sup> F and *hipA*<sub>1</sub><sup>D301Q</sup> R). pFLAG-*hipA*<sub>2</sub><sup>D308Q</sup>: (*hipA*<sub>2</sub><sup>D308Q</sup> F and *hipA*<sub>2</sub><sup>D308Q</sup> R). pFLAG-*hipA*<sub>3</sub><sup>D326Q</sup>: (*hipA*<sub>3</sub><sup>D326Q</sup> F and *hipA*<sub>3</sub><sup>D326Q</sup> R).

pFLAG-*hipB*<sub>1</sub>, pFLAG-*hipB*<sub>2</sub>, pFLAG-*hipB*<sub>3</sub>, pFLAG-*metG*, pFLAG-*lysS*, pFLAG-*trpS*, and pFLAG-*gltX*. For these over expression vectors, the coding region of *hipB*<sub>1</sub>, *hipB*<sub>2</sub>, *hipB*<sub>3</sub>, *metG*, *lysS*, *trpS*, and *gltX* were N-terminally fused to a 1xFLAG tag (amino acid sequence: DYKDDDDK) and placed under control of the *riboA* promoter on the high-copy plasmid pJS71. PCR fragments representing the *riboA* promoter and each coding region with N-terminal 1xFLAG tag fusion were inserted into BamHI/HindIII digested pMR20 using Gibson Assembly. PCR fragments for Gibson assembly were amplified using the following primer pairs: pFLAG-*hipB*<sub>1</sub>: P<sub>riboA</sub> (*riboA* to pJS71 F and *riboA* to FLAG R), *hipB*<sub>1</sub> (*hipB*<sub>1</sub> F and *hipB*<sub>1</sub> R). pFLAG-*hipB*<sub>2</sub>: P<sub>riboA</sub> (*riboA* to pJS71 F and *riboA* to FLAG R), *hipB*<sub>2</sub> (*hipB*<sub>2</sub> F and *hipB*<sub>2</sub> R). pFLAG-*hipB*<sub>3</sub>: P<sub>riboA</sub> (*riboA* to pJS71 F and *riboA* to FLAG R), *hipB*<sub>3</sub> (*hipB*<sub>3</sub> F and *hipB*<sub>3</sub> R). pFLAG-*metG*: P<sub>riboA</sub> (*riboA* to pJS71 and *riboA* to FLAG R), *metG* (*metG* F and *metG* R). pFLAG-*lysS*: P<sub>riboA</sub> (*riboA* to pJS71 and *riboA* to FLAG R), *lysS* (*lysS* F and *lysS* R). pFLAG-*trpS*: P<sub>riboA</sub> (*riboA* to pJS71 F and *riboA* to FLAG R), *trpS* (*trpS* F and *trpS* R). pFLAG-*gltX*: P<sub>riboA</sub> (*riboA* to pJS71 F and *riboA* to FLAG R), *gltX* (*gltX* F and *gltX* R).

*hipBA*<sub>1</sub>, *hipBA*<sub>2</sub>, *hipBA*<sub>3</sub>, *hipBA*<sub>1,2</sub>. For these complementation plasmids, the operon and upstream promoter regions were inserted into HindIII/EcoRI digested pMR20 using Gibson Assembly. PCR fragments for Gibson assembly were amplified using the following primer pairs: *hipBA*<sub>1</sub>: *hipBA*<sub>1</sub> (*hipBA*<sub>1</sub> F and *hipBA*<sub>1</sub> R). *hipBA*<sub>2</sub>: *hipBA*<sub>2</sub> (*hipBA*<sub>2</sub> F and *hipBA*<sub>2</sub> R). *hipBA*<sub>3</sub>: *hipBA*<sub>3</sub> (*hipBA*<sub>3</sub> F and *hipBA*<sub>3</sub> R). *hipBA*<sub>1,2</sub>: *hipBA*<sub>1</sub> (*hipBA*<sub>1</sub> F and *hipBA*<sub>1</sub> to *hipBA*<sub>2</sub> R) *hipBA*<sub>2</sub> (*hipBA*<sub>2</sub> to *hipBA*<sub>1</sub> F and *hipBA*<sub>2</sub> R).

**Growth assays.** For growth curves and end-point growth assays, cells grown to OD<sub>660</sub> 0.2-0.5 in PYE were released into PYE at OD<sub>660</sub> 0.02 and allowed to incubate with shaking at 30°C. Proteins were ectopically expressed from the RiboA promoter by supplementing liquid PYE medium with 1 mM isopropyl thiogalactoside (IPTG) and 1 mM theophylline<sup>53</sup>. At each indicated time or at the end-point, a sample was withdrawn for OD<sub>660</sub> measurement and enumeration of colony forming units (CFU)/ml on solid PYE medium. Unless otherwise specified, mean and standard deviation of three independent biological replicates are reported.

**RNA extraction and reverse transcription.** RNA was extracted using Direct-zol RNA Miniprep Kits from Zymo Research. Purified RNA was reverse transcribed for qPCR using ProtoScript II First-Strand cDNA Transcription kit (NEB) with random hexamers to prime the reaction.

**RT-PCR.** RT-PCR was performed on an Applied Biosciences Step One Plus using Luna SYBR Master Mix from NEB. The thermocycling conditions are as follows: initial heating at 95°C for 20s, followed by 40 cycles of 95°C for 3 s, 60°C for 30s. *rho* was used as an endogenous control for all experiments. Relative transcript levels were calculated using the double delta CT method<sup>54</sup>. Primers used for RT-PCR are listed in Table 1-3.

**Gel detection of phosphoproteins.** Samples for phosphoprotein detection were harvested after inducing protein expression for 1.5 or 3 hours from a starting OD<sub>660</sub> 0.02 in PYE medium. Cells were washed with PBS containing 1% (v/v) phosphatase inhibitor cocktail (Sigma P5726). Proteins were precipitated using 20% (v/v) trichloroacetic acid overnight at -20°C. The precipitate was harvested by centrifugation and washed twice with 1 ml ice-cold acetone. The sample was then resuspended in 60 µL Tris-HCl pH 8.0 containing 1 mM MnCl<sub>2</sub> and Laemmli sample buffer (Bio-Rad 1610737). The samples were heated at 95°C for 5 min, then allowed to cool to room temperature before protein concentration was quantified using Bradford reagent (Bio-Rad). Samples were normalized by protein concentration, and 10-20 µL were loaded into a 10-well 8% bis-acrylamide gels (Bio-Rad 1610158) containing 5, 10 or 20 µM Phos Binding Reagent (APEX-BIO F4002) to test/optimize separation of phosphorylated and non-phosphorylated species by SDS-PAGE electrophoresis. After electrophoresis, the gels were soaked in Western transfer buffer (25mM Tris Base (Gold Bio T-400), 192mM glycine and 10% methanol) containing 10 mM EDTA (10 minutes, 3 times) with agitation before a final soak in Western transfer buffer without EDTA. Protein transfer to PVDF membranes was performed overnight using the wet tank method in Western transfer buffer with 1% SDS on ice. Western blotting was done using anti-FLAG antibodies (1:5000) (Millipore-Sigma F3165) and horseradish peroxidase (HRP)-conjugated anti-mouse antibodies (1:5000) (Millipore-Sigma A8592). Western blots were visualized by using Western Lightning (Perkin Elmer) on a Bio-Rad Gel Doc XR.

**Antibiotic persistence assays.** Antibiotic persistence was measured using a protocol adapted from the MDK method. Overnight exponential-phase cultures were subcultured into fresh PYE medium at an OD<sub>660</sub> of 0.02. Cultures were harvested by centrifugation

after 6 hours ( $OD_{660}$  0.2-0.4) for exponential phase persister assays and after 24 hours ( $OD_{660}$  ~1.0) for stationary phase persister assays. Harvested cells were resuspended in fresh PYE medium for exponential phase persister assays or in spent medium (normalized by  $OD_{660}$ ) for stationary phase persister assays before aliquoting 1 mL/well into a 96 deep-well block. Antibiotic (streptomycin 25-150  $\mu\text{g/mL}$ , kanamycin 25-150  $\mu\text{g/mL}$ , or vancomycin 50-200  $\mu\text{g/mL}$ ) was added at a range of concentrations known to be saturating (10-500x MIC) in order to produce concentration-independent killing. The block was incubated with shaking during the experiment. At the indicated time points, a sample was withdrawn and a ten-fold dilution series was performed in a 96-well plate using fresh PYE medium. These plates were allowed to regrow with incubation and shaking for 7 days. Regrowth in a well indicates that at least 1 surviving cell was present at the inoculation of that well. Survival was measured relative to the time zero CFU dilution plate. Survival was plotted against time to produce a biphasic killing curves indicative of persistence. Reported data points are the mean and standard deviation of two biological replicates, each with six technical replicates. The persister frequency was estimated using the y-intercept of the curve describing the persister fraction.

**Assays of protein, RNA, and DNA synthesis.** Overnight cultures were grown in PYE medium at 30°C. Cells were subcultured in M2G minimal medium to an optical density ( $OD_{660}$ ) of 0.02. M2G cultures grown to an optical density of ~0.2 before diluting back to an optical density of 0.02 in M2G supplemented with 1 mM theophylline and 1 mM IPTG to induce expression of HipA toxins. At the indicated time points, 0.9 ml aliquots were withdrawn and added to 10 Ci of [ $^{35}\text{S}$ ]methionine (protein synthesis), 4 Ci [methyl- $^3\text{H}$ ]thymidine (DNA synthesis), or 0.2 Ci [2- $^{14}\text{C}$ ]uracil (RNA synthesis). After 2 min of incorporation, samples were chased for 10 min with 0.5 mg of cold methionine, 0.5 mg cold thymidine, or 0.5 mg cold uracil, respectively. Cells were harvested by centrifugation, resuspended in 200  $\mu\text{l}$  cold 20% trichloroacetic acid (TCA), and further centrifuged at 15,000  $\times g$  for 30 min at 4°C. The samples were washed twice with 1 ml of cold 96% ethanol. Precipitates were transferred to vials, and the amount of incorporated radioactivity was counted in a liquid scintillation counter averaging counts per minute over 15 minutes using the appropriate energy setting for  $^{35}\text{S}$  or  $^3\text{H}$  isotope counting. Samples were counted twice to verify counting accuracy.

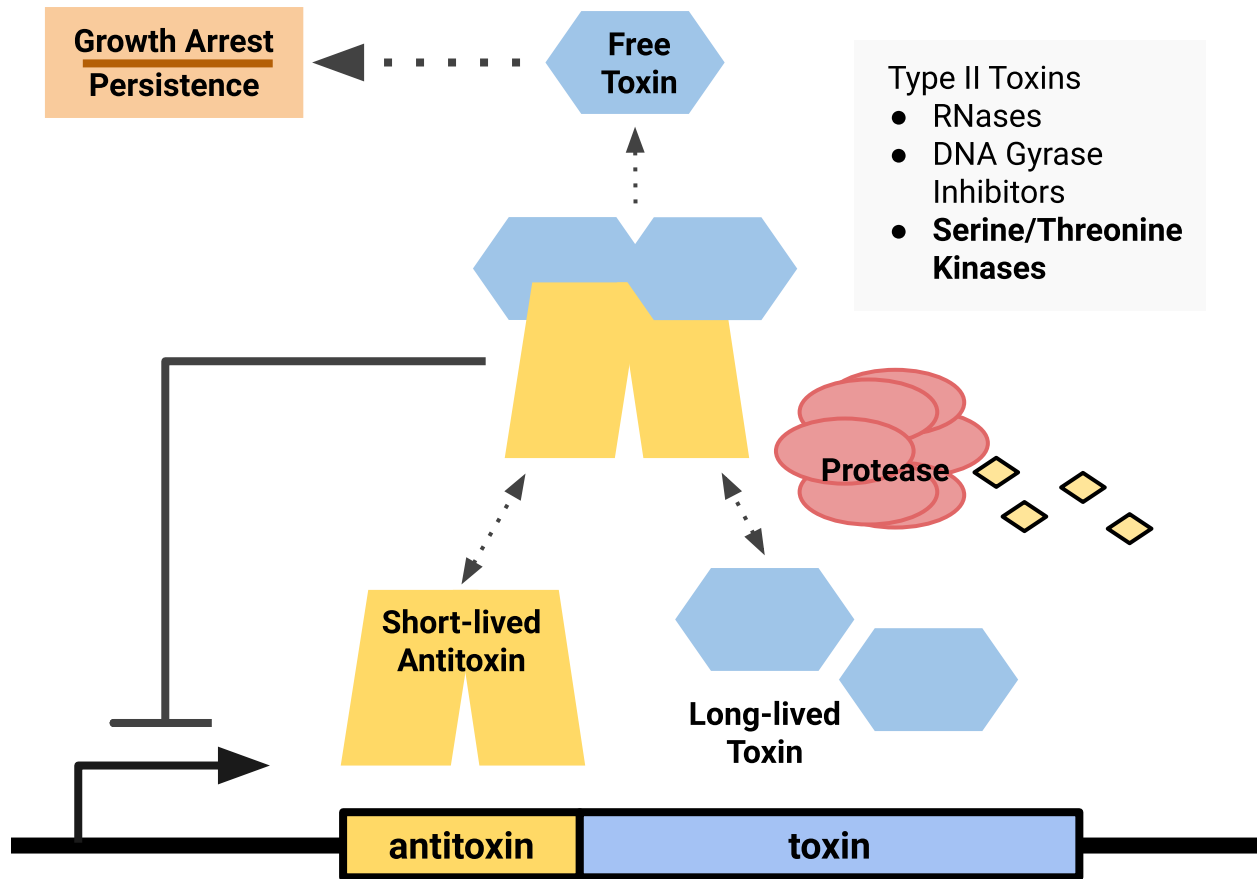


**Figure 1-1. A Type II Toxin-Antitoxin System**

Type II Toxin-Antitoxin Systems are typically encoded in operons with the antitoxin gene preceding the toxin gene. The operon is subject to autorepression by the antitoxin alone or by a complex of the antitoxin and toxin. When free and active, toxins can affect a variety of cellular processes to inhibit growth or cause cell death.

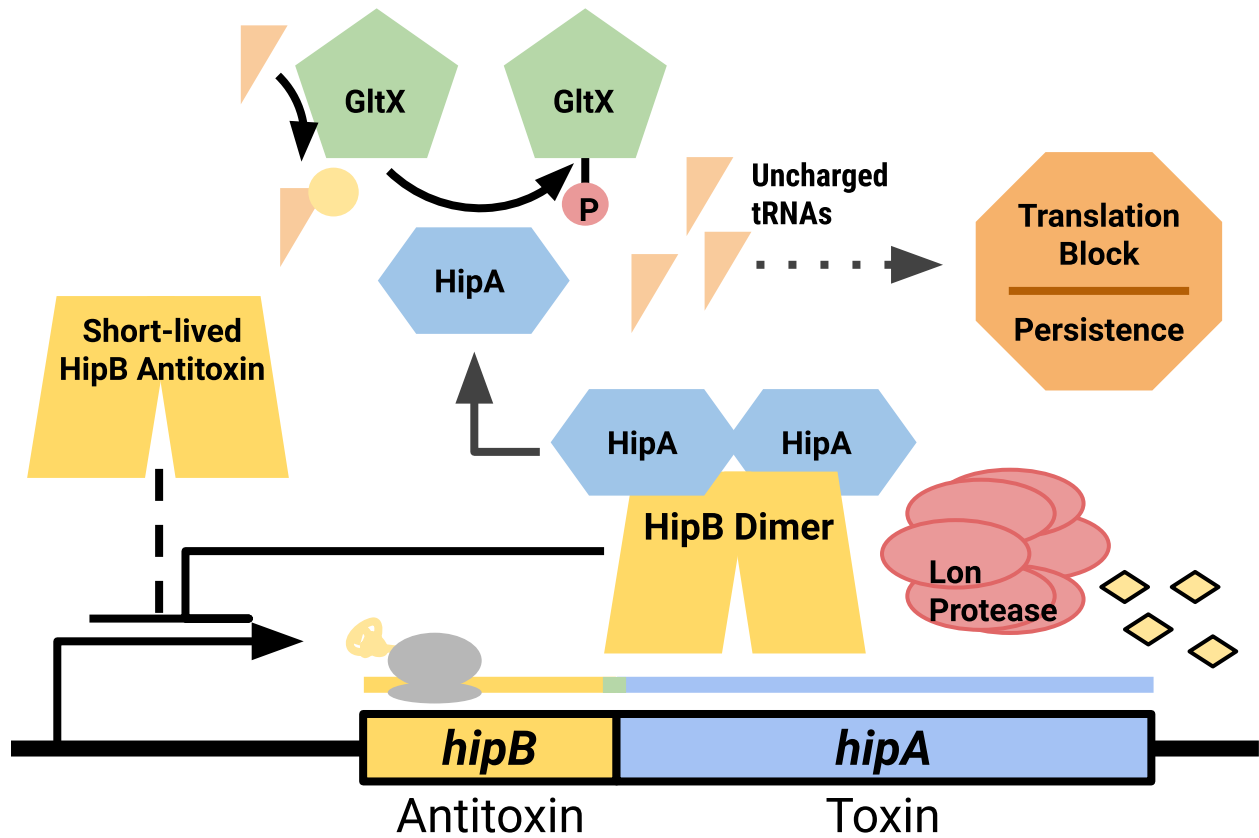


**Figure 1-2. The *E. coli* hipBA module**

When free of inhibition, the *E. coli* HipA toxin phosphorylates the tRNA synthetase GltX. When phosphorylated, GltX no longer charges tRNA, resulting in the cessation of protein synthesis and increasing the likelihood of persister cell formation.

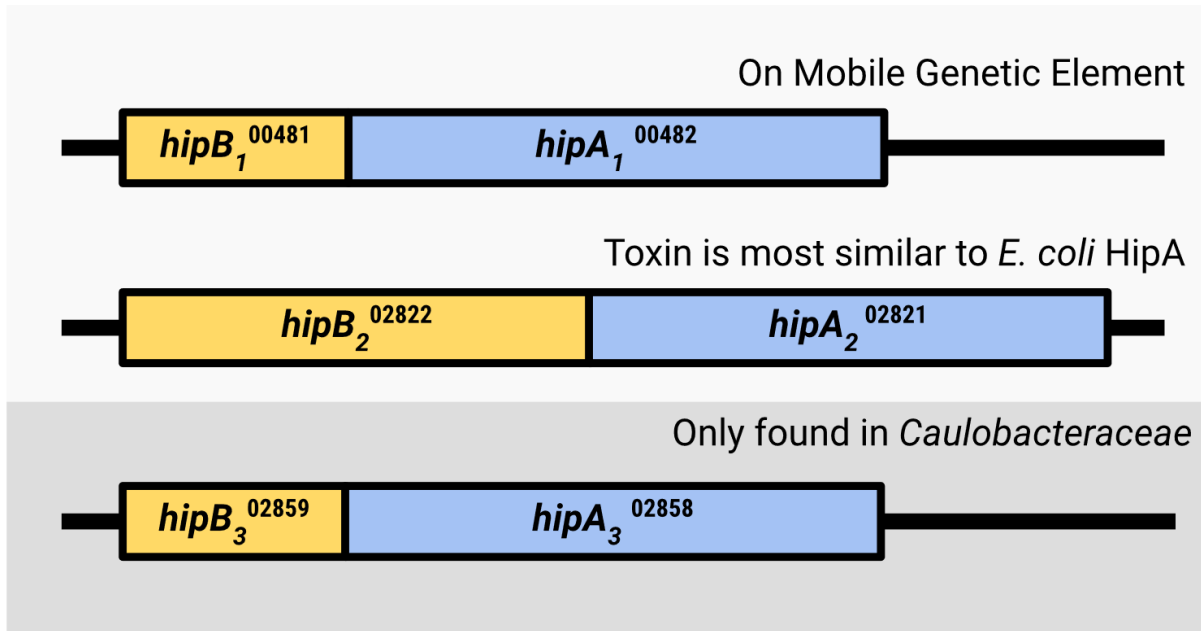


**Figure 1-3. The three *hipBA* modules in *C. crescentus* NA1000**  
 Each module is named in the order of ascending locus tag.

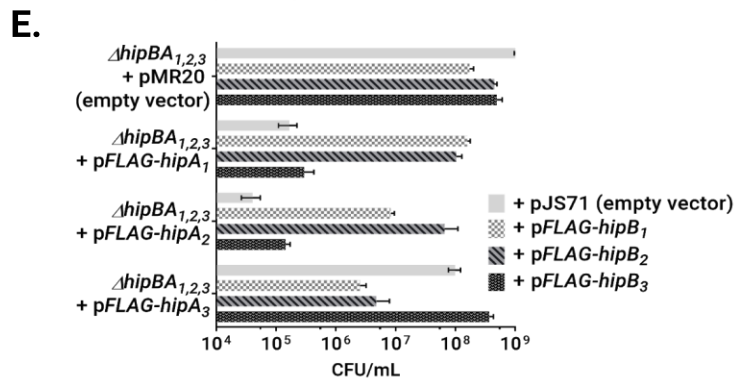
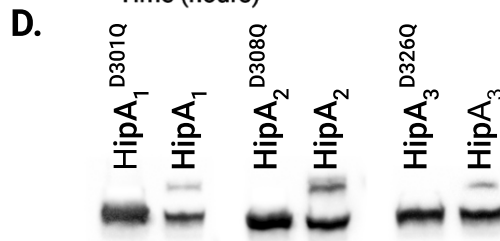
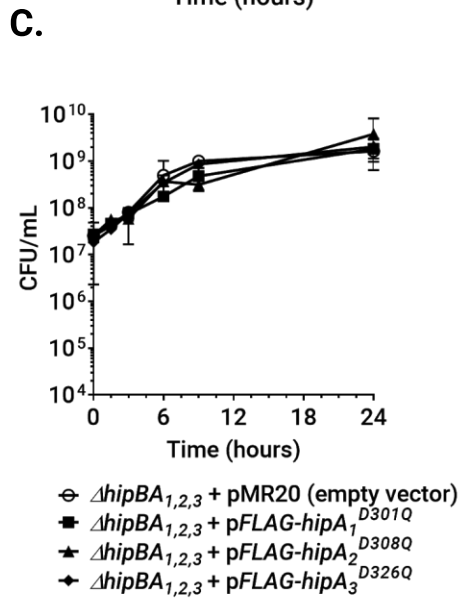
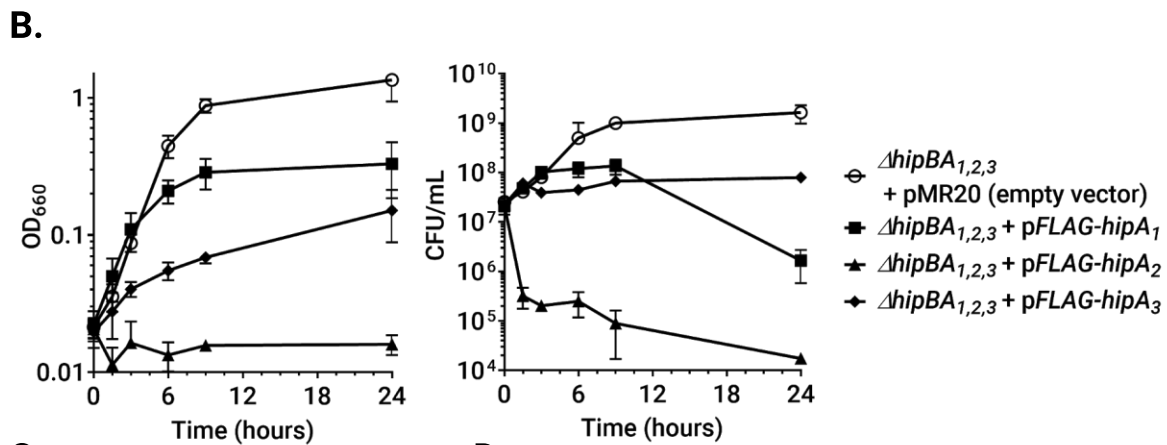
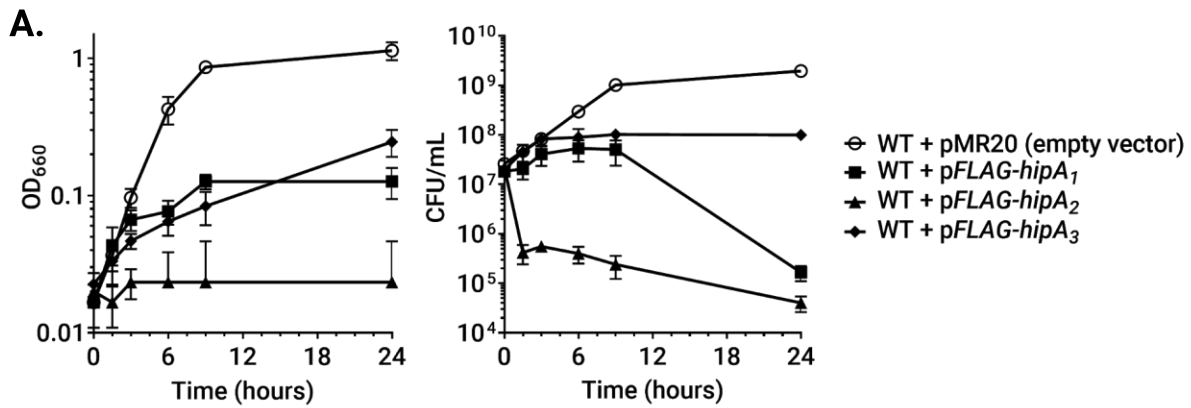




**Figure 1-4. All NA1000 HipA toxins inhibit growth**

Growth curves of NA1000 (A) or  $\Delta hipBA_{1,2,3}$  (B) cells expressing the indicated HipA toxins (C) or kinase-null alleles in exponential phase. HipA proteins were induced at time 0 by the addition of 1 mM IPTG and 1 mM theophylline. (D.) The indicated HipA toxins were expressed in  $\Delta hipBA_{1,2,3}$  cells in exponential phase for 1.5 hours beginning at  $OD_{660} = 0.02$ . Whole-cell lysates were prepared and normalized as described in Methods before Phos-tag mobility shift analysis and Western blotting with anti-FLAG antibodies. (E.) The indicated HipA toxins were expressed from low-copy plasmids, while the indicated HipB antitoxins were expressed from high-copy plasmids, all under control of the RiboA promoter. Exponential phase cultures in PYE medium were subcultured to  $OD_{660} = 0.02$  and supplemented with 1mM IPTG and 1mM theophylline to induce protein expression. After 18 hours, samples were collected for CFU enumeration. Values reported are the mean and standard deviation from three independent biological replicates.

```

E. coli ---MPKLVTWMN--NQRVGEL-TKLANGAHTFKYAPEWLASRYARPLSLSLPLQRGNITS 54
HipA1 MAMTRVLTWV--WGDGVVGS-ALDETGDIRFAYDAAWLADEACPAVSVSLPKQPGAFSR 57
HipA2 MSGPAGLIVRMDGFNLPAGYL-ASDEARAI SFAYDDRYIAAG-GPPLSL SMPLEQVSFGD 58
HipA3 MTTVAEVRW---GS-RIGAVSLEDGAETAVFAYEPSFIASGI-QPAPLMMPLKAGVFSF 55

E. coli D--AVFNFF-----DNLLPDSPI--VRDRIVKRY--HAKSRQPFLLSEIGRDSVGAVT 102
HipA1 R--KTRSF-----AGLLPDDL---QRDNVARAL--GVSQRNDFGLLERLGGDVAGALT 104
HipA2 V--TARAFF-----DNLLPEND---QMQRVMDRE--GLARDDIVGLLSHLGADCSGAI 105
HipA3 PDLPPRSFHGLPGMLADALPKYGHVLIDAWLATQGRSPESFNAVERLCYTGRRGMALE 115

E. coli LIPEDETVTHPI----MA-----WEKLTARLEEVLTAYKADIPLGMIREENDFRISVA 152
HipA1 LWPEGEAPPKRQGGRTA-----PLNDKRLLA ILDELPR---RPFLAGEDGVRLSLA 153
HipA2 CLPIGADPIKVPGLSED-----YELLAPGAI AEIARSLAE---RQRLPDTITDPSPVA 156
HipA3 FSPMAGPRRRVSSKIDIDALVTLASEVLTHR--DLRASADADKADALRDILSVGTSAG 173

E. coli GAQEK TALLRIGNDW--CIPK----GITPTTHIIKLPIGEIRQPNATLDLSQSVDNEYC 206
HipA1 GAQEKLPVVLDGAV--ALPA----LGQPSTHILK PANARWPA-----MTENEALA 198
HipA2 GVQRKIALHTHPQGF AKPRPG---RQVPTTHILKVPETRLR-----DARLEAAA 203
HipA3 GARAKAVIAWNPATN-EVRSQVEAGAGFGYWLLKFDGVS GNRDKELADPKGYGAVEHAY 232

E. coli LLLAKELGLNVPDAEIIKAGNVRAL AVERFDRRWNAERTVLLR LPOEDMCQT----FGLP 262
HipA1 MRLAAAVGLPTAGVEPRRIGERTFLLVTRYDRVSSD-GAVRRLHQEDFCQA----LGVS 253
HipA2 ARLASALGLDVS IPEAIVIDGVDALLITRFDRVV-RD-GVVYRLHQEDFAQA----MGLP 257
HipA3 GQMAAAAGIDVAESRLL EGGRRHFMSKRFDRLDGGGK-----LHMQSLAAIAHLDFNDP 287

E. coli SSVKYESDGGPGIARIMA---FLMGSSEALKDRYDFMKFQVQWLIGATDGHAKNFVSF 318
HipA1 PEHKYAAEGGPIFPDCF-NLVRNVCQPS--APAVLALLDAAIFNVIVGNADAHGKNYSLL 310
HipA2 ATLKYQRNGAPGRQFDAQIARVLDQTEAPALSRTAFLSATIFNLLIGNTDNHAKNHGLL 317
HipA3 VANSYEQA-----LFTMR-----RMGLS--MAQLEEQFRMVFNVLARNQDDHVKNIAFL 335

E. coli IQAGGSYRLTPFYDIISAFPVLGGTGIHISDLK LAMGLNASKGKKAIDK IYPRHFLATA 378
HipA1 HQAG-AIVMAPLYDL MCTAAYPEVH-----AKLAMKIAGR---AQLEAFKADTWRDFG 359
HipA2 YRQGRAPILAPLYDL LPSRMNLDNF-----DQLSFNIGAA---DHPDAITFDDMAFF 367
HipA3 MDRAGRWR LSPAFDITWSYNPDGEW---T--SRHQMSINGKR-----DGFDFADLEACA 384

E. coli KVLRFPEVQMHEILSDFA---RMIPAALDNVKTSLPTDFPENVT----AVESNVLRLHG 431
HipA1 RDIG-----MGPAFVER-RANAQARRVLDQVGPVADAI--AACGFDR 398
HipA2 EVFG-----MRRAAA-----ARFIENVIKPMIEALERATLGLAG 401
HipA3 KTASISRGHVGRIFDEVREAVMRWPTFADAA--GV-DERWRDQIG-----ATVRLEL 433

E. coli R-----LSREYGSK----- 440
HipA1 EALRGLRDLIAERARAVLK---LGQGER----- 423
HipA2 ERLKDDMLIGRETEQLVEVLGLDVAVRERDYYPKVRHALAPS 444
HipA3 RR----- 435

```

**Figure 1-5. Protein alignment of *E. coli* HipA and NA1000 HipA toxins**

Alignment was obtained using ClustalOmega. Functionally critical residues are indicated: \*, catalytic aspartate residue targeted for mutation; ^, Mg<sup>++</sup> binding residues; #, ATP-binding residues; !, autophosphorylated serine residue (Correia et al., 2006).

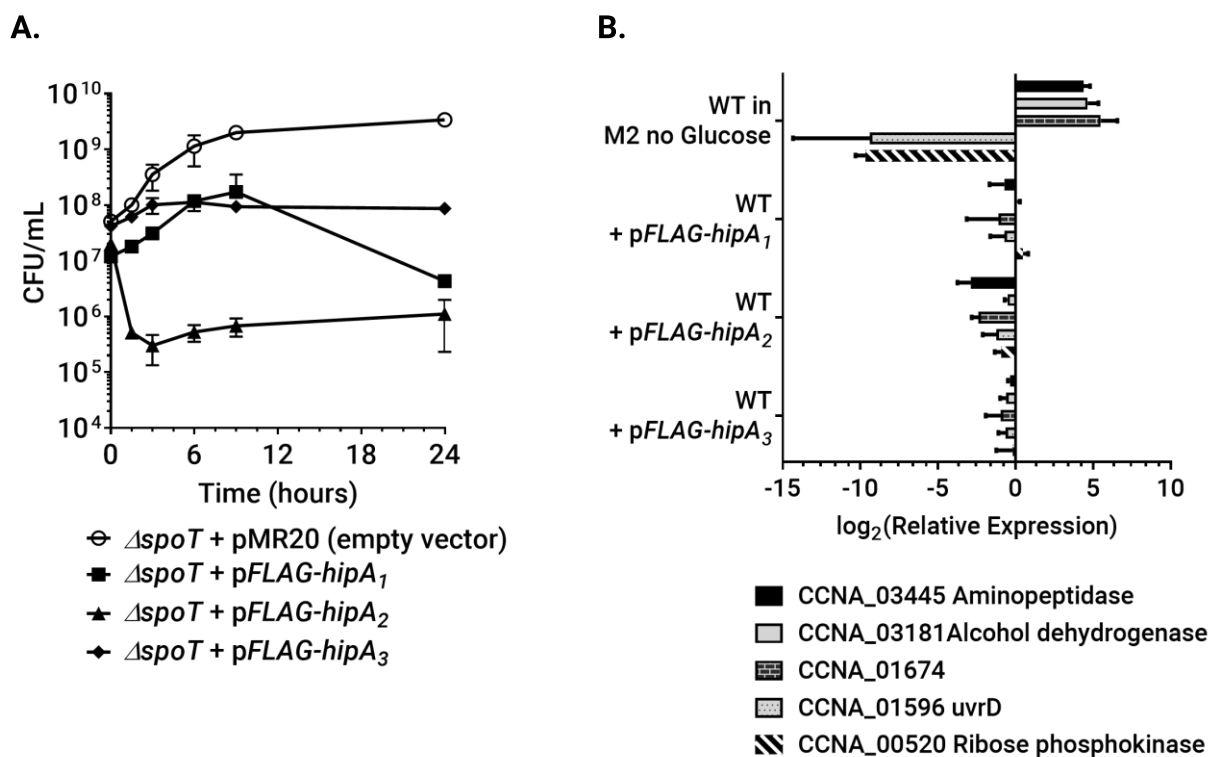
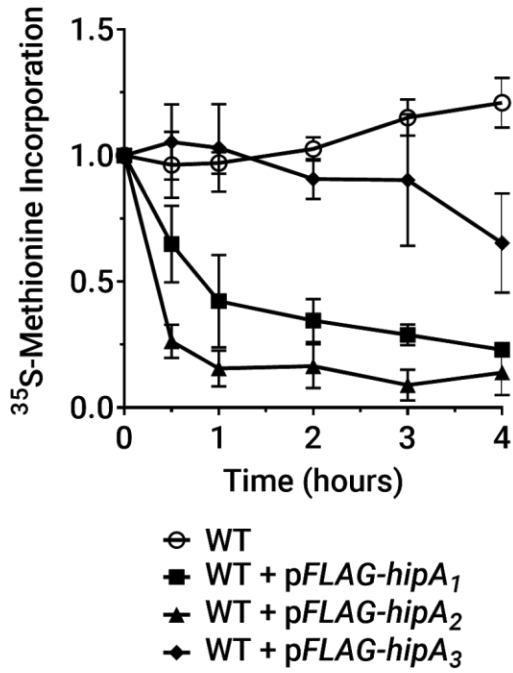


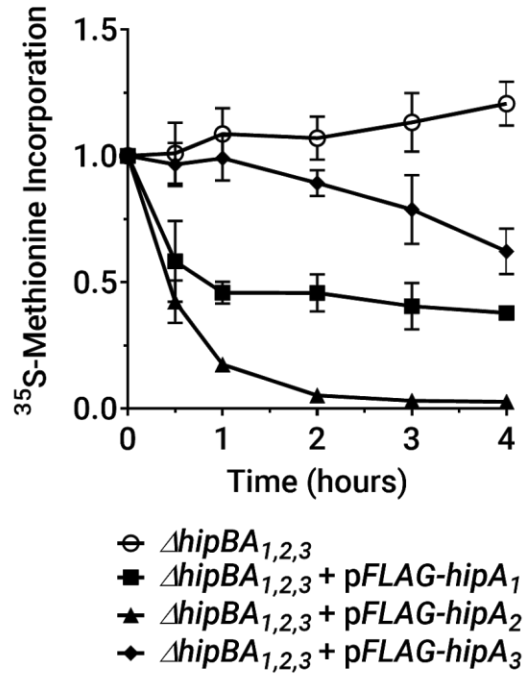
**Figure 1-6 The stringent response is neither required for HipA-mediated growth inhibition, nor does any HipA activate the stringent response when ectopically expressed in exponential phase cultures.**

(A) Growth curves of the  $\Delta spoT$  strain ectopically expressing each indicated HipA toxin performed as in Fig. 1-1A. (B) The indicated strains in exponential phase grown in M2G medium were subcultured to an  $OD_{660} = 0.02$  in M2G supplemented with 1mM IPTG and 1mM theophylline to express HipA toxins. As a positive control the wild-type strain (NA1000) was subcultured in M2 medium lacking the carbon source to induce the stringent response. RNA was harvested after 3 hours of HipA expression or carbon starvation, and the indicated genes were subjected to RT-PCR analysis as described in Methods. *rho* was used as an endogenous calibrator gene. Relative expression to an unstarved M2G control was determined using the double delta Ct analysis. Values reported are the mean and standard deviation of three biological replicates, each used in two technical replicates.

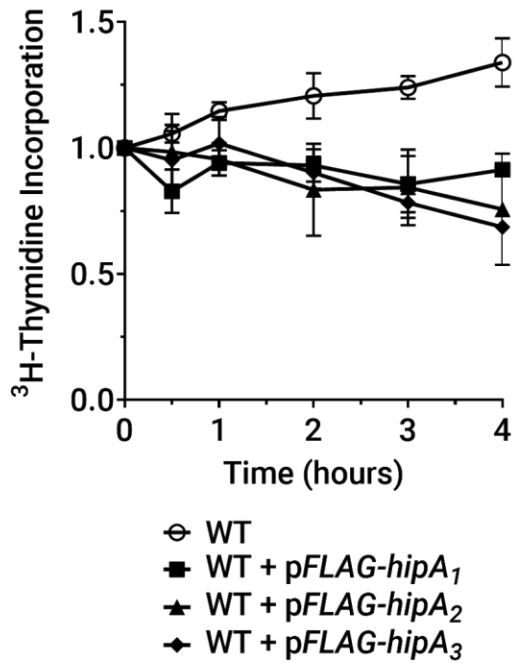
A.



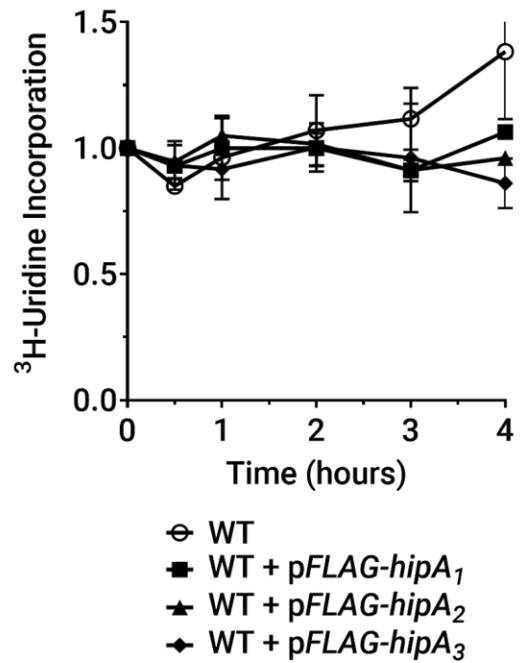
B.



C.

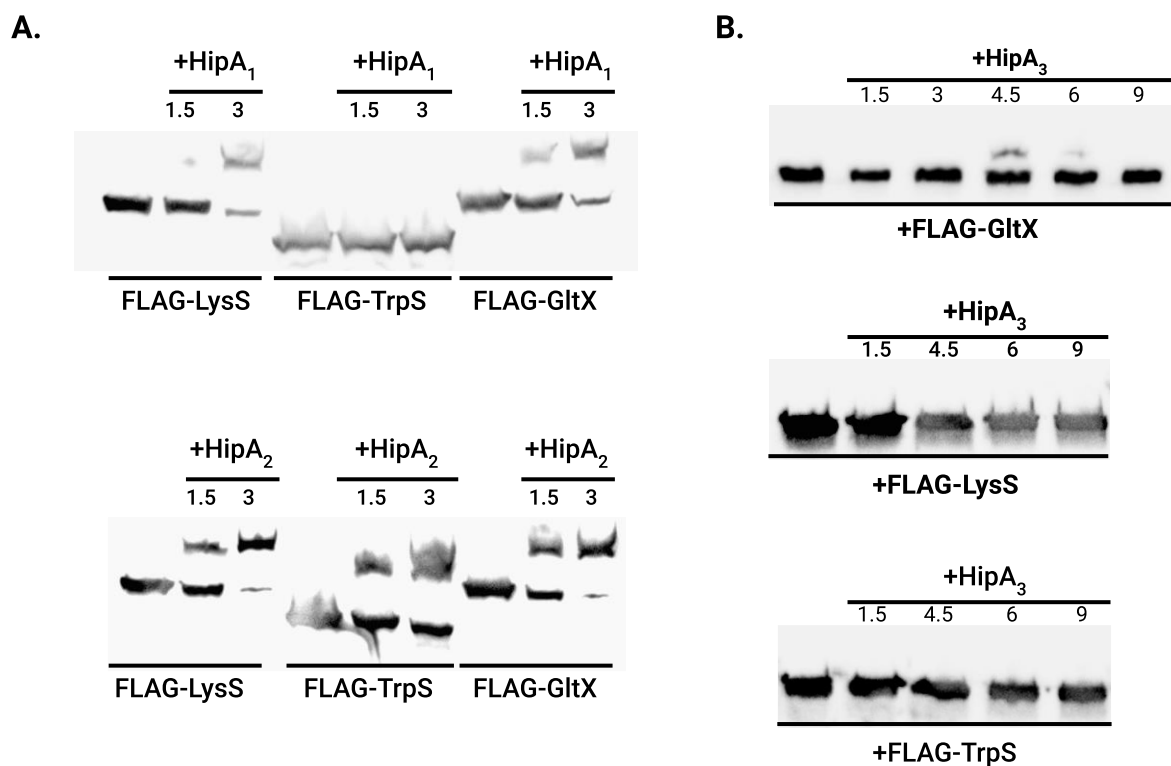


D.



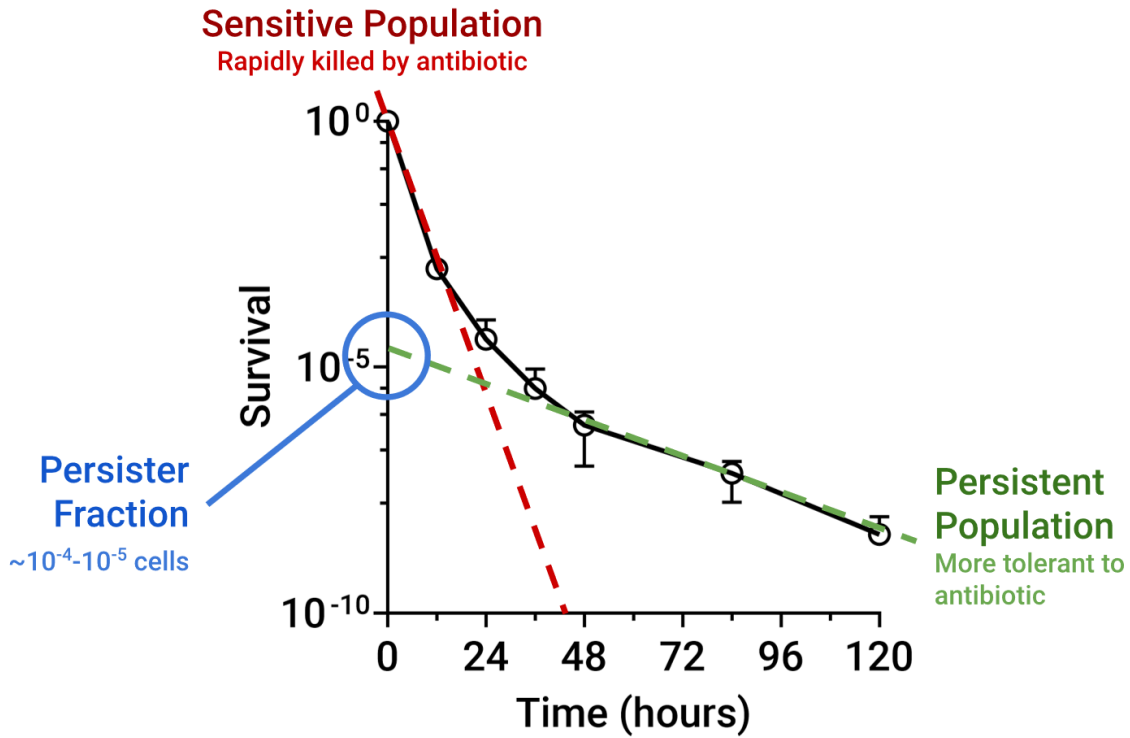
**Figure 1-7. Ectopic expression of HipA toxins affects protein synthesis, but does not alter the synthesis of DNA or RNA.**

Assays were conducted in M2G medium to monitor the incorporation of radiolabeled monomers into protein, DNA or RNA. Rates of incorporation are expressed relative to the incorporation of the culture at time zero, before toxin induction. Values reported are the mean and standard deviation of three biological replicates. (A), (B) Relative <sup>35</sup>S-methionine incorporation when HipA proteins are ectopically expressed in wild-type or *ΔhipBA<sub>1,2,3</sub>* strain backgrounds. (C) Relative <sup>3</sup>H-thymidine incorporation when HipA is ectopically expressed in NA1000. (D) Relative <sup>3</sup>H-uridine incorporation when HipA is ectopically expressed in NA1000.



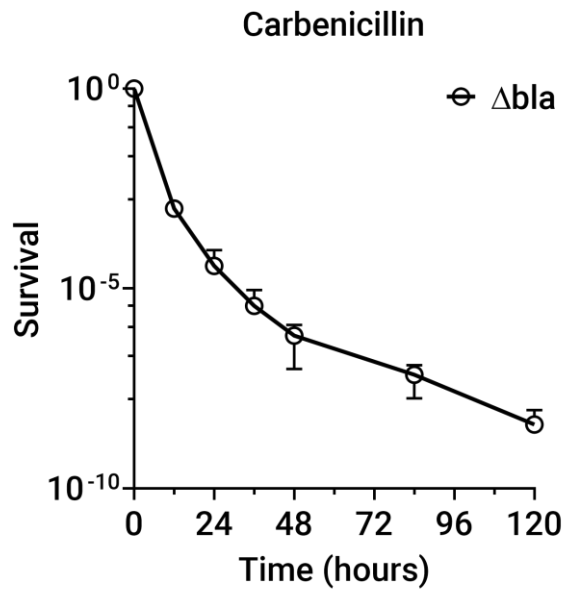
**Figure 1-8. NA1000 HipAs phosphorylate distinct aminoacyl-tRNA synthetases.**

Each strain expressed the indicated HipA toxin from a low-copy plasmid and the indicated aminoacyl-tRNA synthetase from a high-copy plasmid, all under control of the RiboA promoter. Exponential phase PYE cultures were subcultured to OD<sub>660</sub> = 0.02 and supplemented with 1 mM IPTG and 1 mM theophylline to induce protein expression. Samples coexpressing HipA toxins and tRNA synthetases were collected at the indicated times (hours) and processed as described in Methods for Phos-tag mobility shift analysis and Western blotting with anti-FLAG antibodies. Samples of cultures only expressing tRNA synthetases were collected after 3 hours of induced protein expression. (A) HipA<sub>1</sub> and HipA<sub>2</sub> (B) HipA<sub>3</sub>.



**Figure 1-9. Biphasic killing kinetics**

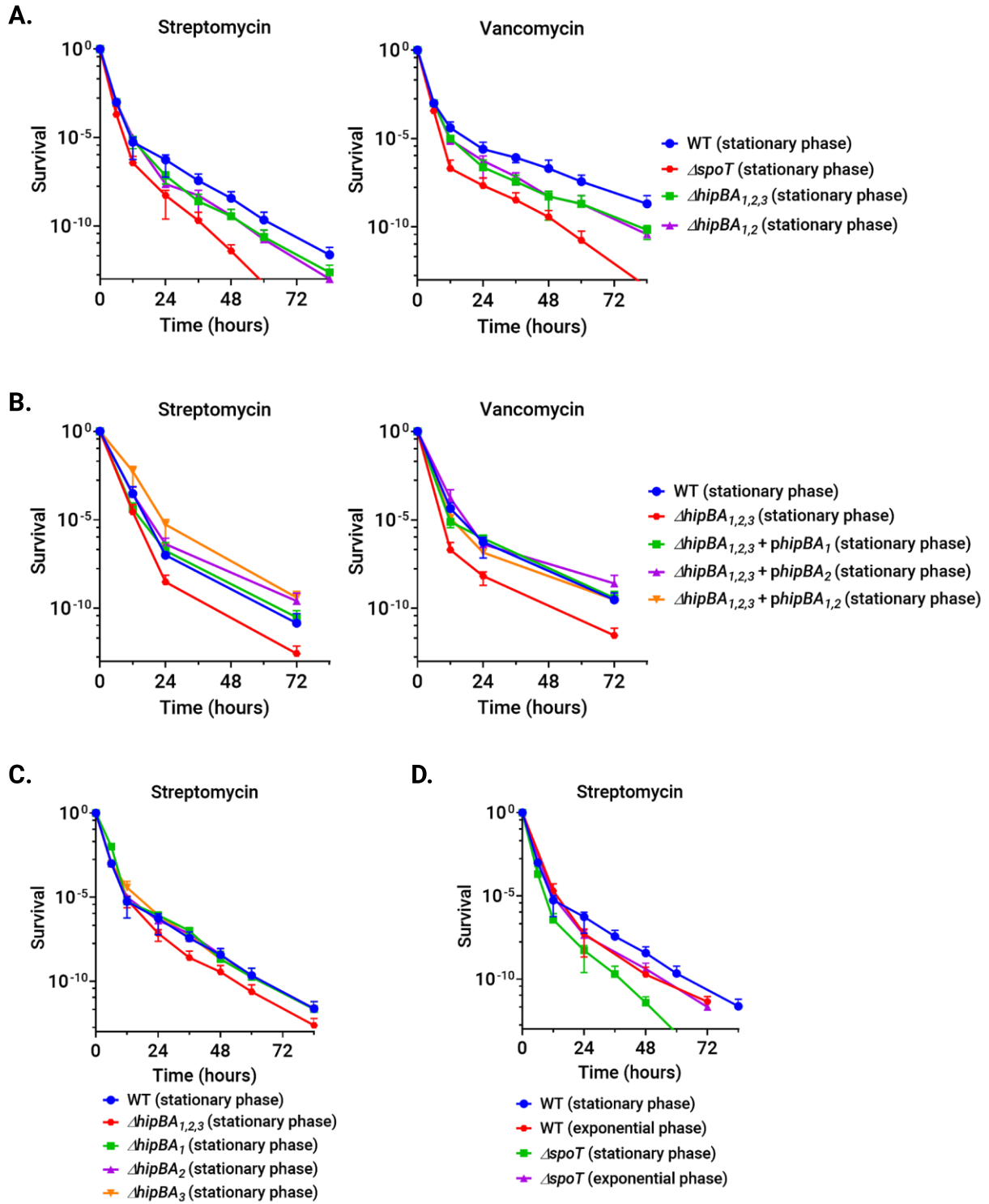
When a population containing persister cells is treated with a lethal concentration of a bactericidal antibiotic, biphasic killing is observed. The larger, normally growing, sensitive population is killed quickly (red) while the persistent population is killed much more slowly (green).



**Figure 1-10. A  $\Delta bla$  strain has persistence toward the beta-lactam antibiotic carbenicillin.**

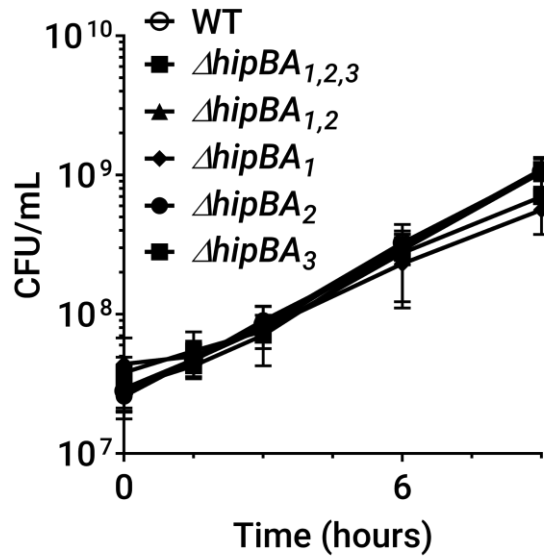
NA1000 has a natural resistance to beta-lactam antibiotics due to the presence of a beta-lactamase, *bla*, on the chromosome. Survival of a  $\Delta bla$  strain that lacks beta-lactamase when grown to stationary phase in PYE media and treated with carbenicillin.





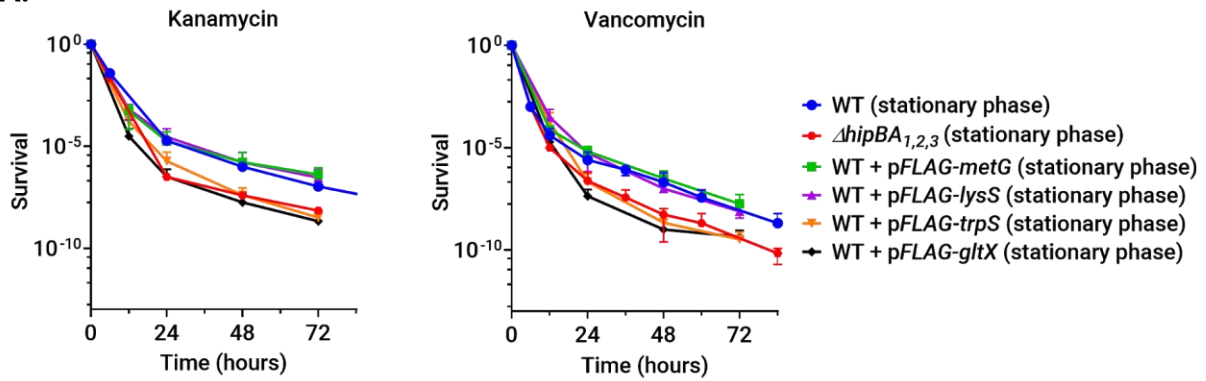
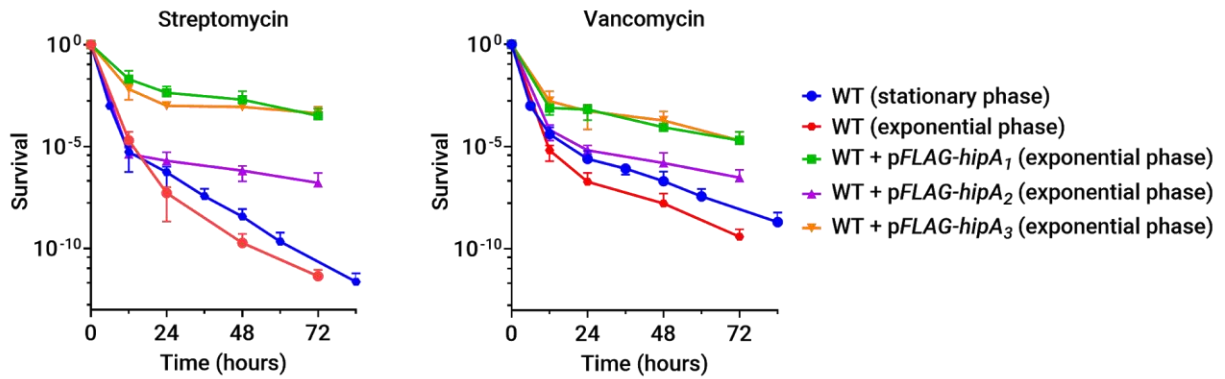
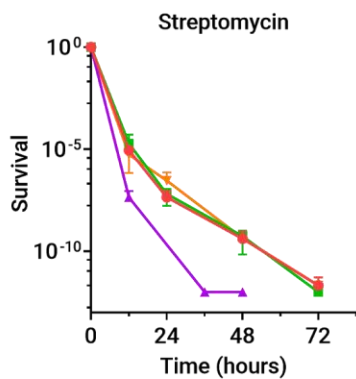
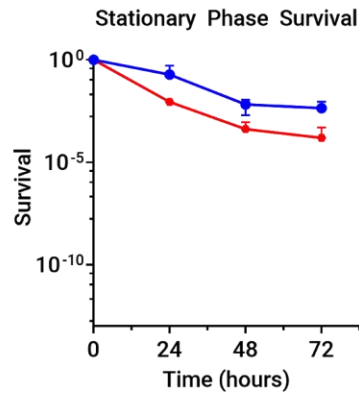
**Figure 1-11. HipBA<sub>1</sub>, HipBA<sub>2</sub>, and SpoT contribute to persister cell formation in stationary phase *C. crescentus* cultures.**

(A) Survival of  $\Delta hipBA_{1,2,3}$ ,  $\Delta hipBA_{1,2}$ , and  $\Delta spoT$  strains grown to stationary phase in PYE medium and treated with streptomycin or vancomycin. (B) Survival of a  $\Delta hipBA_{1,2,3}$  strain with plasmids bearing the wild type *hipBA*<sub>1</sub> and/or *hipBA*<sub>2</sub> operons grown and tested at the same conditions described in 5A. (C) Survival of single *hipBA* module operon knockouts grown to stationary phase and treated with streptomycin. (A), (D) Comparison of the survival of exponential and stationary phase cultures of NA1000 and  $\Delta spoT$  strains treated with streptomycin.



**Figure 1-12. NA1000  $\Delta hipBA$  strains do not have obvious growth defects.**

Growth curves of the constructed *hipBA* module knockout strains in PYE medium. Exponential phase cultures were diluted to  $OD_{660}=0.02$  for the experiment. At the indicated time points, samples were withdrawn for CFU enumeration. Reported data are the mean and standard deviation of three independent biological replicates.

**A.****B.****C.****D.**

- $\Delta spoT$  (exponential phase)
- $\Delta spoT$  + pFLAG-*hipA*<sub>1</sub> (exponential phase)
- $\Delta spoT$  + pFLAG-*hipA*<sub>2</sub> (exponential phase)
- $\Delta spoT$  + pFLAG-*hipA*<sub>3</sub> (exponential phase)

**Figure 1-13. The persister fraction can be modulated by expressing HipA toxins or certain tRNA synthetase targets.**

(A) Survival of WT strains expressing tRNA synthetases grown to stationary phase in PYE media and treated with kanamycin and vancomycin. (B) WT strains expressing HipA toxins for three hours in exponential phase cultures before treatment with streptomycin and vancomycin. (C)  $\Delta spoT$  strain expressing HipA toxins under the conditions described in 6B and treated with streptomycin. (D)  $\Delta spoT$  strain has impaired long-term survival in stationary phase.

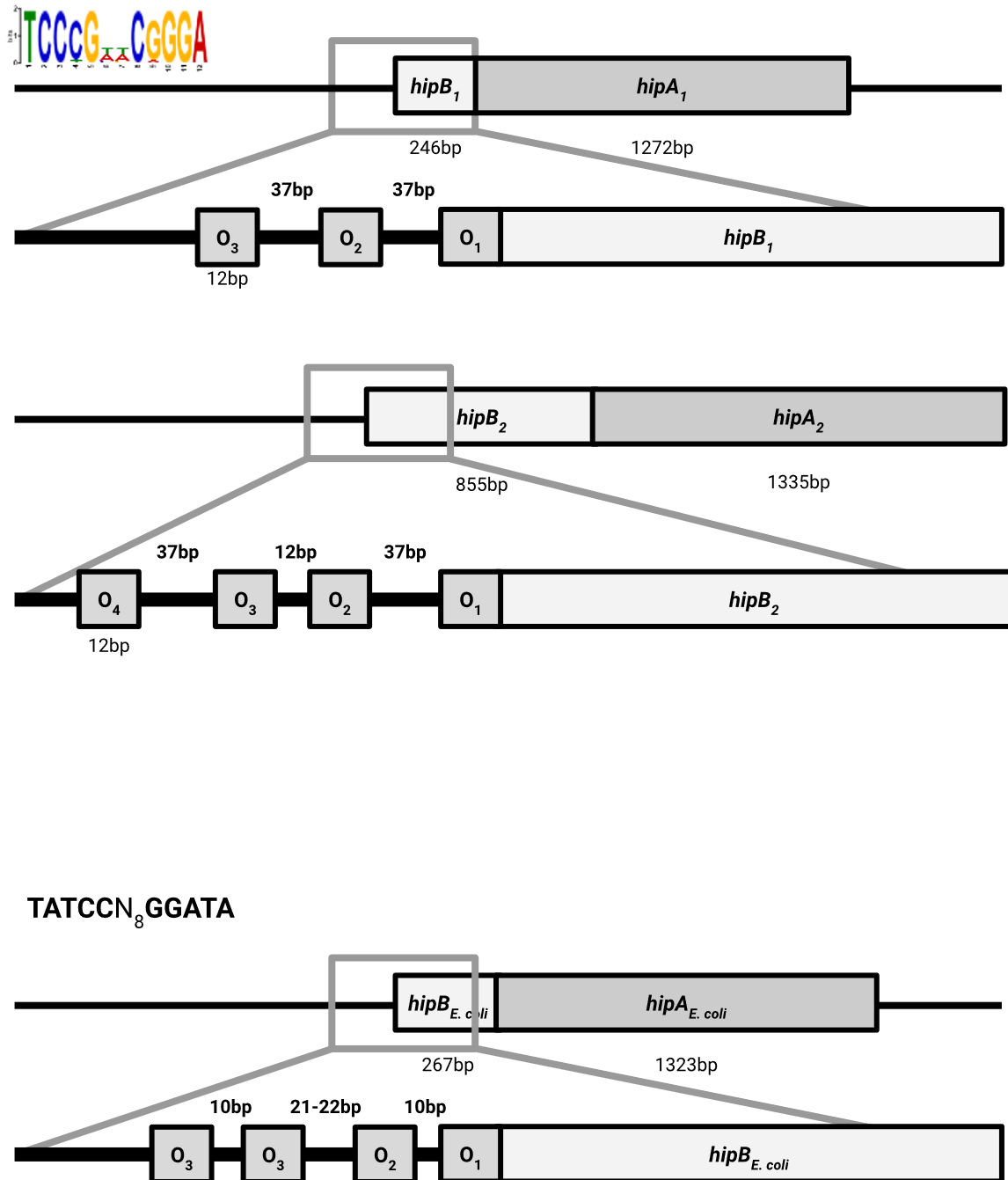


**Figure 1-14. Identical putative binding motifs are observed in the promoter regions upstream of *hipBA*<sub>1</sub> and *hipBA*<sub>2</sub>.**

Repetitive inverted repeats were identified using the EMBOSS bioinformatics suite. *E. coli* promoter region and operator sites is shown for reference<sup>24,45</sup>.

**Table 1. Strains**

<b>Name</b>	<b>Description</b>	<b>Reference</b>
WT	Wild-type <i>Caulobacter</i> NA1000	54
WT + pJS71	NA1000 pJS71	This study
WT + pMR20	NA1000 pMR20	This study
WT + pFLAG-hipA <sub>1</sub>	NA1000 pFLAG-hipA <sub>1</sub>	This study
WT + pFLAG-hipA <sub>2</sub>	NA1000 pFLAG-hipA <sub>2</sub>	This study
WT + pFLAG-hipA <sub>3</sub>	NA1000 pFLAG-hipA <sub>3</sub>	This study
$\Delta$ hipBA <sub>1</sub>	$\Delta$ hipBA <sub>1</sub>	This study
$\Delta$ hipBA <sub>2</sub>	$\Delta$ hipBA <sub>2</sub>	This study
$\Delta$ hipBA <sub>3</sub>	$\Delta$ hipBA <sub>3</sub>	This study
$\Delta$ hipBA <sub>1,2</sub>	$\Delta$ hipBA <sub>1</sub> $\Delta$ hipBA <sub>2</sub>	This study
$\Delta$ hipBA <sub>1,2,3</sub>	$\Delta$ hipBA <sub>1</sub> $\Delta$ hipBA <sub>2</sub> $\Delta$ hipBA <sub>3</sub>	This study
$\Delta$ hipBA <sub>1,2,3</sub> + pJS71	$\Delta$ hipBA <sub>1,2,3</sub> pJS71	This study
$\Delta$ hipBA <sub>1,2,3</sub> + pMR20	$\Delta$ hipBA <sub>1,2,3</sub> pMR20	This study
$\Delta$ hipBA <sub>1,2,3</sub> + pJS71 + pMR20	$\Delta$ hipBA <sub>1,2,3</sub> pJS71 pMR20	This study
$\Delta$ hipBA <sub>1,2,3</sub> + pFLAG-hipA <sub>1</sub>	$\Delta$ hipBA <sub>1</sub> $\Delta$ hipBA <sub>2</sub> $\Delta$ hipBA <sub>3</sub> pFLAG-hipA <sub>1</sub>	This study
$\Delta$ hipBA <sub>1,2,3</sub> + pFLAG-hipA <sub>2</sub>	$\Delta$ hipBA <sub>1</sub> $\Delta$ hipBA <sub>2</sub> $\Delta$ hipBA <sub>3</sub> pFLAG-hipA <sub>2</sub>	This study
$\Delta$ hipBA <sub>1,2,3</sub> + pFLAG-hipA <sub>3</sub>	$\Delta$ hipBA <sub>1</sub> $\Delta$ hipBA <sub>2</sub> $\Delta$ hipBA <sub>3</sub> pFLAG-hipA <sub>3</sub>	This study
$\Delta$ hipBA <sub>1,2,3</sub> + pFLAG-hipA <sub>1</sub> <sup>D301Q</sup>	$\Delta$ hipBA <sub>1</sub> $\Delta$ hipBA <sub>2</sub> $\Delta$ hipBA <sub>3</sub> pFLAG-hipA <sub>1</sub> <sup>D301Q</sup>	This study
$\Delta$ hipBA <sub>1,2,3</sub> + pFLAG-hipA <sub>2</sub> <sup>D308Q</sup>	$\Delta$ hipBA <sub>1</sub> $\Delta$ hipBA <sub>2</sub> $\Delta$ hipBA <sub>3</sub> pFLAG-hipA <sub>2</sub> <sup>D308Q</sup>	This study
$\Delta$ hipBA <sub>1,2,3</sub> + pFLAG-hipA <sub>3</sub> <sup>D326Q</sup>	$\Delta$ hipBA <sub>1</sub> $\Delta$ hipBA <sub>2</sub> $\Delta$ hipBA <sub>3</sub> pFLAG-hipA <sub>3</sub> <sup>D326Q</sup>	This study
$\Delta$ hipBA <sub>1,2,3</sub> + pFLAG-hipB <sub>1</sub>	$\Delta$ hipBA <sub>1</sub> $\Delta$ hipBA <sub>2</sub> $\Delta$ hipBA <sub>3</sub> pFLAG-hipB <sub>1</sub>	This study
$\Delta$ hipBA <sub>1,2,3</sub> + pFLAG-hipB <sub>2</sub>	$\Delta$ hipBA <sub>1</sub> $\Delta$ hipBA <sub>2</sub> $\Delta$ hipBA <sub>3</sub> pFLAG-hipB <sub>2</sub>	This study
$\Delta$ hipBA <sub>1,2,3</sub> + pFLAG-hipB <sub>3</sub>	$\Delta$ hipBA <sub>1</sub> $\Delta$ hipBA <sub>2</sub> $\Delta$ hipBA <sub>3</sub> pFLAG-hipB <sub>3</sub>	This study
$\Delta$ hipBA <sub>1,2,3</sub> + pFLAG-hipA <sub>1</sub> + pFLAG-hipB <sub>1</sub>	$\Delta$ hipBA <sub>1</sub> $\Delta$ hipBA <sub>2</sub> $\Delta$ hipBA <sub>3</sub> pFLAG-hipA <sub>1</sub> pFLAG-hipB <sub>1</sub>	This study
$\Delta$ hipBA <sub>1,2,3</sub> + pFLAG-hipA <sub>2</sub> + pFLAG-hipB <sub>1</sub>	$\Delta$ hipBA <sub>1</sub> $\Delta$ hipBA <sub>2</sub> $\Delta$ hipBA <sub>3</sub> pFLAG-hipA <sub>2</sub> pFLAG-hipB <sub>1</sub>	This study
$\Delta$ hipBA <sub>1,2,3</sub> + pFLAG-hipA <sub>3</sub> + pFLAG-hipB <sub>1</sub>	$\Delta$ hipBA <sub>1</sub> $\Delta$ hipBA <sub>2</sub> $\Delta$ hipBA <sub>3</sub> pFLAG-hipA <sub>3</sub> pFLAG-hipB <sub>1</sub>	This study

$\Delta hipBA_{1,2,3} + pFLAG-hipA_1 + pFLAG-hipB_2$	$\Delta hipBA_1 \Delta hipBA_2 \Delta hipBA_3 pFLAG-hipA_1 pFLAG-hipB_2$	This study
$\Delta hipBA_{1,2,3} + pFLAG-hipA_2 + pFLAG-hipB_2$	$\Delta hipBA_1 \Delta hipBA_2 \Delta hipBA_3 pFLAG-hipA_2 pFLAG-hipB_2$	This study
$\Delta hipBA_{1,2,3} + pFLAG-hipA_3 + pFLAG-hipB_2$	$\Delta hipBA_1 \Delta hipBA_2 \Delta hipBA_3 pFLAG-hipA_3 pFLAG-hipB_2$	This study
$\Delta hipBA_{1,2,3} + pFLAG-hipA_1 + pFLAG-hipB_3$	$\Delta hipBA_1 \Delta hipBA_2 \Delta hipBA_3 pFLAG-hipA_1 pFLAG-hipB_3$	This study
$\Delta hipBA_{1,2,3} + pFLAG-hipA_2 + pFLAG-hipB_3$	$\Delta hipBA_1 \Delta hipBA_2 \Delta hipBA_3 pFLAG-hipA_2 pFLAG-hipB_3$	This study
$\Delta hipBA_{1,2,3} + pFLAG-hipA_3 + pFLAG-hipB_3$	$\Delta hipBA_1 \Delta hipBA_2 \Delta hipBA_3 pFLAG-hipA_3 pFLAG-hipB_3$	This study
$\Delta spoT$	$\Delta spoT$	37
$\Delta spoT + pFLAG-hipA_1$	$\Delta spoT pFLAG-hipA_1$	This study
$\Delta spoT + pFLAG-hipA_2$	$\Delta spoT pFLAG-hipA_2$	This study
$\Delta spoT + pFLAG-hipA_3$	$\Delta spoT pFLAG-hipA_3$	This study
$\Delta hipBA_{1,2,3} + pMR20 + pFLAG-metG$	$\Delta hipBA_1 \Delta hipBA_2 \Delta hipBA_3 pMR20 pFLAG-MetG$	This study
$\Delta hipBA_{1,2,3} + pMR20 + pFLAG-lysS$	$\Delta hipBA_1 \Delta hipBA_2 \Delta hipBA_3 pMR20 pFLAG-lysS$	This study
$\Delta hipBA_{1,2,3} + pMR20 + pFLAG-TrpS$	$\Delta hipBA_1 \Delta hipBA_2 \Delta hipBA_3 pMR20 pFLAG-TrpS$	This study
$\Delta hipBA_{1,2,3} + pMR20 + pFLAG-GltX$	$\Delta hipBA_1 \Delta hipBA_2 \Delta hipBA_3 pMR20 pFLAG-GltX$	This study
$\Delta hipBA_{1,2,3} + pFLAG-hipA_1 + pFLAG-metG$	$\Delta hipBA_1 \Delta hipBA_2 \Delta hipBA_3 pFLAG-hipA_1 pFLAG-metG$	This study
$\Delta hipBA_{1,2,3} + pFLAG-hipA_1 + pFLAG-lysS$	$\Delta hipBA_1 \Delta hipBA_2 \Delta hipBA_3 pFLAG-hipA_1 pFLAG-lysS$	This study
$\Delta hipBA_{1,2,3} + pFLAG-hipA_1 + pFLAG-trpS$	$\Delta hipBA_1 \Delta hipBA_2 \Delta hipBA_3 pFLAG-hipA_1 pFLAG-trpS$	This study
$\Delta hipBA_{1,2,3} + pFLAG-hipA_1 + pFLAG-gltX$	$\Delta hipBA_1 \Delta hipBA_2 \Delta hipBA_3 pFLAG-hipA_1 pFLAG-gltX$	This study
$\Delta hipBA_{1,2,3} + pFLAG-hipA_2 + pFLAG-metG$	$\Delta hipBA_1 \Delta hipBA_2 \Delta hipBA_3 pFLAG-hipA_2 pFLAG-metG$	This study
$\Delta hipBA_{1,2,3} + pFLAG-hipA_2 + pFLAG-lysS$	$\Delta hipBA_1 \Delta hipBA_2 \Delta hipBA_3 pFLAG-hipA_2 pFLAG-lysS$	This study
$\Delta hipBA_{1,2,3} + pFLAG-hipA_2 + pFLAG-trpS$	$\Delta hipBA_1 \Delta hipBA_2 \Delta hipBA_3 pFLAG-hipA_2 pFLAG-trpS$	This study



$\Delta hipBA_{1,2,3}$ + pFLAG-hipA <sub>2</sub> + pFLAG-gltX	$\Delta hipBA_1 \Delta hipBA_2 \Delta hipBA_3$ pFLAG-hipA <sub>2</sub> pFLAG-gltX	This study
$\Delta hipBA_{1,2,3}$ + pFLAG-hipA <sub>3</sub> + pFLAG-metG	$\Delta hipBA_1 \Delta hipBA_2 \Delta hipBA_3$ pFLAG-hipA <sub>3</sub> pFLAG-metG	This study
$\Delta hipBA_{1,2,3}$ + pFLAG-hipA <sub>3</sub> + pFLAG-lysS	$\Delta hipBA_1 \Delta hipBA_2 \Delta hipBA_3$ pFLAG-hipA <sub>3</sub> pFLAG-lysS	This study
$\Delta hipBA_{1,2,3}$ + pFLAG-hipA <sub>3</sub> + pFLAG-trpS	$\Delta hipBA_1 \Delta hipBA_2 \Delta hipBA_3$ pFLAG-hipA <sub>3</sub> pFLAG-trpS	This study
$\Delta hipBA_{1,2,3}$ + pFLAG-hipA <sub>3</sub> + pFLAG-gltX	$\Delta hipBA_1 \Delta hipBA_2 \Delta hipBA_3$ pFLAG-hipA <sub>3</sub> pFLAG-gltX	This study

**Table 2. Plasmids**

<b>Name</b>	<b>Description</b>	<b>Reference</b>
pMR20	Broad-host-range, low-copy-number vector; tetR	
pJS71	Broad host-range cloning vector; high copy; chlorR; pBBR1MCS derivative with unique EcoRI site	(J. M. Skerker unpublished)
pNPTS138	kanR; sacB-containing integration vector	(M.R. K. Alley, unpublished)
pCYH1	pNPTS138 vector for knocking out hipBA1 (CCNA_00481-00482)	This study
pCYH2	pNPTS138 vector for knocking out hipBA2 (CCNA_02821-02822)	This study
pCYH3	pNPTS138 vector for knocking out hipBA3 (CCNA_02858-02859)	This study
p <i>hipA</i> <sub>1</sub>	pMR20 - <i>PriboA</i> - <i>hipA</i> <sub>1</sub> (CCNA_00482)	This study
p <i>hipA</i> <sub>2</sub>	pMR20 - <i>PriboA</i> - <i>hipA</i> <sub>2</sub> (CCNA_02821)	This study
p <i>hipA</i> <sub>3</sub>	pMR20 - <i>PriboA</i> - <i>hipA</i> <sub>3</sub> (CCNA_02858)	This study
p <i>FLAG-hipA</i> <sub>1</sub>	pMR20 - <i>PriboA</i> - <i>FLAG-hipA</i> <sub>1</sub> (CCNA_00482)	This study
p <i>FLAG-hipA</i> <sub>2</sub>	pMR20 - <i>PriboA</i> - <i>FLAG-hipA</i> <sub>2</sub> (CCNA_02821)	This study
p <i>FLAG-hipA</i> <sub>3</sub>	pMR20 - <i>PriboA</i> - <i>FLAG-hipA</i> <sub>3</sub> (CCNA_02858)	This study
p <i>FLAG-hipA</i> <sub>1</sub> <sup>D301Q</sup>	pMR20 - <i>PriboA</i> - <i>FLAG-hipA</i> <sub>1</sub> <sup>D301Q</sup>	This study
p <i>FLAG-hipA</i> <sub>2</sub> <sup>D308Q</sup>	pMR20 - <i>PriboA</i> - <i>FLAG-hipA</i> <sub>2</sub> <sup>D308Q</sup>	This study
p <i>FLAG-hipA</i> <sub>3</sub> <sup>D326Q</sup>	pMR20 - <i>PriboA</i> - p <i>FLAG-hipA</i> <sub>3</sub> <sup>D326Q</sup>	This study
p <i>FLAG-hipB</i> <sub>1</sub>	JS71 - <i>PriboA</i> - <i>FLAG-hipB</i> <sub>1</sub> (CCNA_00481)	This study
p <i>FLAG-hipB</i> <sub>2</sub>	JS71 - <i>PriboA</i> - <i>FLAG-hipB</i> <sub>2</sub> (CCNA_02822)	This study
p <i>FLAG-hipB</i> <sub>3</sub>	JS71 - <i>PriboA</i> - <i>FLAG-hipB</i> <sub>3</sub> (CCNA_02859)	This study
p <i>FLAG-metG</i>	JS71 - <i>PriboA</i> - <i>FLAG-metG</i> (CCNA_01547)	This study
p <i>FLAG-lysS</i>	JS71 - <i>PriboA</i> - <i>FLAG-lysS</i> (CCNA_00082)	This study
p <i>FLAG-trpS</i>	JS71 - <i>PriboA</i> - <i>FLAG-trpS</i> (CCNA_00062)	This study
p <i>FLAG-gltX</i>	JS71 - <i>PriboA</i> - <i>FLAG-gltX</i> (CCNA_01982)	This study
p <i>hipBA</i> <sub>1</sub>	pMR20 - <i>hipBA</i> <sub>1</sub>	This study
p <i>hipBA</i> <sub>2</sub>	pMR20 - <i>hipBA</i> <sub>2</sub>	This study
p <i>hipBA</i> <sub>3</sub>	pMR20 - <i>hipBA</i> <sub>3</sub>	This study
p <i>hipBA</i> <sub>1,2</sub>	pMR20 - <i>hipBA</i> <sub>1,2</sub>	This study

**Table 3. Primers**

<b>Name</b>	<b>Sequence (5'-3')</b>	<b>Purpose</b>
<i>hipBA</i> <sub>1</sub> Up F	attgaagccggctggcgccaTCGACCCGGGCGATCTTC	<i>hipBA</i> <sub>1</sub> chromosomal knockout
<i>hipBA</i> <sub>1</sub> Up R	tctagcgctcGAGGGTCATGAAAATTCTCCCG	
<i>hipBA</i> <sub>1</sub> Dn F	catgaccctcGAGCGCTAGACTCGATCCCGC	<i>hipBA</i> <sub>1</sub> chromosomal knockout
<i>hipBA</i> <sub>1</sub> Dn R	cgtcacggccgaagctagcgGCCAGGACGGCGACACC	
<i>hipBA</i> <sub>2</sub> Up F	attgaagccggctggcgccaTTGCCTCTTGAGGAGCCG	<i>hipBA</i> <sub>2</sub> chromosomal knockout
<i>hipBA</i> <sub>2</sub> Up R	acacctcctaCAGGAGCATAAGTAGCTAACGAAG	
<i>hipBA</i> <sub>2</sub> Dn F	tatgctcctgtagGAGGTGTTGCGCATGAGG	<i>hipBA</i> <sub>2</sub> chromosomal knockout
<i>hipBA</i> <sub>2</sub> Dn R	cgtcacggccgaagctagcgAAGATCACCCCGCTGTCTG	
<i>hipBA</i> <sub>3</sub> Up F	attgaagccggctggcgccaCCCGGGCGACAAGAAGGC	<i>hipBA</i> <sub>3</sub> chromosomal knockout
<i>hipBA</i> <sub>3</sub> Up R	cctaccgcctAAATTTTCATAAATCGCCTCTTGTGGCG	
<i>hipBA</i> <sub>3</sub> Dn F	tatgaaatttAGGCGGTAGGCGGGGGAT	<i>hipBA</i> <sub>3</sub> chromosomal knockout
<i>hipBA</i> <sub>3</sub> Dn R	cgtcacggccgaagctagcgGACAGCGGCACCAGCCGT C	
<i>riboA</i> to pJS71 F	cggccgctctagaactagtgTGGTGCAAACCTTTTCGC	pJS71 protein expression vector
<i>riboA</i> to pMR10/pMR 20 F	ctatgaccatgattacgccaTGGTGCAAACCTTTTCGC	pMR10/pMR20 expression vector
<i>riboA</i> to <i>FLAG</i> R	cttgtcgtcatcgtctttgtagtcCATCTTGTTGATACCCCC	riboA promoter for protein expression
<i>riboA</i> to <i>hipA</i> <sub>1</sub> R	tagtcatcgcCATCTTGTTGATACCCCC	
<i>riboA</i> to <i>hipA</i> <sub>2</sub> R	cgggcccactCATCTTGTTGATACCCCC	
<i>riboA</i> to <i>hipA</i> <sub>3</sub> R	cgacggtggtCATCTTGTTGATACCCCC	
<i>hipA</i> <sub>1</sub> to <i>riboA</i> F	caacaagatgGCGATGACTAGAGTGCTGACG	<i>hipA</i> <sub>1</sub> for pMR20 expression vector
<i>hipA</i> <sub>1</sub> F	gactacaaagacgatgacgacaagGCGATGACTAGAGTG CTGACG	<i>FLAG-hipA</i> <sub>1</sub> for pMR20 expression vector
<i>hipA</i> <sub>1</sub> R	ttgtaaacgacggccagtgCTAGCGCTCGCCCTGACC	
<i>hipA</i> <sub>2</sub> to <i>riboA</i> F	caacaagatgAGTGGGCCCGCAGGCCTG	<i>hipA</i> <sub>2</sub> for pMR20 expression vector

<i>hipA<sub>2</sub></i> F	gactacaaagacgatgacgacaagAGTGGGCCCGCAGGCCTG	<i>FLAG-hipA<sub>2</sub></i> for pMR20 expression vector
<i>hipA<sub>2</sub></i> R	ttgtaaaacgacggccagtgTCAACTCGGCGCCAAGGCG	
<i>hipA<sub>3</sub></i> to <i>riboA</i> F	caacaagatgACCACCGTCGCCGAGGTT	<i>hipA<sub>3</sub></i> for pMR20 expression vector
<i>hipA<sub>3</sub></i> F	gactacaaagacgatgacgacaagACCACCGTCGCCGAGGTT	<i>FLAG-hipA<sub>3</sub></i> for pMR20 expression vector
<i>hipA<sub>3</sub></i> R	ttgtaaaacgacggccagtgCTACCGCCTGAGCTCCAG	
<i>hipA<sub>1</sub></i> <sup>D301Q</sup> F	tcttgccgtgagcctggcggtgcccagc	<i>hipA<sub>1</sub></i> <sup>D301Q</sup> mutagenic primers
<i>hipA<sub>1</sub></i> <sup>D301Q</sup> R	cgtcggcaacgcccaggctcacggcaaga	
<i>hipA<sub>2</sub></i> <sup>D308Q</sup> F	tggttctggcgtgggtctgagtattgccaatcagaagatt	<i>hipA<sub>2</sub></i> <sup>D308Q</sup> mutagenic primers
<i>hipA<sub>2</sub></i> <sup>D308Q</sup> R	aatcttctgattggcaatactcagaaccacgccaagaacca	
<i>hipA<sub>3</sub></i> <sup>D326Q</sup> F	gttcttgacgtggtcctgctggttcgcccag	<i>hipA<sub>3</sub></i> <sup>D326Q</sup> mutagenic primers
<i>hipA<sub>3</sub></i> <sup>D326Q</sup> R	ctggcgcgaaaccagcaggaccacgtcaagaac	
<i>hipB<sub>1</sub></i> F	gactacaaagacgatgacgacaagACCCTCCTCCGGCAA GGC	<i>FLAG-hipB<sub>1</sub></i> for pJS71 expression vector
<i>hipB<sub>1</sub></i> R	cgaggtcgacggtatcgataCTAGTCATCGCCACCGCTC AC	
<i>hipB<sub>2</sub></i> F	gactacaaagacgatgacgacaagCTCCTGAGCGGGAGC GAAAAC	<i>FLAG-hipB<sub>2</sub></i> for pJS71 expression vector
<i>hipB<sub>2</sub></i> R	cgaggtcgacggtatcgataTCATCTGGGCGCCGCCAT	
<i>hipB<sub>3</sub></i> F	gactacaaagacgatgacgacaagAAATTTGAATCTCTCC TGTCC	<i>FLAG-hipB<sub>3</sub></i> for pJS71 expression vector
<i>hipB<sub>3</sub></i> R	cgaggtcgacggtatcgataTCATTTTTTCATCGCCCCAC	
<i>gltX</i> F	gactacaaagacgatgacgacaagTCGAACCCACCCCT ACC	<i>FLAG-gltX</i> for pJS71 expression vector
<i>gltX</i> R	cgaggtcgacggtatcgataTCATGCGCGAGGCGCTAG	
<i>lysS</i> F	gactacaaagacgatgacgacaagTTTGAAGGCCTCTCCC CC	<i>FLAG-lysS</i> for pJS71 expression vector
<i>lysS</i> R	cgaggtcgacggtatcgataTCAGCCCAGCTTTTCCTC	
<i>metG</i> F	gactacaaagacgatgacgacaagGCTCGCATCCTGATTA CCTCCG	<i>FLAG-metG</i> for pJS71 expression vector
<i>metG</i> R	cgaggtcgacggtatcgataTACTCCGCGCCGCCGAA	
<i>trpS</i> F	gactacaaagacgatgacgacaagACCGACCAAGCTCCC GTC	<i>FLAG-trpS</i> for pJS71 expression vector
<i>trpS</i> R	cgaggtcgacggtatcgataCTACGCGCCCCAGAAGCC	
<i>hipBA<sub>1</sub></i> F	ctatgaccatgattacccaGGGGCCCAGCCCCATGGC	

<i>hipBA</i> <sub>1</sub> R	ttgtaaaacgacggccagtgCTAGCGCTCGCCCTGACCC AG	<i>hipBA</i> <sub>1</sub> operon and promoter for pMR10 complementation vector
<i>hipBA</i> <sub>2</sub> F	ctatgaccatgattacgccaTCAACTCGGCGCCAAGGC	<i>hipBA</i> <sub>2</sub> operon and promoter for pMR10 complementation vector
<i>hipBA</i> <sub>2</sub> R	ttgtaaaacgacggccagtgCTGCGGGGAGGGTGTGGG	
<i>hipBA</i> <sub>1</sub> to <i>hipBA</i> <sub>2</sub> R	gccgagttgaCTAGCGCTCGCCCTGACCCAG	<i>hipBA</i> <sub>1</sub> and <i>hipBA</i> <sub>2</sub> operons for pMR10 complementation vector
<i>hipBA</i> <sub>2</sub> to <i>hipBA</i> <sub>1</sub> F	cgagcgctagTCAACTCGGCGCCAAGGC	
<i>hipBA</i> <sub>3</sub> F	ctatgaccatgattacgccaCCCCACCGGCGCCAGGAG	<i>hipBA</i> <sub>3</sub> operon and promoter for pMR10 complementation vector
<i>hipBA</i> <sub>3</sub> R	ttgtaaaacgacggccagtgGCGCGTCGCGCGGCGTCA	
CCNA_0344 5 qPCR F	CTGGATCTGTCTCGCCTTGG	RT-PCR oligonucleotides
CCNA_0344 5 qPCR R	GGTGGGATGGGGCTTCTG	
CCNA_0318 1 qPCR F	TTCAGACGCTTGAGACCACC	
CCNA_0318 1 qPCR R	CGTACATGGTTTTTCGGCACG	
CCNA_0167 4 qPCR F	CAGACCCTAGCGGACACTCC	
CCNA_0167 4 qPCR R	GGCGTGAACATCTCGTCGTA	
CCNA_0159 6 qPCR F	ATGTTTCCCGACACCGACTC	
CCNA_0159 6 qPCR R	CTGCTCGGGGTTTCAGGC	
CCNA_0052 0 qPCR F	GCGATCGCGGAATATCTCGAC	
CCNA_0052 0 qPCR R	CTGGTCGACTGGATGACGAA	
<i>rho1</i> F	AGACACCGAAAACCAGGTTCC	

<i>rho1</i> R	CGCTTCAGTGGTGATGTCGG	
<i>rho2</i> F	ACCGAAGACACCGAAAACCAG	
<i>rho2</i> R	GCCGCTTCAGTGGTGATGT	

## References

1. Van Melderren, L. Toxin-antitoxin systems: why so many, what for? *Curr. Opin. Microbiol.* **13**, 781–785 (2010).
2. Hayes, F. & Van Melderren, L. Toxins-antitoxins: diversity, evolution and function. *Crit. Rev. Biochem. Mol. Biol.* **46**, 386–408 (2011).
3. Hall, A. M., Gollan, B. & Helaine, S. Toxin-antitoxin systems: reversible toxicity. *Curr. Opin. Microbiol.* **36**, 102–110 (2017).
4. Hörak, R. & Tamman, H. Desperate times call for desperate measures: benefits and costs of toxin-antitoxin systems. *Curr. Genet.* **63**, 69–74 (2017).
5. Loris, R. & Garcia-Pino, A. Disorder- and dynamics-based regulatory mechanisms in toxin-antitoxin modules. *Chem. Rev.* **114**, 6933–6947 (2014).
6. Tsuchimoto, S. & Ohtsubo, E. Autoregulation by cooperative binding of the Pemi and PemK proteins to the promoter region of the pem operon. *Mol. Gen. Genet.* **237**, 81–88 (1993).
7. Hayes, F. Toxins-antitoxins: plasmid maintenance, programmed cell death, and cell cycle arrest. *Science* **301**, 1496–1499 (2003).
8. Pandey, D. P. & Gerdes, K. Toxin-antitoxin loci are highly abundant in free-living but lost from host-associated prokaryotes. *Nucleic Acids Res.* **33**, 966–976 (2005).
9. Díaz-Orejas, R., Espinosa, M. & Yeo, C. C. The Importance of the Expendable: Toxin-Antitoxin Genes in Plasmids and Chromosomes. *Front. Microbiol.* **8**, 1479 (2017).
10. Wozniak, R. A. F. & Waldor, M. K. A toxin-antitoxin system promotes the maintenance of an integrative conjugative element. *PLoS Genet.* **5**, e1000439 (2009).
11. Goeders, N. & Van Melderren, L. Toxin-antitoxin systems as multilevel interaction systems. *Toxins* **6**, 304–324 (2014).
12. Kędzierska, B. & Hayes, F. Emerging Roles of Toxin-Antitoxin Modules in Bacterial Pathogenesis. *Molecules* **21**, (2016).
13. Lobato-Márquez, D., Díaz-Orejas, R. & García-Del Portillo, F. Toxin-antitoxins and bacterial virulence. *FEMS Microbiol. Rev.* **40**, 592–609 (2016).
14. Levin-Reisman, I. *et al.* Antibiotic tolerance facilitates the evolution of resistance. *Science* **355**, 826–830 (2017).
15. Lewis, K. Persister cells. *Annu. Rev. Microbiol.* **64**, 357–372 (2010).
16. Balaban, N. Q., Merrin, J., Chait, R., Kowalik, L. & Leibler, S. Bacterial persistence as a phenotypic switch. *Science* **305**, 1622–1625 (2004).
17. Veening, J.-W., Smits, W. K. & Kuipers, O. P. Bistability, epigenetics, and bet-hedging in bacteria. *Annu. Rev. Microbiol.* **62**, 193–210 (2008).
18. Wood, T. K., Knabel, S. J. & Kwan, B. W. Bacterial persister cell formation and dormancy. *Appl. Environ. Microbiol.* **79**, 7116–7121 (2013).
19. Moyed, H. S. & Bertrand, K. P. *hipA*, a newly recognized gene of *Escherichia coli* K-12 that affects frequency of persistence after inhibition of murein synthesis. *J. Bacteriol.* **155**, 768–775 (1983).
20. Moyed, H. S. & Broderick, S. H. Molecular cloning and expression of *hipA*, a gene of *Escherichia coli* K-12 that affects frequency of persistence after inhibition of murein synthesis. *J. Bacteriol.* **166**, 399–403 (1986).

21. Black, D. S., Kelly, A. J., Mardis, M. J. & Moyed, H. S. Structure and organization of hip, an operon that affects lethality due to inhibition of peptidoglycan or DNA synthesis. *J. Bacteriol.* **173**, 5732–5739 (1991).
22. Black, D. S., Irwin, B. & Moyed, H. S. Autoregulation of hip, an operon that affects lethality due to inhibition of peptidoglycan or DNA synthesis. *J. Bacteriol.* **176**, 4081–4091 (1994).
23. Korch, S. B., Henderson, T. A. & Hill, T. M. Characterization of the hipA7 allele of Escherichia coli and evidence that high persistence is governed by (p)ppGpp synthesis. *Mol. Microbiol.* **50**, 1199–1213 (2003).
24. Schumacher, M. A. *et al.* HipBA-promoter structures reveal the basis of heritable multidrug tolerance. *Nature* **524**, 59–64 (2015).
25. Germain, E., Castro-Roa, D., Zenkin, N. & Gerdes, K. Molecular mechanism of bacterial persistence by HipA. *Mol. Cell* **52**, 248–254 (2013).
26. Semanjski, M. *et al.* The kinases HipA and HipA7 phosphorylate different substrate pools in Escherichia coli to promote multidrug tolerance. *Sci. Signal.* **11**, (2018).
27. Bokinsky, G. *et al.* HipA-triggered growth arrest and  $\beta$ -lactam tolerance in Escherichia coli are mediated by RelA-dependent ppGpp synthesis. *J. Bacteriol.* **195**, 3173–3182 (2013).
28. Hauryliuk, V., Atkinson, G. C., Murakami, K. S., Tenson, T. & Gerdes, K. Recent functional insights into the role of (p)ppGpp in bacterial physiology. *Nat. Rev. Microbiol.* **13**, 298–309 (2015).
29. Poindexter, J. S. BIOLOGICAL PROPERTIES AND CLASSIFICATION OF THE CAULOBACTER GROUP. *Bacteriol. Rev.* **28**, 231–295 (1964).
30. Poindexter, J. S. The caulobacters: ubiquitous unusual bacteria. *Microbiol. Rev.* **45**, 123–179 (1981).
31. Kasari, V., Mets, T., Tenson, T. & Kaldalu, N. Transcriptional cross-activation between toxin-antitoxin systems of Escherichia coli. *BMC Microbiol.* **13**, 45 (2013).
32. Gupta, A., Venkataraman, B., Vasudevan, M. & Gopinath Bankar, K. Co-expression network analysis of toxin-antitoxin loci in Mycobacterium tuberculosis reveals key modulators of cellular stress. *Sci. Rep.* **7**, 5868 (2017).
33. Correia, F. F. *et al.* Kinase activity of overexpressed HipA is required for growth arrest and multidrug tolerance in Escherichia coli. *J. Bacteriol.* **188**, 8360–8367 (2006).
34. Schumacher, M. A. *et al.* Role of unusual P loop ejection and autophosphorylation in HipA-mediated persistence and multidrug tolerance. *Cell Rep.* **2**, 518–525 (2012).
35. Aakre, C. D. *et al.* Evolving new protein-protein interaction specificity through promiscuous intermediates. *Cell* **163**, 594–606 (2015).
36. Walling, L. R. & Butler, J. S. Structural Determinants for Antitoxin Identity and Insulation of Cross Talk between Homologous Toxin-Antitoxin Systems. *J. Bacteriol.* **198**, 3287–3295 (2016).
37. Lesley, J. A. & Shapiro, L. SpoT regulates DnaA stability and initiation of DNA replication in carbon-starved Caulobacter crescentus. *J. Bacteriol.* **190**, 6867–6880 (2008).



38. Boutte, C. C. & Crosson, S. The complex logic of stringent response regulation in *Caulobacter crescentus*: starvation signalling in an oligotrophic environment. *Mol. Microbiol.* **80**, 695–714 (2011).
39. Korch, S. B. & Hill, T. M. Ectopic overexpression of wild-type and mutant *hipA* genes in *Escherichia coli*: effects on macromolecular synthesis and persister formation. *J. Bacteriol.* **188**, 3826–3836 (2006).
40. Brauner, A., Shores, N., Fridman, O. & Balaban, N. Q. An Experimental Framework for Quantifying Bacterial Tolerance. *Biophys. J.* **112**, 2664–2671 (2017).
41. Balaban, N. Q. *et al.* Definitions and guidelines for research on antibiotic persistence. *Nat. Rev. Microbiol.* **17**, 441–448 (2019).
42. Docquier, J.-D. *et al.* CAU-1, a subclass B3 metallo-beta-lactamase of low substrate affinity encoded by an ortholog present in the *Caulobacter crescentus* chromosome. *Antimicrob. Agents Chemother.* **46**, 1823–1830 (2002).
43. Svenningsen, M. S., Veress, A., Harms, A., Mitarai, N. & Semsey, S. Birth and Resuscitation of (p)ppGpp Induced Antibiotic Tolerant Persister Cells. *Sci. Rep.* **9**, 6056 (2019).
44. Boutte, C. C., Henry, J. T. & Crosson, S. ppGpp and polyphosphate modulate cell cycle progression in *Caulobacter crescentus*. *J. Bacteriol.* **194**, 28–35 (2012).
45. Lin, C.-Y., Awano, N., Masuda, H., Park, J.-H. & Inouye, M. Transcriptional repressor HipB regulates the multiple promoters in *Escherichia coli*. *J. Mol. Microbiol. Biotechnol.* **23**, 440–447 (2013).
46. Agirrezabala, X. *et al.* The ribosome triggers the stringent response by RelA via a highly distorted tRNA. *EMBO Rep.* **14**, 811–816 (2013).
47. Winther, K. S., Roghanian, M. & Gerdes, K. Activation of the Stringent Response by Loading of RelA-tRNA Complexes at the Ribosomal A-Site. *Mol. Cell* **70**, 95–105.e4 (2018).
48. Vang Nielsen, S. *et al.* Serine-Threonine Kinases Encoded by Split *hipA* Homologs Inhibit Tryptophanyl-tRNA Synthetase. *MBio* **10**, (2019).
49. Sekine, S.-I. *et al.* ATP binding by glutamyl-tRNA synthetase is switched to the productive mode by tRNA binding. *EMBO J.* **22**, 676–688 (2003).
50. Sekine, S.-I. *et al.* Structural bases of transfer RNA-dependent amino acid recognition and activation by glutamyl-tRNA synthetase. *Structure* **14**, 1791–1799 (2006).
51. Ely, B. Genetics of *Caulobacter crescentus*. *Methods Enzymol.* **204**, 372–384 (1991).
52. Bertani, G. Studies on lysogenesis. I. The mode of phage liberation by lysogenic *Escherichia coli*. *J. Bacteriol.* **62**, 293–300 (1951).
53. Topp, S. *et al.* Synthetic riboswitches that induce gene expression in diverse bacterial species. *Appl. Environ. Microbiol.* **76**, 7881–7884 (2010).
54. Marks, M. E. *et al.* The genetic basis of laboratory adaptation in *Caulobacter crescentus*. *J. Bacteriol.* **192**, 3678–3688 (2010).

## **Chapter 2**

### **A novel role for a HipBA toxin-antitoxin system in *C. crescentus* stress tolerance**

Charlie Y. Huang and Kathleen R. Ryan

Department of Plant & Microbial Biology, University of California, Berkeley, USA

## Introduction

Toxin Antitoxin modules ordinarily maintain themselves in a homeostatic inactive state unless the host organism encounters a perturbation that disrupts the stability of the antitoxin<sup>1,2</sup>. If the antitoxin supply cannot be replenished, the toxin is released and can act on downstream targets to inhibit growth or cause death<sup>3,4</sup>. In the case of TA systems as selfish genetic elements, the perturbation is a genetic change that removes the TA operon from the host organism through loss of a plasmid, excision of a mobile genetic element, or mutations that affect the expression and activity of the operon. This 'addictive' quality ensures the propagation of the TA operon. However, in the case of stress-responsive TA elements, the antitoxin is degraded in response to an environmental cue such as nutrient deprivation or antibiotic treatment<sup>5,6</sup>. The toxin is then able to affect downstream targets and in the case of TA-mediated persister cell formation, improve organismal survival<sup>7,8</sup>. Many modules can be activated by stressful conditions that disrupt antitoxin synthesis such as amino acid starvation<sup>5</sup>, antibiotic treatment that inhibit translation or transcription<sup>9</sup> and DNA damage<sup>10,11</sup>. Furthermore, different modules can respond to different stress conditions and multiple proteases are implicated in their activation<sup>12</sup>. Thus, TA modules have the potential to exhibit higher-order logic and have been reported to contribute to the choreography of complex processes such as biofilm formation<sup>13-16</sup>. Nonetheless, the potential for TA systems to mediate bacterial stress responses is largely unexplored.

We have dissected the roles of *C. crescentus* *hipBA* modules in persister cell formation. *hipBA*<sub>1</sub> and *hipBA*<sub>2</sub> contribute to the accumulation of persister cells in stationary phase cultures grown in PYE medium; however, a  $\Delta$ *hipBA*<sub>3</sub> strain does not have a persistence defect in stationary phase (**Figs. 1-11 A-C**). This is curious as *hipBA*<sub>3</sub> is a *bona fide* TA module. HipA<sub>3</sub> functions as a kinase and inhibits growth in *C. crescentus* when ectopically expressed. While HipA<sub>1</sub> and HipA<sub>2</sub> are more potent toxins and have strong effects on protein synthesis, <sup>35</sup>S-methionine incorporation is moderately reduced when HipA<sub>3</sub> expression is induced, indicating that HipA<sub>3</sub> does target protein synthesis to some degree (**Figs. 1-7 A-B**). Indeed, we detect that HipA<sub>3</sub> weakly phosphorylates the GltX tRNA synthetase in Phos-tag mobility shift assays (**Fig. 1-8B**). DNA replication and transcription were not altered when HipA<sub>3</sub> expression was induced (**Figs. 1-7 C-D**). HipB<sub>3</sub> is the only cognate antitoxin of the HipA<sub>3</sub> toxin (**Fig. 1-4E**); *hipBA*<sub>3</sub> appears insulated from the other two NA1000 *hipBA* modules. Intriguingly, an increase in persistence mediated by the stringent response was observed when HipA<sub>3</sub> expression was induced in exponential phase PYE cultures (**Fig. 1-13B**). Thus, HipA<sub>3</sub> may affect persistence under conditions not yet tested and likely targets cellular processes not affected by HipA<sub>1</sub> or HipA<sub>2</sub> to inhibit growth.

Here, we report a new role for a *hipBA* TA system in *C. crescentus* stress resistance. Instead of being stochastically active in a small subpopulation, the *hipBA*<sub>3</sub> module is activated on a larger scale in response to phosphate starvation. Strains without the *hipBA*<sub>3</sub> module are ultrasensitive to peroxide stress during phosphate limitation, indicating that HipA<sub>3</sub> is important for survival under these conditions. Furthermore, HipA<sub>3</sub> activation results in the transcriptional upregulation of *dps*, a ferritin-like protein that has recently been implicated in peroxide and osmotic stress tolerance in

*Caulobacter* and other organisms<sup>17–20</sup>. Finally, we find that the HslUV protease is responsible for degrading the HipB<sub>3</sub> antitoxin in phosphate-limited conditions. This novel integration of a *hipBA* TA system into bacterial stress tolerance reveals another role in the diverse repertoire of these evolutionarily successful modules.

## Results

To dissect the biological role of *hipBA*<sub>3</sub> in *C. crescentus*, we looked for a phenotype associated with the loss of the module. We were previously unable to detect a persistence defect in a strain lacking the  $\Delta$ *hipBA*<sub>3</sub> module despite the increase in persistence observed when HipA<sub>3</sub> was ectopically expressed in exponential phase cultures. We reasoned that *hipBA*<sub>3</sub> could active in other conditions not tested. Curiously, a slight fitness defect was observed in competition experiments conducted in PYE medium; when exponential-phase marked wild-type NA1000 and  $\Delta$ *hipBA*<sub>3</sub> cultures are coinoculated into fresh PYE medium at equal CFU/mL, NA1000 consistently outcompetes the  $\Delta$ *hipBA*<sub>3</sub> strain at the transition from exponential phase to stationary phase (**Fig. 2-1**). The mild fitness defect observed at this transition indicates that the *hipBA*<sub>3</sub> module is important during this time and that HipA<sub>3</sub> could be active during this period.

### HipA<sub>3</sub> is activated in response to phosphate limitation

To observe *hipBA*<sub>3</sub> activation, we monitored transcript abundance of the *hipBA*<sub>3</sub> operon. A characteristic of Type-II Toxin-Antitoxin systems is tight autoregulation at the transcriptional level<sup>21–23</sup>. In addition to binding and inactivating the toxin, Type-II antitoxins also bind and repress the transcription of their own operon. If the antitoxin is degraded, this autorepression is ameliorated, and the operon can be transcribed to replenish the antitoxin supply. Since the destruction of HipB causes both derepression of the toxin-antitoxin operon and liberation of HipA, the accumulation of *hipBA*<sub>3</sub> transcripts can serve as an indicator of free and active HipA<sub>3</sub> toxin. We profiled *hipBA*<sub>3</sub> transcript abundance in a wild type NA1000 strain throughout all phases of growth in PYE medium and observed an ~8 fold increase during the exponential-to-stationary phase transition for a brief period of time before returning to basal levels (**Fig. 2-2A**). We infer that the HipB<sub>3</sub> antitoxin is degraded and HipA<sub>3</sub> is active during this short window before HipB<sub>3</sub> is resynthesized to repress transcription of its operon and sequester the HipA<sub>3</sub> toxin. The brief increase in *hipBA*<sub>3</sub> transcript abundance does not occur if the HipB<sub>3</sub> antitoxin is expressed from the RiboA promoter on a high-copy plasmid, supporting the assertion that HipB<sub>3</sub> represses *hipBA*<sub>3</sub> transcription and validating *hipBA*<sub>3</sub> transcript abundance as a readout for HipB<sub>3</sub> stability and HipA<sub>3</sub> activity. We conclude that the *hipBA*<sub>3</sub> module is turned on during a brief window during the transition to stationary phase in PYE medium, and that HipA<sub>3</sub> phosphorylates one or more targets important to fitness at that time.

We hypothesized that *hipBA*<sub>3</sub> is activated in response to the depletion of one or more nutrients from PYE medium. Curiously, we did not observe an increase in *hipBA*<sub>3</sub> transcript abundance during the exponential-stationary phase transition in the defined minimal medium M2G (**Fig 2-2A**). This suggested that the nutrient whose depletion

activates HipA<sub>3</sub> in PYE medium may not be exhausted as cultures transition from exponential to stationary phase in M2G. To determine which nutrient(s) affect HipA<sub>3</sub> activation, exponential phase cultures were shifted from nutritionally replete M2G medium to M2 lacking either carbon or nitrogen (**Fig 2-2B**). No change in *hipBA*<sub>3</sub> transcript abundance was observed during these shifts, indicating that *hipBA*<sub>3</sub> does not respond to carbon or nitrogen starvation alone. Phosphate salts are the buffering system in M2G medium and removing these salts would significantly alter its osmotic balance. We therefore selected M5G minimal medium, which has previously been used to study the effects of phosphate limitation on stalk outgrowth<sup>24,25</sup>. We observed an increase in *hipBA*<sub>3</sub> transcription when NA1000 exponential phase cells were shifted from balanced phosphate conditions (200 μM) in M5G to phosphate-limited conditions (30 μM) (**Fig 2B**). These results indicate that phosphate limitation activates *hipBA*<sub>3</sub> transcription, likely due to the inactivation of the HipB<sub>3</sub> antitoxin.

### **HipB<sub>3</sub> is degraded by the HslUV protease during phosphate limitation**

To release HipA from inhibition in *E. coli*, the HipB antitoxin is proteolyzed by the Lon protease<sup>8</sup>. However, it is possible that a toxin could instead be activated via sequestration of the antitoxin protein by other cellular components. To discriminate between these hypotheses, we incubated wild-type *C. crescentus* and several protease-deficient mutants in phosphate-limited conditions and compared their *hipBA*<sub>3</sub> transcript levels (**Fig. 2-3**). We selected ATP-dependent proteases as *E. coli* HipB is degraded by Lon and ATP-dependent proteases are implicated in antitoxin degradation in many cases<sup>12,21,26</sup>. Both the  $\Delta lon$  and  $\Delta clpP$  protease mutants increase *hipBA*<sub>3</sub> transcript abundance in response to phosphate limitation, indicating that HipB<sub>3</sub> is properly degraded and HipA<sub>3</sub> is activated. However, *hipBA*<sub>3</sub> transcript abundance does not change during phosphate limitation in the  $\Delta hslV$  protease mutant. We conclude that HslV is the protease responsible for degrading HipB<sub>3</sub> in response to phosphate limitation, most likely in concert with its associated ATPase HslU.

### **The *hipBA*<sub>3</sub> module is important for peroxide stress tolerance**

The growth defect we observed in the  $\Delta hipBA$ <sub>3</sub> strain was mild, so to further dissect the role of HipA<sub>3</sub>, we looked for additional phenotypes associated with the  $\Delta hipBA$ <sub>3</sub> genotype. We uncovered a window of ultrasensitivity to peroxide in  $\Delta hipBA$ <sub>3</sub> cultures during the exponential-to-stationary phase transition in PYE medium (**Fig 2-4A**). During this time,  $\Delta hipBA$ <sub>3</sub> cells have significantly reduced survival when challenged with 1 mM peroxide for 30 minutes relative to a wild type strain. This window of peroxide ultrasensitivity coincides with the period of increased *hipBA*<sub>3</sub> transcript abundance (**Fig 2-2A**). While antitoxins are known to bind and repress their own operons, it has also been reported that the HipB antitoxin regulates several other genes in *E. coli*<sup>13</sup>. Thus, the period of peroxide ultrasensitivity observed in the  $\Delta hipBA$ <sub>3</sub> strain could be due to either to improper transcriptional regulation by HipB<sub>3</sub> or to the lack of HipA<sub>3</sub> kinase activity. To distinguish between the contributions of HipA<sub>3</sub> and HipB<sub>3</sub>, we complemented the peroxide ultrasensitivity phenotype with alleles of the entire *hipBA*<sub>3</sub> operon. We chose this approach because of actual or potential technical problems with expression

of HipB<sub>3</sub> or HipA<sub>3</sub> individually. Free energy simulations and crystal structures indicate that HipB-HipA complexes bind DNA more strongly than HipB alone<sup>22,23</sup>. Thus, complementing the  $\Delta hipBA_3$  strain with only HipB<sub>3</sub> could yield a false negative result. Conversely, ectopic expression of HipA<sub>3</sub> alone is known to be toxic. The window of ultrasensitivity to peroxide was complemented by the wild type  $hipBA_3$  operon on a plasmid, but not by a  $hipBA_3^{D326Q}$  operon, which encodes an amino acid substitution in the HipA<sub>3</sub> kinase active site (**Fig. 2-4A**). The HipA<sub>3</sub><sup>D326Q</sup> allele was previously demonstrated to lack kinase activity and is not toxic when ectopically expressed (**Figs. 1-4 C-D**). Therefore, it is specifically the kinase activity of HipA<sub>3</sub> that complements the peroxide ultrasensitivity phenotype. HipA<sub>3</sub> must phosphorylate a target during this window that is important for peroxide stress tolerance in *C. crescentus*.

HipA<sub>3</sub> may interface with well-characterized stress response pathways to provide peroxide resistance. To explore this possibility, we compared the peroxide sensitivity of the  $\Delta hipBA_3$  strain to strains lacking SigT or SpoT. SigT is an extracytoplasmic sigma factor that is induced a variety of stress conditions from heat shock to osmotic stress and is important for survival against oxidative stress<sup>27,28</sup>. The (p)ppGpp synthetase/hydrolase SpoT is the sole source of the alarmone (p)ppGpp in *C. crescentus* and therefore, governs the stringent response<sup>29,30</sup>. *C. crescentus* has a highly customized stringent response that activates under carbon and nitrogen starvation, but has not been reported to respond to other nutrient limiting conditions<sup>30,31</sup>. However, the *C. crescentus* stringent response upregulates several genes involved in oxidative stress response, including the catalase KatG and superoxide dismutase SodA<sup>27</sup>. Neither  $\Delta sigT$  nor  $\Delta spoT$  strains demonstrate peroxide ultrasensitivity during a growth curve in PYE medium (**Fig 2-4B**). KatG is the sole catalase enzyme encoded in the *C. crescentus* genome<sup>32,33</sup>. The ultrasensitivity to peroxide could be explained if KatG levels were altered in the  $\Delta hipBA_3$  strain. However, the amount of KatG protein, determined by Western blot, is similar in NA1000 and  $\Delta hipBA_3$  strains during the exponential-to-stationary phase transition in PYE cultures (**Fig. 2-4C**). We have not eliminated the possibility that HipA<sub>3</sub> regulates KatG activity via phosphorylation but taken together with the remaining data concerning SigT and SpoT, our model is that HipA<sub>3</sub> provides peroxide resistance through a mechanism apart from these known stress response pathways.

### **HipA<sub>3</sub> transcriptionally upregulates the ferritin-like protein Dps**

Because HipA<sub>3</sub> is activated in response to phosphate limitation (demonstrated in M5G medium), we hypothesized that phosphate limitation is the signal that activates HipA<sub>3</sub> during the exponential-to-stationary phase transition in PYE medium. We therefore supplemented PYE medium with 50  $\mu$ M phosphate and measured peroxide sensitivity at distinct points during the growth curve. Phosphate supplementation restored peroxide resistance to the  $\Delta hipBA_3$  strain (**Fig 2-5A**), indicating that phosphate availability is necessary for peroxide stress tolerance. This result further suggests HipA<sub>3</sub> contributes to peroxide resistance by phosphorylating a target that compensates for phosphate limitation.

In addition to KatG, the ferritin-like protein, Dps, plays an important role in protecting many organisms, including *C. crescentus*, from oxidative stress<sup>17–20,34</sup>. A Dps-deficient mutant was reported to be ultrasensitive to peroxide, similar to the  $\Delta hipBA_3$  strain<sup>17</sup>. Dps has been proposed to protect the cell through its DNA binding and ferroxidase activity; specifically, Dps detoxifies peroxide through the iron storage reaction<sup>18,35</sup>. Based on these results and because KatG levels were unaffected in a  $\Delta hipBA_3$  strain, we hypothesized that HipA<sub>3</sub> could phosphorylate targets that affect Dps abundance or activity. When Dps is ectopically expressed in a  $\Delta hipBA_3$  mutant on a low-copy plasmid under the control of an inducible *riboA* promoter, peroxide sensitivity is restored during all phases of growth in PYE medium; no ultrasensitivity to peroxide is observed (**Fig. 2-5A**), suggesting that Dps acts downstream of HipA<sub>3</sub>. Since Dps is known to be upregulated during the exponential-to-stationary phase growth transition, we monitored *dps* transcript abundance in wild type NA1000 and  $\Delta hipBA_3$  strains during all phases of growth in PYE medium<sup>17</sup>. During the transition to stationary phase, *dps* transcripts were ~4 fold less abundant in the  $\Delta hipBA_3$  mutant than in NA1000 (**Fig. 2-5B**), indicating that HipA<sub>3</sub> likely plays a role in upregulating *dps* expression under phosphate-limited conditions. To test this model, we monitored *dps* transcripts during phosphate limitation in  $\Delta hslV$  cells, which lack the protease responsible for degrading HipB<sub>3</sub> and cannot activate HipA<sub>3</sub>. As predicted, *dps* transcripts are reduced in the  $\Delta hslV$  strain relative to wild type during phosphate limitation (**Fig 2-5C**). Finally, if the inability to activate HipA<sub>3</sub> reduces *dps* transcription, ectopic HipA<sub>3</sub> expression should upregulate *dps* transcription. Indeed, we observe a ~7 fold increase in *dps* transcripts when HipA<sub>3</sub> is ectopically expressed in exponential phase NA1000 cultures grown in PYE medium (**Fig 2-5D**). Taken together, these data indicate that HipA<sub>3</sub> is responsible for the upregulation of *dps* transcription under phosphate limiting conditions. Since catalytically inactive HipA<sub>3</sub> failed to restore peroxide resistance, we infer that phosphorylation of an intermediate protein or proteins by HipA<sub>3</sub> is required to activate *dps* transcription.

## Discussion

Here we report the novel integration of a TA system into stress tolerance in *C. crescentus*. *hipBA<sub>3</sub>* is activated in response to phosphate limitation. Using *hipBA<sub>3</sub>* transcript abundance as a readout for HipA<sub>3</sub> activation, we observe an increase in *hipBA<sub>3</sub>* transcripts in defined minimal medium when phosphate is depleted (**Fig. 2-2B**), indicating that HipB<sub>3</sub> is proteolyzed and HipA<sub>3</sub> is active. This increase could only be detected if HipA<sub>3</sub> was activated on a larger scale than in a small subpopulation. This increase is temporary and transcript levels quickly return to basal levels as HipB<sub>3</sub> is resynthesized, restoring repression of the operon and inhibiting HipA<sub>3</sub>. We also observe a similar brief increase in *hipBA<sub>3</sub>* transcript abundance during the exponential phase to stationary phase transition in wild type NA1000 cultures grown in PYE medium (**Fig. 2-2A**). It is likely that phosphate is a limiting nutrient in PYE medium. Yeast extract and peptone, the principal components of PYE medium, are reported to only contain small amounts of phosphate<sup>36</sup>. Thus, instead of affecting a small subpopulation through stochastic activation, the *hipBA<sub>3</sub>* module is activated across the bacterial population in response to phosphate limitation.

Consistent with the population-wide activation of *hipBA*<sub>3</sub> in response to phosphate limitation, we observed a fitness defect during the exponential-to-stationary phase transition in the  $\Delta hipBA_3$  strain when grown in PYE medium (**Fig. 2-1**). Further dissection revealed this fitness defect coincides with major ultrasensitivity to peroxide during the brief window when HipA<sub>3</sub> was determined to be active in cultures grown in PYE (**Fig. 2-4A**). This peroxide ultrasensitivity phenotype can be complemented with a plasmid bearing the wild type *hipBA*<sub>3</sub> operon, but not the *hipBA*<sub>3</sub><sup>D326Q</sup> operon encoding a kinase-dead HipA<sub>3</sub> (**Fig. 2-4A**). Furthermore, supplementing PYE medium with phosphate eliminates the window of peroxide ultrasensitivity in the  $\Delta hipBA_3$  strain (**Fig. 2-5A**). This indicates that the target phosphorylated by HipA<sub>3</sub> is important for peroxide stress tolerance and likely requires phosphate to function.

We hypothesized that HipA<sub>3</sub> might activate one or more well-characterized stress response pathways in *C. crescentus* and that therefore, the ultrasensitivity to peroxide observed in the  $\Delta hipBA_3$  strain would be mirrored in mutants lacking these stress response pathways. SigT is an extracytoplasmic sigma factor that is important for oxidative stress response; a  $\Delta sigT$  strain has significantly increased sensitivity to peroxide<sup>28</sup>. SpoT regulates the *C. crescentus* stringent response and synthesizes (p)ppGpp under nutrient limiting conditions. While SpoT has not been reported to respond to phosphate limitation, several genes involved in oxidative stress response, including the catalase KatG are upregulated during by the stringent response<sup>30</sup>. Furthermore, all NA1000 HipA toxins, including HipA<sub>3</sub>, mediate the formation of persister cells through SpoT (**Figs. 1-13 B-C**). However, neither a  $\Delta sigT$  nor a  $\Delta spoT$  mutant had similar peroxide ultrasensitivity at any phase of growth (**Fig. 2-4B**). The protein levels of catalase, KatG, were also similar between the  $\Delta hipBA_3$  strain and wild type NA1000 during the exponential phase to stationary phase transition (**Fig. 2-4C**). Thus, HipA<sub>3</sub> operates through a pathway distinct from traditional characterized peroxide stress response pathways in *C. crescentus*.

We determined that HipA<sub>3</sub> transcriptionally upregulates Dps. A *C. crescentus* strain lacking Dps has similar ultrasensitivity to peroxide stress as  $\Delta hipBA_3$ , and ectopic Dps expression complements the peroxide ultrasensitivity of  $\Delta hipBA_3$  cells (**Fig. 2-5A**)<sup>17</sup>. Ectopic HipA<sub>3</sub> expression results in an accumulation of *dps* transcripts (**Fig. 2-5D**). When grown in PYE medium, *C. crescentus* upregulates *dps* transcription during the exponential-to-stationary phase transition; however, that upregulation is delayed in the  $\Delta hipBA_3$  strain (**Fig. 2-5B**). The delay in *dps* transcription could leave *C. crescentus* with less Dps during this period and temporarily vulnerable to peroxide stress. The transcriptional regulators that provide basal *dps* expression in exponential phase and increased expression later in stationary phase are unknown. Previous work demonstrated that *dps* transcription is not induced in response to hydrogen peroxide, and is not regulated by Fur and OxyR, which in other bacteria respond to iron limitation and oxidative stress, respectively<sup>17</sup>.

Surprisingly, phosphate supplementation of PYE medium also complements the peroxide ultrasensitivity phenotype of the  $\Delta hipBA_3$  strain. A floating phosphate layer has been observed on the surface of developing iron mineral cores in ferritin, and it has



been hypothesized to assist in recruiting iron and growing the ferric hydroxide cores<sup>37</sup>. Phosphate is also a component of at least one bacterial Dps iron mineral core<sup>19</sup>. The iron storage reaction performed by Dps consumes peroxide as a reactant<sup>34</sup>. Thus, if *dps* is transcribed too late under conditions where phosphate is being depleted, there may not be sufficient phosphate to facilitate the development of iron mineral cores, and Dps would be unable to efficiently remove peroxide from the intracellular environment. Consistent with this model, strains that lack the *hipBA*<sub>3</sub> operon or the HslV protease do not upregulate *dps* transcription in response to phosphate limitation (**Fig. 2-5C**). In our proposed model, *hipBA*<sub>3</sub> plays a role in regulating *dps* as an early warning signal for phosphate limitation; HipA<sub>3</sub> phosphorylates a target that results in the transcriptional upregulation of *dps* so that there is sufficient phosphate to ensure development of Dps iron mineral cores and therefore, efficient removal of peroxide before intracellular damage can occur (**Fig. 2-6**).

In our experiments examining the contribution of *hipBA* TA systems to persistence in *C. crescentus*, we were unable to detect a persistence defect associated with the loss of *hipBA*<sub>3</sub> in stationary phase PYE cultures. However, the exponential-to-stationary phase transition was never tested. Ectopic expression of HipA<sub>3</sub> in exponential phase cultures dramatically increased persister cell formation, and HipA<sub>3</sub> weakly phosphorylated the glutamyl tRNA synthetase, GltX (**Fig. 1-8B**). To reconcile these results, we speculate that HipA<sub>3</sub> normally contributes to persister cell formation under phosphate limiting conditions (**Fig. 2-6**). Future work will use single-cell measurements to confirm that HipA<sub>3</sub> is activated population-wide in response to phosphate limitation and will uncover molecular links between HipA<sub>3</sub> and persister cell formation. In contrast to *E. coli* HipB, which is degraded by the Lon protease, *C. crescentus* HipB<sub>3</sub> is proteolyzed by HslUV (**Fig. 2-3**). Additional work will determine how HslUV detects phosphate limitation and selectively degrades the HipB<sub>3</sub> antitoxin. Our results establish a novel integration of a HipBA toxin-antitoxin system into bacterial stress tolerance and demonstrate another way in which robust and ubiquitous toxin-antitoxin modules can neofunctionalize.

## Methods

**Strains and growth conditions.** Strains used in this study are listed in Table 2-1. All *Caulobacter crescentus* strains derive from the laboratory strain NA1000. *Caulobacter* strains were grown at 30°C in rich PYE, minimal medium supplemented with 0.2% glucose (M2G, M5G) <sup>25,38,39</sup>. PYE medium was supplemented with antibiotics when appropriate at the following concentrations (µg/mL): kanamycin (5); nalidixic acid (20); oxytetracycline (1). *E. coli* was grown in Luria broth at 37°C, supplemented with antibiotics when appropriate at the following concentrations (µg/mL) for liquid (L) or solid (S) medium: kanamycin, 30 (L), 50 (S); tetracycline, 12 (L/S)<sup>40</sup>. Proteins were ectopically expressed from the RiboA promoter by supplementing liquid PYE medium with 1 mM isopropyl thiogalactoside (IPTG) and 1 mM theophylline<sup>41</sup>.

**Plasmid construction.** *Caulobacter crescentus* NA1000 genomic DNA or purified plasmids were used as template with Q5 High Fidelity DNA Polymerase (New England Biolabs (NEB)) to amplify fragments for cloning. Fragments were isolated after gel electrophoresis using the Zymoclean Gel DNA Recovery kit (Zymo Research). NEB restriction enzymes were used to digest purified plasmids. Gibson assembly was performed using NEB Hi-Fi DNA Assembly Master Mix. Plasmid constructs were confirmed by DNA sequencing. Plasmid descriptions are listed in Table 2-2, and primers used for plasmid construction are described in Table 2-3.

*hipBA<sub>3</sub>*. The complementation vector was constructed by placing the *hipBA<sub>3</sub>* coding region and 500bp upstream promoter region in a pMR10 backbone. *hipBA<sub>3</sub>* F and *hipBA<sub>3</sub>* R primers were used to amplify the operon and promoter. The final plasmid was assembled via Gibson cloning into a HindIII/EcoRI-digested pMR10 backbone.

*hipBA<sub>3</sub><sup>D326Q</sup>*. Mutagenic primers *hipBA<sub>3</sub><sup>D326Q</sup>* F and *hipBA<sub>3</sub><sup>D326Q</sup>* R were used to amplify *hipBA<sub>3</sub>*. For final assembly, the amplified plasmid was treated with KLD Enzyme Mix (NEB) before transformation into *E. coli* competent cells.

*pdps*. The expression vector was constructed by placing the *dps* (CCNA\_02966) coding region under control of the *riboA* promoter. The *riboA* promoter was amplified using *riboA* to pMR10/pMR20 F and *riboA* to *dps* R primers. *dps* was amplified using *dps* F and *dps* R primers. The final plasmid was assembled via Gibson cloning into a HindIII/EcoRI-digested pMR20 backbone.

*pFLAG-hipA<sub>3</sub>*. The expression vector was constructed by placing the *hipA<sub>3</sub>* (CCNA\_02858) coding region N-terminally fused to a 1xFLAG tag (DYKDDDDK) under control of the *riboA* promoter. The *riboA* promoter was amplified using *riboA* to pMR10/pMR20 F and *riboA* to *FLAG* R primers. *hipA<sub>3</sub>* was amplified using *hipA<sub>3</sub>* F and *hipA<sub>3</sub>* R primers. The final plasmid was assembled via Gibson cloning into a HindIII/EcoRI-digested pMR20 backbone.

*pFLAG-hipB<sub>3</sub>*. The expression vector was constructed by placing the *hipB<sub>3</sub>* (CCNA\_02859) coding region N-terminally fused to a 1xFLAG tag (DYKDDDDK) under control of the *riboA* promoter. The *riboA* promoter was amplified using *riboA* to *riboA* to

pJS71 F and *riboA* to FLAG R primers. *hipB<sub>3</sub>* was amplified using *hipB<sub>3</sub>* F and *hipB<sub>3</sub>* R primers. The final plasmid was assembled via Gibson cloning into a HindIII/BamHI-digested pJS71 backbone.

**Fitness assays.** For competition experiments, cells grown to OD<sub>660</sub> 0.2-0.5 in PYE were coinoculated into PYE in equal OD fractions totaling OD<sub>660</sub> 0.02 and allowed to incubate with shaking at 30°C. At each indicated time or at the end-point, a sample was withdrawn for OD<sub>660</sub> measurement and enumeration of colony forming units (CFU)/ml on solid PYE medium (to enumerate all strains) and solid PYE medium containing kanamycin (to select for the marked wild type strain). Unless otherwise specified, mean and standard deviation of three independent biological replicates are reported.

**Peroxide survival assays.** Cells grown to OD<sub>660</sub> 0.2-0.5 in PYE were released into fresh PYE at OD<sub>660</sub> 0.02 and allowed to incubate with shaking at 30°C. At indicated OD<sub>660</sub>, samples were taken for CFU enumeration before and after 1mM peroxide treatment for 30 minutes.

**RNA extraction and reverse transcription.** RNA was extracted using Direct-zol RNA Miniprep Kits from Zymo Research. Purified RNA was reverse transcribed for qPCR using ProtoScript II First-Strand cDNA Transcription kit (NEB) with random hexamers to prime the reaction.

**RT-PCR.** RT-PCR was performed on an Applied Biosciences Step One Plus using Luna SYBR Master Mix from NEB. The thermocycling conditions are as follows: initial heating at 95°C for 20s, followed by 40 cycles of 95°C for 3 s, 60°C for 30s. *rho* was used as an endogenous control for all experiments. Primers used for RT-PCR are listed in Table 2-3.

**Western blot detection of proteins.** Samples for Western blot detection were harvested at OD<sub>660</sub> 0.4 in PYE medium for late exponential phase samples and at OD<sub>660</sub>~0.8-1.0 for stationary phase samples. The volume of culture collected was normalized by OD<sub>660</sub>. Cells were pelleted and resuspended in 60 µL water containing diluted 1X Laemmli sample buffer (Bio-Rad 1610737). The samples were heated at 95°C for 5 min, then allowed to cool to room temperature before 20 µL were loaded into a 10-well 12% bis-acrylamide gels (Bio-Rad 1610158) for separation by SDS-PAGE electrophoresis. After electrophoresis, protein transfer to PVDF membranes was performed overnight using the wet tank method in Western transfer buffer (3.03g/L Tris base, 14.4g/L glycine, 100mL/L methanol) with on ice. Western blotting was done using anti-katG antibodies (1:375) (Millipore-Sigma F3165) and horseradish peroxidase (HRP)-conjugated anti-rabbit antibodies (1:5000) (ThermoFisher 31460). Western blots were visualized by using Western Lightning (Perkin Elmer) on a Bio-Rad Gel Doc XR.

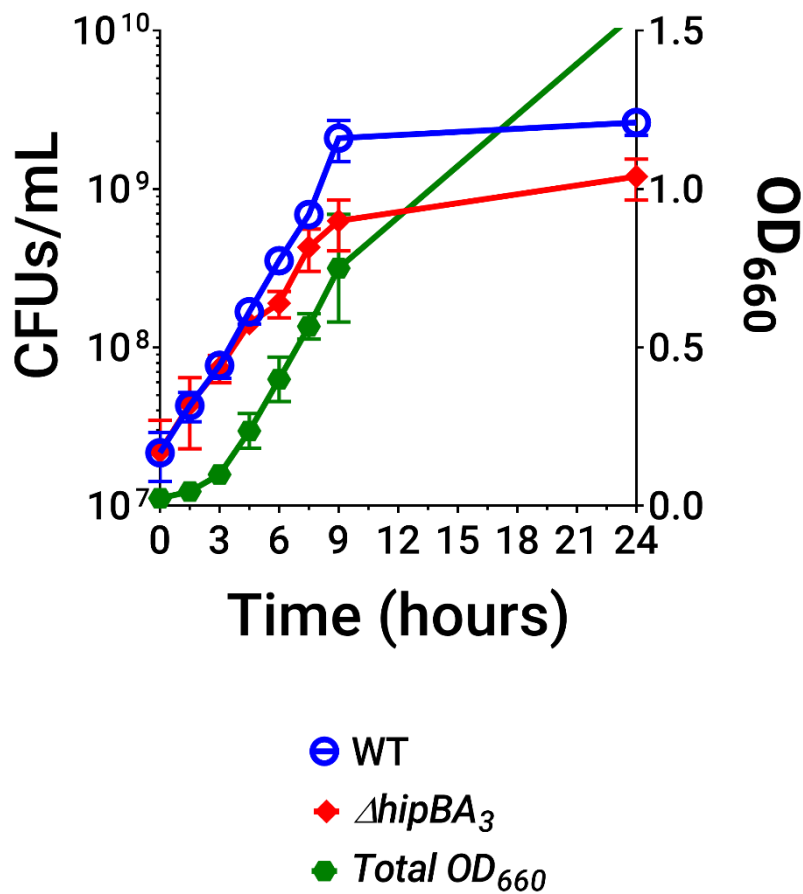


**Figure 2-1. The *hipBA<sub>3</sub>* has a mild fitness defect when competed against a marked NA1000 strain.**

*hipBA<sub>3</sub>* and marked NA1000 strains in exponential phase were coinoculated into PYE medium at OD<sub>660</sub>=0.01 each and incubated with shaking. Samples were withdrawn at the indicated times for OD<sub>660</sub> measurement and CFU enumeration of PYE solid media with and without kanamycin to distinguish between the strains. Values reported are the mean of three biological replicates.

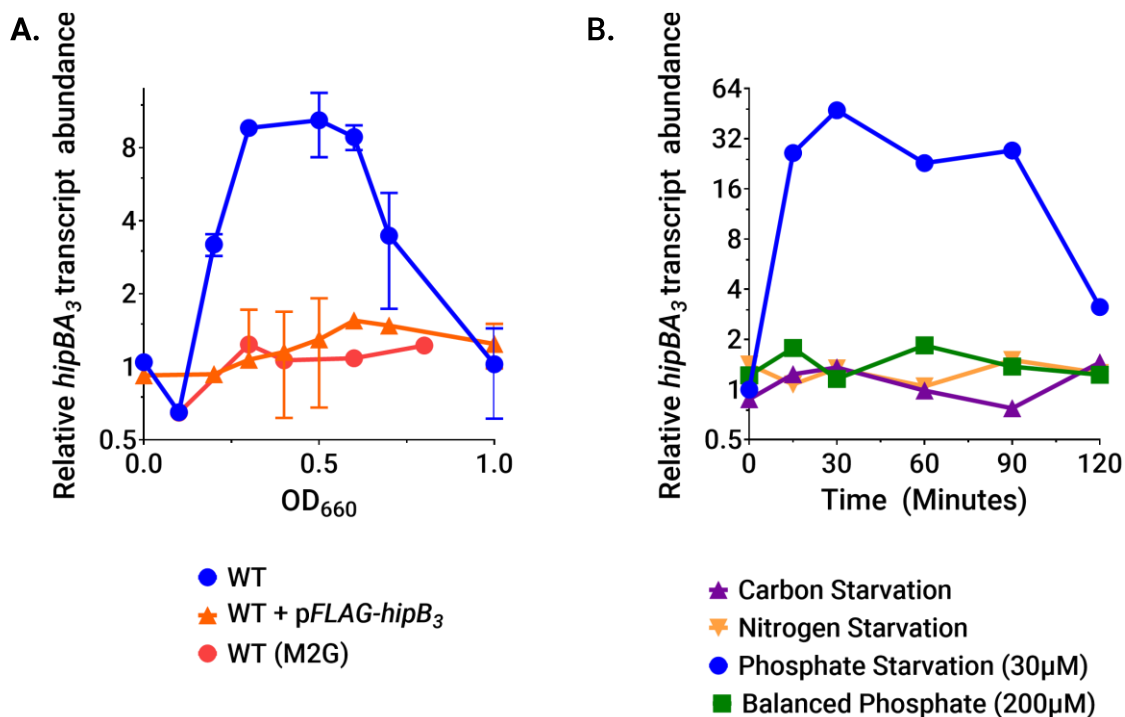


**Figure 2-2. *hipBA3* is active during late exponential phase in cultures grown in PYE medium and responds to phosphate starvation.**

(A) WT strains in exponential phase grown in PYE or M2G were subcultured to  $OD_{660}=0.02$  in PYE or M2G media, respectively. PYE was supplemented with 1mM IPTG and 1mM theophylline to express HipB<sub>3</sub>. Samples were collected at indicated  $OD_{660}$  for RNA extraction and subject to RT-PCR analysis to quantify *hipBA3* transcript abundance. Relative expression was determined using the double delta Ct analysis. Values reported are the mean and standard deviation of three biological replicates, each used in two technical replicates. (B) WT strains in exponential phase in M2G (carbon and nitrogen starvation) or M5G (phosphate starvation) were subcultured into media starved of the indicated nutrient at  $OD_{660}=0.1$ . Samples were collected at the indicated times for RNA extraction and subject to RT-PCR analysis to quantify *hipBA3* transcript abundance. Relative expression was determined using the double delta Ct analysis.

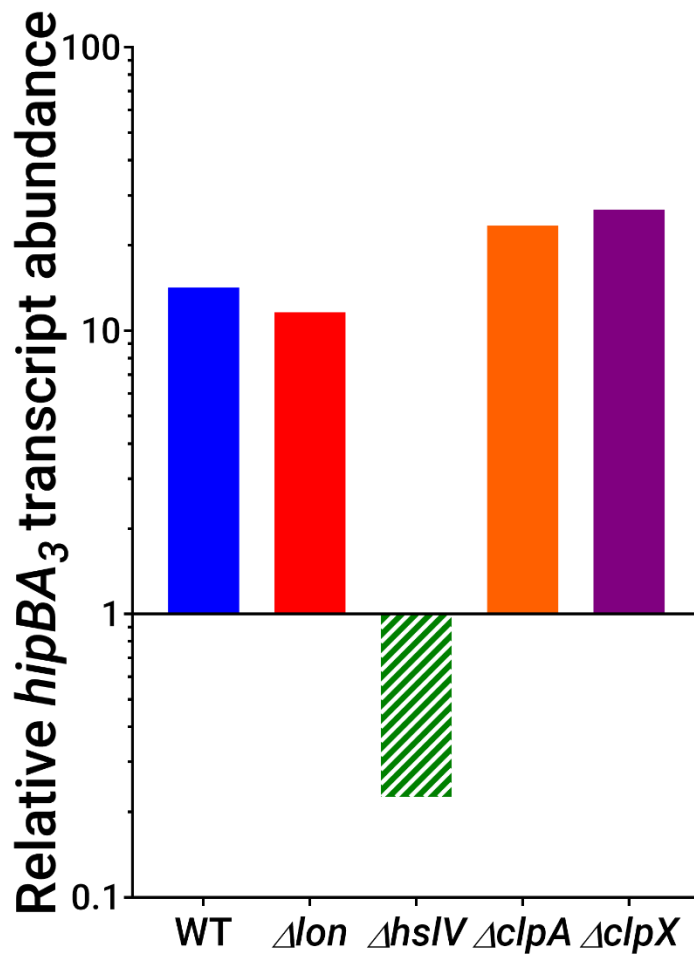


**Figure 2-3. HslUV is the protease responsible for degrading HipB<sub>3</sub> during phosphate starvation**

The indicated strains in exponential phase grown in M5G phosphate-replete medium were subcultured into M5G medium with 30  $\mu$ M phosphate at OD<sub>660</sub> = 0.1. RNA was harvested after 30 minutes of starvation, and *hipBA*<sub>3</sub> transcript abundance was determined using RT-PCR analysis. Expression relative to unstarved M5G controls was determined using the double delta Ct analysis.

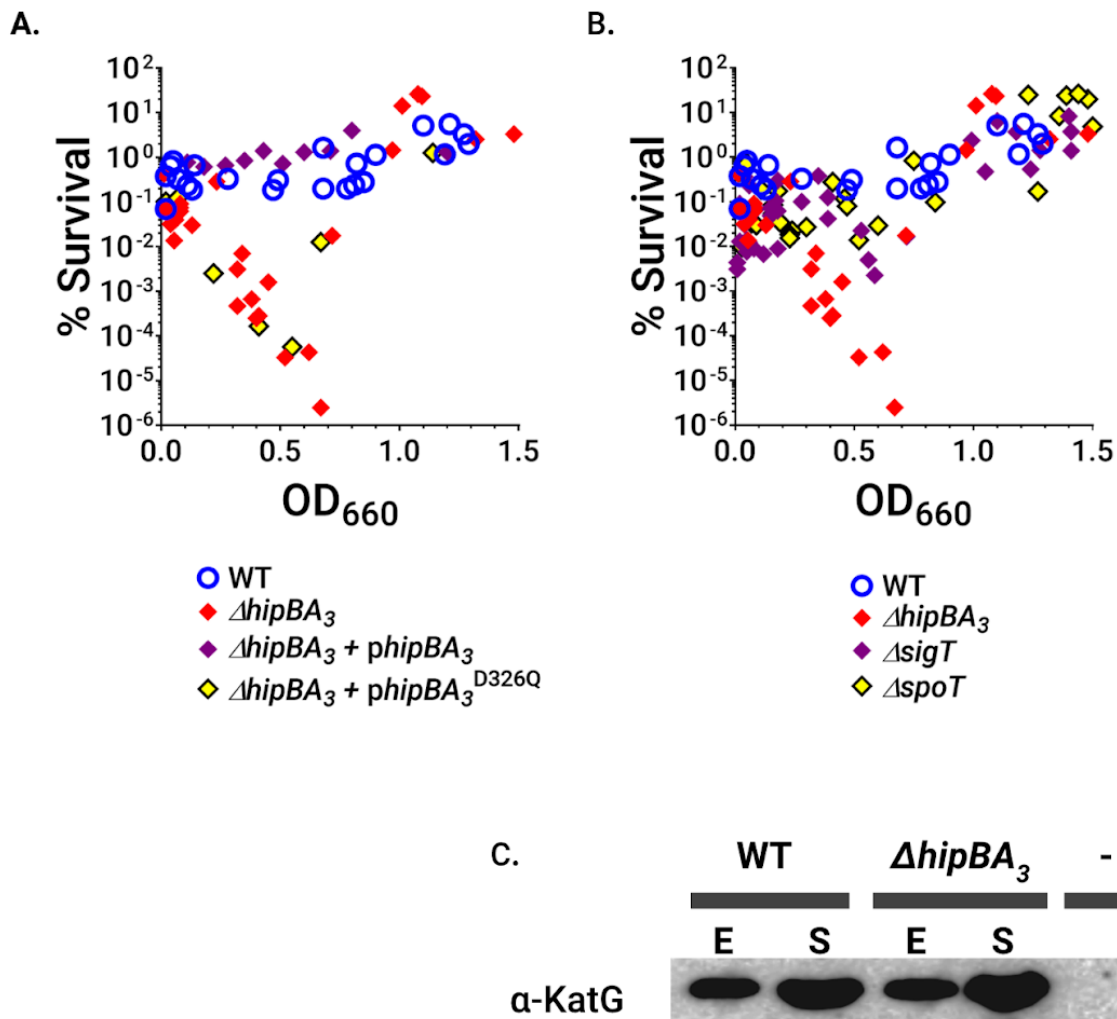
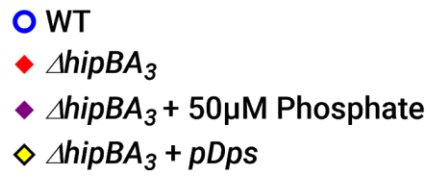
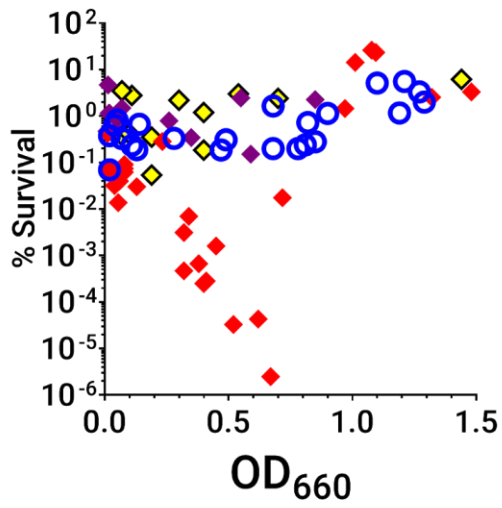
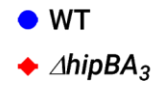
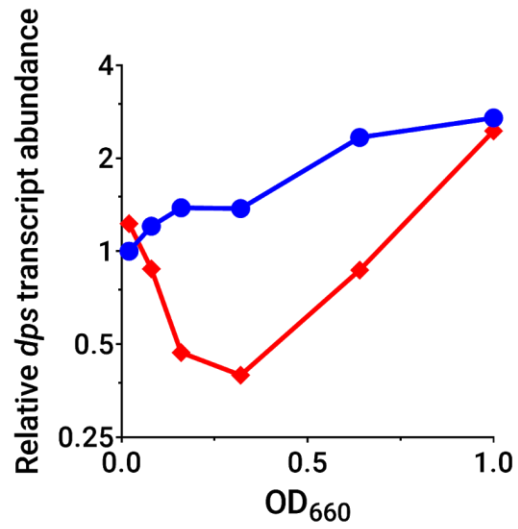


**Figure 2-4. HipA<sub>3</sub> kinase activity is required for peroxide tolerance during the exponential phase to stationary phase transition.** (A) Peroxide survival assays in PYE media indicate the  $\Delta hipBA_3$  strain has a window of ultrasensitivity to 1mM peroxide stress that can be complemented with the wild type  $hipBA_3$  operon on a low copy plasmid, but not a  $hipBA_3^{D326Q}$  operon with a mutation in the HipA<sub>3</sub> kinase active site. (B) Peroxide survival assays on  $\Delta sigT$  and  $\Delta spoT$  do not reveal peroxide ultrasensitivity. (C) Western blot measuring KatG catalase in WT and  $\Delta hipBA_3$  strains during the exponential phase to stationary phase transition in PYE medium. Samples were collected during late exponential phase (E) at  $OD_{660} \sim 0.4$  and stationary phase (S) at  $OD_{660} \sim 0.8-1.0$ . Whole cell lysates were prepared and normalized as described in Methods before Western blotting with anti-KatG antibodies.

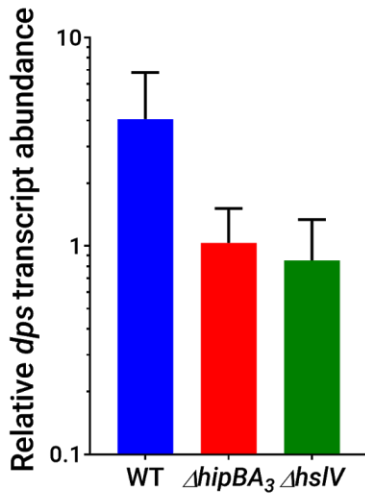
A.



B.



C.



D.

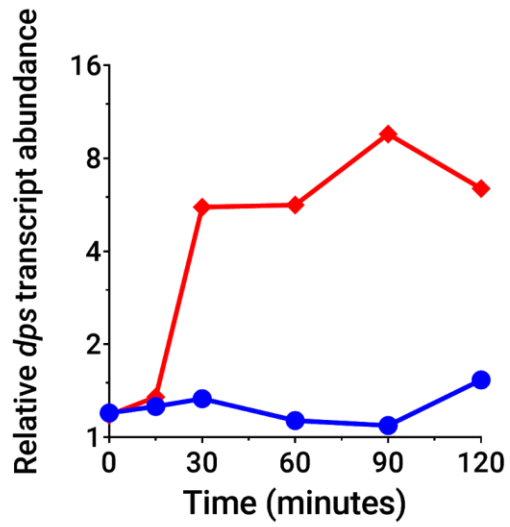




**Figure 2-5. HipA<sub>3</sub> transcriptionally upregulates Dps expression** (A) Peroxide survival assays in PYE medium indicate that the window of ultrasensitivity to 1mM peroxide stress can be complemented by ectopic Dps expression under the control of an inducible *riboA* promoter on a low-copy plasmid or phosphate supplementation to the PYE medium. (B) Measurements of *dps* transcripts through all phases of growth in PYE medium. Exponential phase cultures of the indicated strains grown in PYE medium were subcultured to OD<sub>660</sub>=0.02 and incubated with shaking. At the indicated OD<sub>660</sub>, samples were withdrawn for RT-PCR. Relative expression to an initial exponential phase control culture was determined using double delta CT analysis. (C) Relative *dps* transcript abundance during phosphate limitation. The indicated strains in exponential phase grown in M5G medium were subcultured to OD<sub>660</sub>=0.1 in M5G with reduced phosphate (30μM phosphate) to activate HipA<sub>3</sub> and induce *dps* transcription. After 30 minutes, samples were collected for RT-PCR. Relative expression to an unstarved M5G control was determined using double delta CT analysis. Values reported are the mean and standard deviation of three biological replicates and two technical replicates. (D) Measurements of *dps* transcripts after ectopic HipA<sub>3</sub> expression. Exponential phase cultures of the indicated strains were subcultured into PYE medium at OD<sub>660</sub>=0.02. HipA<sub>3</sub> proteins were induced at time=0 by the addition of 1 mM IPTG and 1 mM theophylline. Samples were withdrawn at indicated time points for RT-PCR analysis. Relative expression to an initial exponential phase control culture was determined using double delta CT analysis.

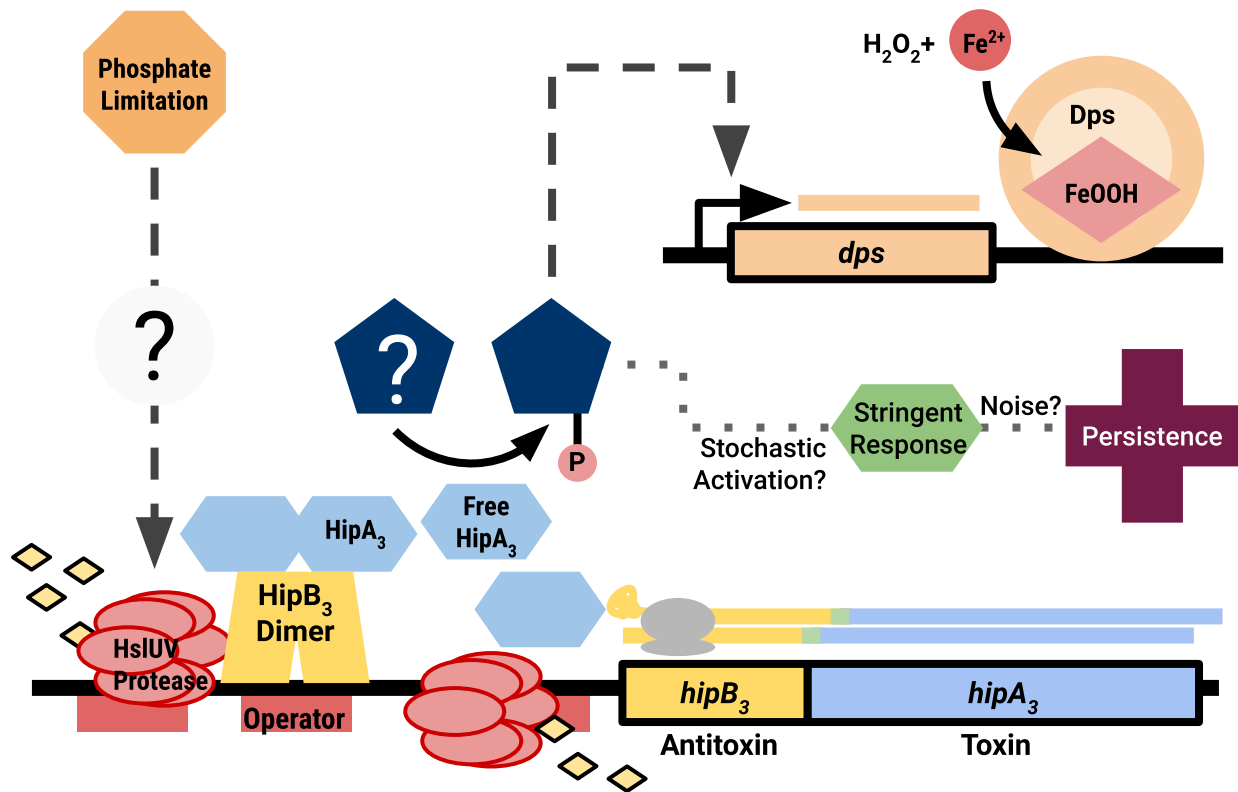


**Figure 2-6. A model for HipBA<sub>3</sub> in *C. crescentus* stress tolerance**

The HslUV protease responds to a phosphate limitation cue and degrades the HipB<sub>3</sub> antitoxin; consequently, HipA<sub>3</sub> is free and active. HipA<sub>3</sub> phosphorylates a downstream target that directly or indirectly upregulates *dps* transcription. In this model, the activation of HipA<sub>3</sub> is an early warning indicator of phosphate starvation and Dps is synthesized when sufficient phosphate is present to efficiently develop the iron mineral core, which removes peroxide during via the iron storage reaction. HipA<sub>3</sub> also phosphorylates a target that increases persistence via stringent response activation.

**Table 1. Strains**

<b>Name</b>	<b>Description</b>	<b>Reference</b>
WT	Wild-type Caulobacter NA1000	42
$\Delta hipBA_3$	$\Delta hipBA_3$	This study
$\Delta lon$	$\Delta lon$	43
$\Delta hslV$	$\Delta hslV$	J. Modell, unpublished
$\Delta clpA$	$\Delta clpA$	44
$\Delta clpX$	$\Delta clpX$	45
$\Delta sigT$	$\Delta sigT$	28
$\Delta spoT$	$\Delta spoT$	29
WT + pFLAG-hipB <sub>3</sub>	WT pFLAG-hipB <sub>3</sub>	This study
$\Delta hipBA_3$ + phipBA <sub>3</sub>	$\Delta hipBA_3$ phipBA <sub>3</sub>	This study
$\Delta hipBA_3$ + phipBA <sub>3</sub> <sup>D326Q</sup>	$\Delta hipBA_3$ phipBA <sub>3</sub> <sup>D326Q</sup>	This study
$\Delta hipBA_3$ + pdps	$\Delta hipBA_3$ pdps	This study
$\Delta hipBA_3$ + pFLAG-hipA <sub>3</sub>	$\Delta hipBA_3$ pFLAG-hipA <sub>3</sub>	This study

**Table 2. Plasmids**

<b>Name</b>	<b>Description</b>	<b>Reference</b>
pMR20	Broad-host-range, low-copy-number vector; tetR	
p <i>hipBA</i> <sub>3</sub>	pMR10 - <i>hipBA</i> <sub>3</sub>	This study
p <i>hipBA</i> <sub>3</sub> <sup>D326Q</sup>	pMR10 - <i>hipBA</i> <sub>3</sub> <sup>D326Q</sup>	This study
p <i>dps</i>	pMR20 - <i>PriboA</i> - <i>dps</i> (CCNA_02966)	This study
p <i>FLAG-hipA</i> <sub>3</sub>	pMR20 - <i>PriboA</i> - <i>FLAG-hipA</i> <sub>3</sub> (CCNA_02858)	This study
p <i>FLAG-hipB</i> <sub>3</sub>	JS71 - <i>PriboA</i> - <i>FLAG-hipB</i> <sub>3</sub> (CCNA_02859)	This study

**Table 3. Primers**

<b>Name</b>	<b>Sequence (5'-3')</b>	<b>Purpose</b>
<i>hipBA</i> <sub>3</sub> Up F	attgaagccggctggcgccaCCCGGGCGACAAGAAGGC	<i>hipBA</i> <sub>3</sub> chromosomal knockout
<i>hipBA</i> <sub>3</sub> Up R	cctaccgcctAAATTTTCATAAATCGCCTCTTGTGGCG	
<i>hipBA</i> <sub>3</sub> Dn F	tatgaaatttAGGCGGTAGGCGGGGGAT	<i>hipBA</i> <sub>3</sub> chromosomal knockout
<i>hipBA</i> <sub>3</sub> Dn R	cgtcacggcccgaagctagcgGACAGCGGCACCAGCCGT C	
<i>riboA</i> to pMR10/pMR20 F	ctatgaccatgattacgccaTGGTGCAAACCTTTTCGC	pMR10/pMR20 expression vector
<i>riboA</i> to pJS71 F	cggccgctctagaactagtgTGGTGCAAACCTTTTCGC	pJS71 protein expression vector
<i>riboA</i> to FLAG R	cttgtcgtcatcgtctttgtagtcCATCTTGTTGATACCCCC	<i>riboA</i> promoter for protein expression
<i>riboA</i> to <i>dps</i> R	aagcggcggcCATCTTGTTGATACCCCC	
<i>hipA</i> <sub>3</sub> F	gactacaaagacgatgacgacaagACCACCGTCGCCGAG GTT	FLAG- <i>hipA</i> <sub>3</sub> for pMR20 expression vector
<i>hipA</i> <sub>3</sub> R	ttgtaaaacgacggccagtgCTACCGCCTGAGCTCCAG	
<i>hipB</i> <sub>3</sub> F	gactacaaagacgatgacgacaagAAATTTGAATCTCTCC TGTCC	FLAG- <i>hipB</i> <sub>3</sub> for pJS71 expression vector
<i>hipB</i> <sub>3</sub> R	cgaggtcgacggtatcgataCTAGTCATCGCCACCGCTC AC	
<i>dps</i> F	caacaagatgGCCGCCGCTTTGAACACC	<i>dps</i> for pMR10 expression vector
<i>dps</i> R	ttgtaaaacgacggccagtgCTACTTTAGGCCGAGCGTG G	
<i>hipA</i> <sub>3</sub> <sup>D326Q</sup> F	gttcttgacgtggtcctgctggttcgcgccag	<i>hipA</i> <sub>3</sub> <sup>D326Q</sup> mutagenic primers
<i>hipA</i> <sub>3</sub> <sup>D326Q</sup> R	ctggcgcgaaaccagcaggaccacgtcaagaac	
<i>hipBA</i> <sub>3</sub> F	ctatgaccatgattacgccaCCCCACCGGCGCCCAGGAG	<i>hipBA</i> <sub>3</sub> operon and promoter for pMR10 complementation vector
<i>hipBA</i> <sub>3</sub> R	ttgtaaaacgacggccagtgGCGCGTCGCGCGGCGTCA	
<i>hipBA</i> <sub>3</sub> F	GGCGGTCTTCGCCTATGAG	RT-PCR oligonucleotides
<i>hipBA</i> <sub>3</sub> R	GGCAGATCGGGAAAGCTGAA	

<i>dps</i> (CCNA_02966) ) F	CTTTGAACACCGGGCTGACT	
<i>dps</i> (CCNA_02966) ) R	TCCAGTGATAGCCATGCGTC	
<i>rho1 F</i>	AGACACCGAAAACCAGGTTCC	
<i>rho1 R</i>	CGCTTCAGTGGTGATGTCGG	
<i>rho2 F</i>	ACCGAAGACACCGAAAACCAG	
<i>rho2 R</i>	GCCGCTTCAGTGGTGATGT	

## References

1. Van Melder, L. Toxin-antitoxin systems: why so many, what for? *Curr. Opin. Microbiol.* **13**, 781–785 (2010).
2. Magnuson, R. & Yarmolinsky, M. B. Corepression of the P1 addiction operon by Phd and Doc. *J. Bacteriol.* **180**, 6342–6351 (1998).
3. Jensen, R. B. & Gerdes, K. Programmed cell death in bacteria: proteic plasmid stabilization systems. *Mol. Microbiol.* **17**, 205–210 (1995).
4. Magnuson, R. D. Hypothetical functions of toxin-antitoxin systems. *J. Bacteriol.* **189**, 6089–6092 (2007).
5. Christensen, S. K., Mikkelsen, M., Pedersen, K. & Gerdes, K. RelE, a global inhibitor of translation, is activated during nutritional stress. *Proc. Natl. Acad. Sci. U. S. A.* **98**, 14328–14333 (2001).
6. Christensen, S. K., Pedersen, K., Hansen, F. G. & Gerdes, K. Toxin-antitoxin loci as stress-response-elements: ChpAK/MazF and ChpBK cleave translated RNAs and are counteracted by tmRNA. *J. Mol. Biol.* **332**, 809–819 (2003).
7. Germain, E., Castro-Roa, D., Zenkin, N. & Gerdes, K. Molecular mechanism of bacterial persistence by HipA. *Mol. Cell* **52**, 248–254 (2013).
8. Kaspy, I. *et al.* HipA-mediated antibiotic persistence via phosphorylation of the glutamyl-tRNA-synthetase. *Nat. Commun.* **4**, 3001 (2013).
9. Sat, B. *et al.* Programmed cell death in Escherichia coli: some antibiotics can trigger mazEF lethality. *J. Bacteriol.* **183**, 2041–2045 (2001).
10. Hazan, R., Sat, B. & Engelberg-Kulka, H. Escherichia coli mazEF-mediated cell death is triggered by various stressful conditions. *J. Bacteriol.* **186**, 3663–3669 (2004).
11. Sat, B., Reches, M. & Engelberg-Kulka, H. The Escherichia coli mazEF suicide module mediates thymineless death. *J. Bacteriol.* **185**, 1803–1807 (2003).
12. Muthuramalingam, M., White, J. C. & Bourne, C. R. Toxin-Antitoxin Modules Are Pliable Switches Activated by Multiple Protease Pathways. *Toxins* **8**, (2016).
13. Ren, D., Bedzyk, L. A., Thomas, S. M., Ye, R. W. & Wood, T. K. Gene expression in Escherichia coli biofilms. *Appl. Microbiol. Biotechnol.* **64**, 515–524 (2004).
14. Kasari, V., Kurg, K., Margus, T., Tenson, T. & Kaldalu, N. The Escherichia coli mqsR and ygiT genes encode a new toxin-antitoxin pair. *J. Bacteriol.* **192**, 2908–2919 (2010).
15. Wang, X. *et al.* A new type V toxin-antitoxin system where mRNA for toxin GhoT is cleaved by antitoxin GhoS. *Nat. Chem. Biol.* **8**, 855–861 (2012).
16. Soo, V. W. C. & Wood, T. K. Antitoxin MqsA represses curli formation through the master biofilm regulator CsgD. *Sci. Rep.* **3**, 3186 (2013).
17. de Castro Ferreira, I. G., Rodrigues, M. M., da Silva Neto, J. F., Mazzon, R. R. & do Valle Marques, M. Role and regulation of ferritin-like proteins in iron homeostasis and oxidative stress survival of Caulobacter crescentus. *Biometals* **29**, 851–862 (2016).
18. Karas, V. O., Westerlaken, I. & Meyer, A. S. The DNA-Binding Protein from Starved Cells (Dps) Utilizes Dual Functions To Defend Cells against Multiple Stresses. *J. Bacteriol.* **197**, 3206–3215 (2015).

19. Castruita, M. *et al.* Overexpression and characterization of an iron storage and DNA-binding Dps protein from *Trichodesmium erythraeum*. *Appl. Environ. Microbiol.* **72**, 2918–2924 (2006).
20. Ishikawa, T. *et al.* The iron-binding protein Dps confers hydrogen peroxide stress resistance to *Campylobacter jejuni*. *J. Bacteriol.* **185**, 1010–1017 (2003).
21. Hayes, F. & Kędzierska, B. Regulating toxin-antitoxin expression: controlled detonation of intracellular molecular timebombs. *Toxins* **6**, 337–358 (2014).
22. Lin, C.-Y., Awano, N., Masuda, H., Park, J.-H. & Inouye, M. Transcriptional repressor HipB regulates the multiple promoters in *Escherichia coli*. *J. Mol. Microbiol. Biotechnol.* **23**, 440–447 (2013).
23. Schumacher, M. A. *et al.* HipBA-promoter structures reveal the basis of heritable multidrug tolerance. *Nature* **524**, 59–64 (2015).
24. Ely, B. [17] Genetics of *Caulobacter crescentus*. in *Methods in Enzymology* **204**, 372–384 (Academic Press, 1991).
25. Domian, I. J., Quon, K. C. & Shapiro, L. Cell type-specific phosphorylation and proteolysis of a transcriptional regulator controls the G1-to-S transition in a bacterial cell cycle. *Cell* **90**, 415–424 (1997).
26. Hansen, S. *et al.* Regulation of the *Escherichia coli* HipBA toxin-antitoxin system by proteolysis. *PLoS One* **7**, e39185 (2012).
27. Britos, L. *et al.* Regulatory response to carbon starvation in *Caulobacter crescentus*. *PLoS One* **6**, e18179 (2011).
28. Alvarez-Martinez, C. E., Lourenço, R. F., Baldini, R. L., Laub, M. T. & Gomes, S. L. The ECF sigma factor sigma(T) is involved in osmotic and oxidative stress responses in *Caulobacter crescentus*. *Mol. Microbiol.* **66**, 1240–1255 (2007).
29. Lesley, J. A. & Shapiro, L. SpoT regulates DnaA stability and initiation of DNA replication in carbon-starved *Caulobacter crescentus*. *J. Bacteriol.* **190**, 6867–6880 (2008).
30. Boutte, C. C. & Crosson, S. The complex logic of stringent response regulation in *Caulobacter crescentus*: starvation signalling in an oligotrophic environment. *Mol. Microbiol.* **80**, 695–714 (2011).
31. Chiaverotti, T. A., Parker, G., Gallant, J. & Agabian, N. Conditions that trigger guanosine tetraphosphate accumulation in *Caulobacter crescentus*. *J. Bacteriol.* **145**, 1463–1465 (1981).
32. Italiani, V. C. S., da Silva Neto, J. F., Braz, V. S. & Marques, M. V. Regulation of catalase-peroxidase KatG is OxyR dependent and Fur independent in *Caulobacter crescentus*. *J. Bacteriol.* **193**, 1734–1744 (2011).
33. Steinman, H. M., Fareed, F. & Weinstein, L. Catalase-peroxidase of *Caulobacter crescentus*: function and role in stationary-phase survival. *J. Bacteriol.* **179**, 6831–6836 (1997).
34. Zhao, G. *et al.* Iron and hydrogen peroxide detoxification properties of DNA-binding protein from starved cells. A ferritin-like DNA-binding protein of *Escherichia coli*. *J. Biol. Chem.* **277**, 27689–27696 (2002).
35. Calhoun, L. N. & Kwon, Y. M. Structure, function and regulation of the DNA-binding protein Dps and its role in acid and oxidative stress resistance in *Escherichia coli*: a review. *J. Appl. Microbiol.* **110**, 375–386 (2011).



36. Becton, Dickinson and Company. BD Bionutrients™ Technical Manual Third Edition. (2006). Available at: [https://www.bdbiosciences.com/documents/bionutrients\\_tech\\_manual.pdf](https://www.bdbiosciences.com/documents/bionutrients_tech_manual.pdf). (Accessed: 1st August 2019)
37. Johnson, J. L., Cannon, M., Watt, R. K., Frankel, R. B. & Watt, G. D. Forming the phosphate layer in reconstituted horse spleen ferritin and the role of phosphate in promoting core surface redox reactions. *Biochemistry* **38**, 6706–6713 (1999).
38. Poindexter, J. S. BIOLOGICAL PROPERTIES AND CLASSIFICATION OF THE CAULOBACTER GROUP. *Bacteriol. Rev.* **28**, 231–295 (1964).
39. Ely, B. Genetics of *Caulobacter crescentus*. *Methods Enzymol.* **204**, 372–384 (1991).
40. Bertani, G. Studies on lysogenesis. I. The mode of phage liberation by lysogenic *Escherichia coli*. *J. Bacteriol.* **62**, 293–300 (1951).
41. Topp, S. *et al.* Synthetic riboswitches that induce gene expression in diverse bacterial species. *Appl. Environ. Microbiol.* **76**, 7881–7884 (2010).
42. Marks, M. E. *et al.* The genetic basis of laboratory adaptation in *Caulobacter crescentus*. *J. Bacteriol.* **192**, 3678–3688 (2010).
43. Wright, R., Stephens, C., Zweiger, G., Shapiro, L. & Alley, M. R. *Caulobacter* Lon protease has a critical role in cell-cycle control of DNA methylation. *Genes Dev.* **10**, 1532–1542 (1996).
44. Grünenfelder, B. *et al.* Identification of the protease and the turnover signal responsible for cell cycle-dependent degradation of the *Caulobacter* FliF motor protein. *J. Bacteriol.* **186**, 4960–4971 (2004).
45. Aakre, C. D., Phung, T. N., Huang, D. & Laub, M. T. A bacterial toxin inhibits DNA replication elongation through a direct interaction with the  $\beta$  sliding clamp. *Mol. Cell* **52**, 617–628 (2013).